1978

Geometric nonlinear analysis of plane flexible frame structures.

Hany Ahmed Mohamed. el-Ghazaly
University of Windsor

Recommended Citation

el-Ghazaly, Hany Ahmed Mohamed., "Geometric nonlinear analysis of plane flexible frame structures." (1978). *Electronic Theses and Dissertations.* Paper 2224.

GEOMETRIC NONLINEAR ANALYSIS OF
PLANE FLEXIBLE FRAME STRUCTURES

A THESIS
SUBMITTED TO THE FACULTY OF GRADUATE STUDIES THROUGH
THE DEPARTMENT OF CIVIL ENGINEERING IN PARTIAL
FULFILMENT OF THE REQUIREMENTS FOR THE
DEGREE OF MASTER OF APPLIED SCIENCE
AT THE UNIVERSITY OF WINDSOR

BY

HANY AHMED MOHAMED EL-GHAZALY

WINDSOR, ONTARIO, CANADA

1978

TO MY PARENTS

ABSTRACT

A study of the geometric nonlinear behaviour of structures is performed in this research. The method of analysis reported is applicable to planar frame structures under any loading conditions.

Using an Eulerian moving coordinate system and a nonlinear strain-displacement relationship, nonlinear finite element formulations are developed and employed to calculate the total potential energy of the structure which is then minimized using a scaled unconstrained conjugate gradient algorithm to yield the solution to the structural analysis problem.

The various degrees of geometric nonlinearity include finite deflections, bifurcation buckling and snap-through buckling and these applications demonstrate the potential of the method developed. Special attention is given to the analysis of guyed transmission towers as a practical example of geometrically nonlinear structures.

Comparison with linear solutions indicates that in certain structures, considerations of the geometric nonlinear aspects are essential, otherwise the analysis could be misleading. The results using the present formulation are compared with previous analytical solutions and experimental test results and excellent agreement is obtained; in general, the method presented gives improved accuracy

as compared to other solution procedures.

ACKNOWLEDGEMENTS

The writer would like to express his sincere appreciation and gratitude to his advisor, Dr. G.R. Monforton, Professor in charge of this research, for his continuous encouragement and valuable suggestions and recommendations throughout the research.

Thanks are also due to the University of Windsor Computer Center staff.

The writer is also grateful to the National Research Council for the financial assistance provided during the study period (Grant No. 689).

Special thanks are also extended to Mrs. Barbara Denomey for her patience and cooperation in typing the entire manuscript.

LIST OF SYMBOLS

$\{\tilde{G}_e\}$	gradient vector of the element strain energy with respect to the displacements components defined in the undeformed local coordinates.
$\{\bar{G}_e\}$	gradient vector of the element strain energy with respect to the displacements components defined in the global reference coordinates.
$g(\alpha_i)$	two dimensional function defining the linear search in the minimization process.
$\acute{g}(\alpha_i)$	gradient of the linear search function $g(\alpha_i)$ with respect to α_i.
I	number of elements comprising the structure.
J	number of degrees of freedom of the structure.
k	coupling constant in the bending-tension case.
k_1	coupling constant in the bending-compression case.
k_{ij}	i, j th element in the element stiffness matrix defined in the Eulerian coordinates.
$[K]$	the linear stiffness matrix.
$[\bar{K}]$	the scaled linear stiffness matrix.
k_o	estimate of the location of the function's minimum in the linear search.
ℓ	undeformed length of the frame discrete element.
ℓ_1, m_1	direction cosines of the x axis with respect to the $\bar{X}, \bar{Y}$ coordinates.
P_j	the load corresponding to the j th component of the global displacement vector.
$\{P\}$	the unscaled load vector.
$\{\bar{P}\}$	the scaled load vector.

p, q	subscripts denoting nodal points of a frame discrete element.
P_p, V_p, M_p	end forces developed at end p in the deformed configuration.
P_q, V_q, M_q	end forces developed at end q in the deformed configuration.
R	integration constant of the displacement function in the axial x direction.
$[R]$	diagonal scaling transformation matrix.
r_{jj}	j th diagonal element in the $[R]$ matrix.
s	chord length of the deformed frame element.
$\vec{s}$	conjugate direction.
$[\tilde{T}]$	nonlinear transformation matrix.
$[\bar{T}]$	linear transformation matrix
$\tilde{t}_{ij}$	i, j th element in the nonlinear transformation $[\tilde{T}]$ matrix.
U	total strain energy of the structure.
U_s	element strain energy.
u_p, v_p, v_{x_p}	element displacement components in the Eulerian coordinates at end p.
u_q, v_q, v_{x_q}	element displacement components in the Eulerian coordinates at end q.
$\tilde{u}_p, \tilde{v}_p, \tilde{\lambda}_p$	element displacement components in the local undeformed coordinates at end p.
$\tilde{u}_q, \tilde{v}_q, \tilde{\lambda}_q$	element displacement components in the local undeformed coordinates at end q.
$\bar{u}_p, \bar{v}_p, \bar{\lambda}_p$	element displacement components in the reference global coordinates at end p.
$\bar{u}_q, \bar{v}_q, \bar{\lambda}_q$	element displacement components in the reference global coordinates at end q.
V	element volume.
W	potential of the applied loads acting on the structure.

W_s	potential of the forces developed at the ends of the element.
x, y	Eulerian moving coordinates.
$\tilde{x}, \tilde{y}$	local undeformed (Lagrangian) coordinates.
$\bar{X}, \bar{Y}$	reference global coordinates.
$\{z\}$	scaled displacement vector.

Greek Letters

α	the axis along which the function is minimized in the linear search routine.
$\overset{*}{\alpha}$	the distance along the α axis that corresponds to the minimum of the function in the linear search.
α_e	location of the minimum of the function along the α axis that corresponds to the minimum of the fitted third degree polynomial.
γ	wind load parameter relating the actual wind intensity to the working wind intensity.
Δ	deflection.
$\vec{\nabla \pi}_p$	vector defining the gradient of the total potential energy function.
$\varepsilon(x,y)$	total strain at any point on the frame element defined by the x,y coordinates.
ε_p	prestrain induced in the element.
ε_d	strain of deformation due to applied loads.
$\varepsilon_2, \varepsilon_3$	absolute error value defining the exit criterion in the minimization process.
θ_p, θ_q	relative rotation at ends p and q, respectively.
θ_r	rigid body rotation.
π_p	element potential energy.

Π_p total potential energy of the structural system.

σ stress corresponds to strain ε.

TABLE OF CONTENTS

LIST OF FIGURES

LIST OF TABLES

CHAPTER I

INTRODUCTION .

1.1 General

The need for dependable geometric nonlinear methods
of analysis is evident in the design of flexible light-
weight structures. In this type of structure, situations
involving geometric nonlinearity, but restricted to
linear material behaviour, constitute a significant class
of analysis problems. Moreover, the structural design
of such structures is often governed by elastic stability
requirements. This concern in realistic design situations
has provided strong motivation for extending the finite
element analysis method in order to accommodate geometric
nonlinearities. Accordingly, many research efforts have
been devoted to this objective and several analysis pro-
cedures have emerged.

1.2 Literature Review

In the International Symposium for the use of
electronic computers in Civil Engineering which was held
at Lisbon in Portugal on October 1962 (Ref. 1), Saafan
and Brotton presented a method for the analysis of geo-
metrically nonlinear rigid frame structures. In this
method, a finite deflection scheme was proposed for the
analysis to account for large deflections, but the instabi-
lity effects caused by the axial loading as well as the

bowing effects were neglected.

Shortly after, Saafan (Ref. 2) extended his previous work with Brotton and proposed a modified finite deflection method where the effect of axial force on the flexural stiffness was included in the form of bowing functions. According to Saafan's method, each joint of the frame was provided with a system of spring restraints to take the unbalanced forces between the applied load and the actual member forces meeting at a joint. The solution was defined as the displacement pattern which causes the forces in the spring restraints to be equal to zero. Saafan presented some important recommendations which include the following:

(1) End shorting due to flexure $\frac{1}{2}(\frac{dv}{dx})^2$ may be of the same order of magnitude as the linear extensional term $\frac{du}{dx}$.

(2) The stability and bowing functions may play an important part in the estimation of the theoretical carrying capacity of the structure.

Despite some inconsistencies that were noticed, Saffan's attempt opened the way to further investigators.

Poskitt (Ref. 3) proved that Saafan's method is applicable only to the analysis of structures with low levels of geometric nonlinearity since the method oscillates without reaching a solution at higher levels of geometric nonlinearity.. Poskitt attributed the oscillatory behaviour

to the fact that Saafan employed a first order iterative scheme in finding the solution to the geometrically non-linear problem. In the same paper, Poskitt proposed another iterative finite displacement method which involved a second order iterative scheme, but only the solution to a three-jointed simple A truss was reported.

Tezcan (Ref. 4) in a discussion to Poskitt's paper (Ref. 3), derived a tangent stiffness matrix for frames exhibiting geometric nonlinearity. Tezcan's stiffness matrix came out to be unsymmetric and the unsymmetric character was attributed to the fact that the reciprocal theorem does not apply to structures with large deformations. Later, Oran (Ref. 5) proved that Tezcan's interpretation concerning the symmetry and non-symmetry of the stiffness matrix was highly misleading. Oran reported that the unsymmetric character of Tezcan's stiffness matrix was due to the inconsistent approximations embodied in Tezcan's formulations. Oran proved that the tangent stiffness matrix is always symmetric by defining the elements of the tangent stiffness matrix as the second partial derivatives of the strain energy.

In 1968, Lee, Manuel and Rossow (Ref. 6) proposed an incremental method for the analysis of geometrically nonlinear rigid frames where the critical load was also predicted. The writers investigated both the bifurcation and snap-through types of instability as well as the

post-buckling behaviour of framed structures. The method proposed in that paper was formulated as a system of simultaneous nonlinear equations obtained by combining the general solution of the exact nonlinear differential equation of bending and the equilibrium equations obtained for each of the segments between load points and/or points of inflection, with the prescribed boundary conditions. The resulting system of equations was then solved by the Newton-Raphson iterative method.

Przemieniecki (Ref. 7) discussed the concept of geometric nonlinearity and employed an initial stress (geometric stiffness) matrix to be used in conjunction with a load incrementation process. The nonlinear term $\frac{1}{2}(\frac{dv}{dx})^2$ was included in the strain-displacement relationship and first and third degree polynomials were used to describe the axial and the transverse displacements, respectively. The Lagrangian (initial undeformed) coordinates were used to formulate the equilibrium equations in each step and the elastic as well as the geometric stiffness matrices were updated after each step to account for the change in the geometry due to the incremental deformations. In the same reference, the concept of the elastic stability of structures was discussed in light of the geometric stiffness matrix developed.

Connor, Logcher and Chan (Ref. 8) also presented nonlinear formulations for the analysis of rigid frames.

The effect of flexure and chord rotation on the axial
stiffness was included in the analysis. The appropriate
equations for solution by successive substitution and
Newton-Raphson iteration were also given. A linearized
incremental solution technique which can be described as
a one-cycle Newton-Raphson method was also described. Due
to employing Lagrangian coordinates in formulating the
stiffness equations, the writers limited the use of the
formulations to the cases of small rotations (where the
squares of the rotation angles are negligible compared to
unity). In the same paper, the effect of initial prestrains
was included but an inconsistency in defining the axial
force was noted. A shallow frame, which is a scale model
of a large radome, was solved and the results were given in
the form of a load-deflection curve. Two portal frames
were also solved with successful prediction to the buckling
load.

An excellent review to the problem of geometric
nonlinearity is given by Mallett and Marcal (Ref. 9). In
that paper, three alternative mathematical models and com-
putational procedures were developed for the nonlinear,
pre- and post-buckling analyses. The proposed method was
essentially a load incrementing procedure where the non-
linear term $\frac{1}{2}(\frac{dw}{dx})^2$ was retained in the strain-displacement
relationship; a first and a third degree polynomial were
employed to define the axial and the transverse displacements,

respectively. The element strain energy was split into three terms. The first term is that associated with the usual linear formulation, the second term reflects the coupling effects between the axial and the transverse stiffnesses while the third term involves the nonlinear effects due to bending. The stability critical situation was explained as the mutual degradation of the initial axial and flexural stiffnesses which finally leads to buckling. The equilibrium equations were formulated with respect to a system of fixed local coordinates (Lagrangian). which is inaccurate in handling cases of large rotations unless relatively small load increments are considered. First and second order incremental formulations were also given; it was emphasized that the nonlinear incremental formulations have to be used whenever the strain-displacement relationship contains nonlinear terms. In the same paper, a rational classification to the degrees of geometric non-linearity was presented starting with structures exhibiting linear behaviour up to the point of general instability and ending with the snap-through phenomenon in structures as the lowest and highest degrees of geometric nonlinearity, respectively. The writers reported that incremental methods. are not directly applicable to the prediction of the post-buckling behaviour if it involves the traversing of an unstable region of the load-deflection curve, while the potential energy minimization analysis procedure is uniquely

suited to this purpose. Despite the lack of numerical examples, the paper is one of the best references dealing with the problem of geometric nonlinearity.

A few years later, Baron and Venkatesan published a paper (Ref. 10) dealing with the nonlinear analysis of beam-column elements where the undeformed (Lagrangian) axes were used in formulating the stiffness equations. Two approximate formulations, describing two alternative solutions, one based on a third degree polynomial, and another based on a Fourier series expression for the transverse displacement were given. Finally, a closed form solution to the transverse displacement was presented in the form of trigonometric and hyperbolic functions. The writers also proposed a series as well as a closed form solution to account for the influence of lateral loads between nodes but no method of analysis nor illustrative examples were given. Oran (Ref. 5) raised the question of whether the formulations given by Baron and Venkatesan (Ref. 10), in spite of their complexity, have any superiority to the formulations obtained from the conventional beam-column theory.

A valuable assessment of the solution techniques which are applicable to the solution of the nonlinear algebraic or differential equations characterizing the geometrically nonlinear behaviour of structures, was given by Haisler, Stricklin and Stebbins in Ref. 11. The

writers presented a complete review to the methods of solv-
ing the problem of geometric nonlinearity starting with
the incremental stiffness procedure as first proposed by
Turner, Dill, Martin and Meloche (Ref. 12) and ending with
the self-correcting initial value formulations (Ref. 13).

Martin (Ref. 14) presented a general theory to the
problem of geometric nonlinearity based on an incremental
load approach. Martin applied the theory to various
elements, amongst which was the beam-column element. The
element was assumed straight at the initial state so that
the axial force and the bending effects are uncoupled.
The nonlinear term $\frac{1}{2}(\frac{du}{dx})^2$ was included in addition to the
nonlinear term $\frac{1}{2}(\frac{dv}{dx})^2$; a system of Lagrangian coordinates
to formulate the stiffness equations was used. First and
third degree polynomials were assumed for the axial and the
transverse displacements, respectively.

In 1973, Oran published two consecutive papers
(Refs. 5 and 15) for the development of consistent tangent
stiffness matrices for both the planar and the space frame
elements, respectively. In Ref. 5, Oran presented a
valuable discussion to the previous research done in the
area of geometric nonlinearity in skeletal structures.
The explicit definition of the element tangent stiffness
matrix was given with respect to a system of Eulerian
(deformed) coordinates; a transformation was then applied
to transfer from a local to an arbitrary global reference

coordinate system. The formulations given by Oran reflect
the inherent symmetry of the geometrically nonlinear problem,
with respect to the end rotations while other investigators
(Ref.. 8) failed in reflecting this symmetry. Basically,
the use of the stability and bowing functions was demon-
strated to couple the transverse and the axial stiffnesses.
Oran neglected the difference in length between the chord
and the undeformed member when passing from the local to
the global coordinates. The effect of such an approximation
is questionnable in the analysis of flexible structures.
No method of analysis was given, but it is understood that
the formulations are to be used within the framework of an
incremental load procedure. In Ref. 15, Oran extended his
previous work to account for the analysis of space frames.
The concept was, essentially, the same but the transformation
involved more complications. In that paper, Oran outlined
two solution procedures, one using a load incremental method
and another using Newton-Raphson iteration but no numerical
examples were reported.

Yang (Ref. 16) used an incremental procedure to
predict the behaviour of geometrically nonlinear structures.
Although the writer employed the same stiffness matrix
previously developed by Prezemieniecki (Ref. 7), he described
the use of a new linearized midpoint tangent incremental
approach to reduce the errors included in the conventional
linear incremental method. Some comparative examples were

solved and the agreement with prior work was good.

Young (Ref. 17) recalled the geometric stiffness matrix previously developed by Martin in Ref. 18, but instead of using approximate coefficients to reflect the bending-axial interaction, the exact hyperbolic and tri-gonometric functions were used to get accurate expressions for those coefficients. Young showed that the customary assumption that the deflection curve is a cubic is erro-neous in the cases where the value of the axial load is large.

Recently, Bouchet and Biswas (Ref. 19) presented a method for the analysis of cantilever structures. The method of analysis presented in that paper employed a beam-column finite element in conjunction with transfer matrices and an incremental loading procedure to directly generate the total moments as well as the axial and trans-verse displacements. Moreover, with the aid of a standard Southwell plot, the transverse deflections generated by the compressive axial loads (in the presence of a small perturbing transverse force) were plotted to yield the critical buckling load. The method was restricted to the analysis of cantilevers and stacks where the solution pro-ceeds from the free end without the necessity of computing global elastic and geometric stiffness matrices. Three examples for the analysis of three different stacks were presented with fair agreement with prior work.

An important recommendation about the effect of

the nonlinear terms which are usually neglected in the nonlinear analysis was given in Ref. 20. The writers showed that the term $\frac{1}{2}(\frac{du}{dx})^2$ has to be retained in the strain-displacement relationship if Lagrangian coordinates are used in formulating the stiffness equations, otherwise, some fictitious strains develop under rigid body motion. It was also suggested that the omission of this nonlinear term can only be justified if Eulerian coordinates are used with relatively small load increments. The snap-through buckling of a truss dome was studied to illustrate the writers' opinion.

The energy search method is another approach to solve the structural analysis problem and was proposed in 1965 by Bogner, Mallett, Minich and Schmit in Ref. 21. In this method, the structural analysis problem is viewed as a mathematical programming problem where the total potential energy of the structure is minimized using optimization techniques to yield the displacement vector which corresponds to the equilibrium position of the structure. The method is applicable to the nonlinear as well as the linear analyses. In the case of geometric nonlinear analysis, a nonlinear strain-displacement relationship is employed and expressed with respect to a moving local (Eulerian) coordinates to base the equilibrium on the deformed configuration. The method was applied to the nonlinear analysis of one and two dimensional elements.

In Ref. 22, a comparison between the analytical solution, proposed in Ref. 21, and some experimental test results to some model skeletal structures was reported. Mallett (Ref. 23) discussed the basis of introducing the mathematical programming techniques into the structural analysis problem. Mallett and Berke (Ref. 24) employed the energy search formulations, as originally reported in Ref. 21, to solve more examples covering both the truss and the frame discrete elements showing reasonable agreement with the solution obtained using other methods.

Bogner (Ref. 25) refined the previous work done (Ref. 21) for pin ended truss element by incorporating the eigenvalue approach to detect the buckling of compression members which enabled following the behaviour of the truss structure in the post-buckling zone. A numerical example was given showing the elastic behaviour of a truss structure where the post-buckling as well as the change in the structural configuration due to the slackening of tension elements were demonstrated. The interpretation of the boundary conditions, as well as the force-deformation relationships, are debatable and are discussed and corrected in the present study.

Recently, Bogner's previous work (Ref. 25) was extended in Ref. 26 to account for the material nonlinearity besides the geometric nonlinearity. The complete load-deflection history of a shallow truss-dome supported by a

net of cables was demonstrated.

More recently, Holzer and Somers published a paper
(Ref. 27) dealing with the analysis of frame structures
using the function minimization technique. The use of a
third degree polynomial, as proposed by Holzer and Somers,
to represent the deflection curve is questionnable in
describing the actual deflection of the beam-column,
especially at large values of the axial load as indicated
in Ref. 17. The equilibrium equations were formulated with
respect to the deformed geometry by employing Eulerian
coordinates in the analysis. Static stability investigations
were restricted to the stable domain of the potential energy
function since the method is not suited to predict the
unstable post-buckling behaviour. Holzer extended the
function minimization to include material nonlinearity as
well as dynamic analysis problems.

1.3 Objectives Of The Present Study

The basic purpose of this study is to develop a
consistent formulation and method for the geometrical non-
linear analysis of planar frame structures. The sources of
the geometric nonlinear behaviour as they pertain to the
present study can be summarized as follows:

1. Large deflections and rotations of the nodes
   comprising the structure which necessitate con-
   sidering the equilibrium in the final deformed
   configuration. Employing an efficient Eulerian

moving local coordinates automatically considers the equilibrium in the deformed state. A logical explanation and interpretation to the concept of moving coordinates is given which makes it possible to extend the application of the moving coordinates to more complicated types of elements.

2. The coupling between the axial and the transverse stiffnesses. The introduction of nonlinear terms into the strain-deformation relationship reflects this coupling. Moreover, the strain due to prestressing is directly incorporated into the strain-deformation relationship to include the prestraining effects.

3. Changes in the structural configuration under certain loading conditions, (tension elements such as cables may go slack and do not contribute to the strain energy of the structure). Fortunately, the flexibility of the employed function minimization technique enables considering such situations with relative ease.

A by-product of the present study is to investigate the effect of adding the nonlinear term $\frac{1}{2}(\frac{du}{dx})^2$, which is usually neglected, to the strain-displacement relationship to show the effect of retaining this term in the formulations.

Chapter II presents the nonlinear formulations used

to calculate the strain energy of planar frame element as
well as the analytic gradient components of the element
strain energy with respect to the element end global
displacements. The concept of the Eulerian coordinates is
explained and the effect of the different nonlinear terms
in the strain-displacement relationship is also demonstrated.
A discussion to Bogner's formulations (Ref. 25), which are
only applicable to the pin ended truss element, is presented
to point out some questionnable interpretations which cause
some inaccuracy in satisfying the equilibrium in the deformed
configuration.

Chapter III explains the logic behind the introduction
of the minimization techniques into the structural analysis
problem to create the energy search method. The Fletcher-
Reeves conjugate gradient method is explained as the algorithm
employed for the function minimization. The concept of
scaling transformation is also discussed as applied in the
present work.

Chapter IV is devoted to the numerical evaluation of
the formulations developed in order to assess the efficiency
and accuracy of the proposed formulations. The numerical
examples were carefully selected to cover the various degrees
of geometric nonlinearity in frame structures.

Chapter V considers the problem of geometric non-
linearity as it pertains to the analysis of tall guyed
transmission towers. An example tower is solved to show

the nonlinear behaviour of these towers and also to predict the instability limit under increasing wind loads.

In Chapter VI, conclusions are drawn to show the efficiency and merit of the proposed formulations and method of analysis. The difficulties encountered during the research are also mentioned as a guide for further studies. Recommendations and projections are finally given for future investigations.

CHAPTER II

GENERAL FORMULATIONS

2.1 General

In the following, the formulations necessary for the nonlinear analysis of the general planar frame element are presented within the framework of the energy search method. Expressions for the element strain energy, as well as its analytic gradient, are obtained since both are required for the implementation of the employed function minimization technique. The displacement functions are also given to describe the geometry of the finite element in the final deformed state.

A nonlinear strain-displacement relationship is employed to reflect the coupling between the transverse and the axial stiffnesses. The prestressing effect is also included in the same relationship. In order to study the effect of retaining the nonlinear term $\frac{1}{2}u_x^2$ in the strain-deformation relationship, the formulations are first presented including this term, then the necessary changes to exclude the effect of the term $\frac{1}{2}u_x^2$ are reported. The use of Eulerian moving local coordinates is introduced to formulate the equilibrium equations in terms of the final deformed geometry.

2.2 Eulerian Local Coordinates (x,y), Fig. 1

The concept of employing moving local coordinates attached to the element is introduced in order to serve

17

the following purposes:

a) Allows formulating the element strain energy with respect to the deformed configuration which insures satisfaction of equilibrium in terms of the deformed position of the structure.

b) Separates the contribution of rigid body movement from strain inducing movement.

c) Justifies the use of the small rotation strain-displacement relationship in the cases of large nodal displacements. This can be illustrated by comparing the rotations with respect to the x, y axes (Fig. 1) with the corresponding rotations with respect to the $\tilde{x}$, $\tilde{y}$ axes. It is clear that however large the nodal rotations are with respect to the $\tilde{x}$, $\tilde{y}$ axes, they remain small with respect to the moving x, y coordinates so that the strain-displacement relationship, which is based on the assumption of small rotations, remains valid. If required, the accuracy can be improved by increasing the number of elements comprising the frame member.

d) Allows retaining less nonlinear terms in the strain-displacement relationship. It was proved in the case of a truss-element that the nonlinear term $\frac{1}{2}(\frac{du}{dx})^2$ has to be retained in the strain-displacement relationship if Lagrangian (undeformed)

coordinates are used in formulating the stiffness equations; otherwise, some fictitious strains will develop under rigid body rotations. If Eulerian coordinates are used, the omission of the non-linear term $\frac{1}{2}(\frac{du}{dx})^2$ is justified.

Figure 1 shows the frame discrete element before and after deformations. The $\bar{X}$, $\bar{Y}$ axes are the reference global coordinates where the displacement $\bar{u}$, $\bar{v}$ are measured along $\bar{X}$ and $\bar{Y}$ respectively. The $\tilde{x}$, $\tilde{y}$ are the local coordinates defining the direction of the element in the undeformed position. The undeformed length of the element, ℓ, is expressible as

$$\ell = [(\bar{X}_p - \bar{X}_q)^2 + (\bar{Y}_p - \bar{Y}_q)^2]^{\frac{1}{2}} \qquad (2.1)$$

where $\bar{X}_p$, $\bar{Y}_p$ define the position of end p while $\bar{X}_q$, $\bar{Y}_q$ define the position of end q with respect to the $\bar{X}$, $\bar{Y}$ axes. Note that x, y are the employed Eulerian coordinates where the displacements u, v are measured along the x and y axes, respectively. θ_p and θ_q represent the slope of the tangent at p and q with respect to the x axis. The displacement u_q defines the movement of end q along the x axis. The distance between the element terminals p and q in the deformed state defines the chord length s which may be expressed as follows

$$s = \left\{[(\bar{X}_p + \bar{u}_p) - (\bar{X}_q + \bar{u}_q)]^2 + [(\bar{Y}_p + \bar{v}_p) - (\bar{Y}_q + \bar{v}_q)]^2\right\}^{\frac{1}{2}}$$

$$(2.2)$$

P_p, V_p and M_p are the end forces at end p while P_q, V_q and M_q represent the end forces at end q.

In light of employing Eulerian moving coordinates, referring to Fig. 1, a discussion of the development of the element strain energy is now in order. Before applying the external loads, the element is straight and oriented in the undeformed state. At that stage, the element potential energy is minimum or zero depending on whether the structure is prestressed or not, respectively. As the external loads are applied, the element undergoes two basic types of deformations classified as rigid body deformations and strain-inducing deformations. During the rigid body motion, the element rotates through an angle θ_r with respect to the $\tilde{x}$ axis. The Eulerian local coordinates move with the element in the deformed position. Positively, no additional strains are induced in the element due to this rigid body motion. Besides the rigid body motion, the element is deformed with respect to the x, y axes to satisfy the geometrical admissibility with the rest of the nodes and elements comprising the physical structure. Three basic degrees of freedom, namely u_q, θ_p and θ_q (Fig. 1), are assigned to the element in order to absorb the potential energy of the end forces via inducing strain energy along the fibers. The other displacements, namely u_p, v_p and v_q, characterize the rigid body motion and are imposed to be zero with respect to the x and y coordinates; therefore the

corresponding end forces P_p, V_p and V_q do not appear in the formulations.

2.3 Strain-Displacement Relationship

The strain in the frame element can be generally expressed as

$$\varepsilon(x,y) = \varepsilon_p + \varepsilon_d \qquad (2.3)$$

where $\varepsilon(x,y)$ is the strain at any point in the element, ε_p is the initial centric prestrain due to prestressing, ε_d is the strain of deformation which is given as (Ref. 32)

$$\varepsilon_d = u_x - yv_{xx} + \frac{1}{2}(v_x^2 + u_x^2) \qquad (2.4)$$

The first and second terms in Eq. 2.4 represent the conventional linear terms giving the strain due to the direct axial and bending deformations, respectively. The introduction of the nonlinear term $\frac{1}{2}v_x^2$, besides accounting for relatively large rotations, reflects the coupling between the transverse and the axial stiffnesses as will be shown when deriving the governing equilibrium equations. It is also well known that the mere presence of this term, without regard to magnitude, has a decisive influence on the behaviour predicted in stability critical situations. The nonlinear term $\frac{1}{2}u_x^2$ is retained to avoid the possibility of fictitious strains associated with the rigid body motion. Meanwhile, it is also intended to investigate the effectiveness of employing Eulerian coordinates in compensating for the omission of the

nonlinear term $\frac{1}{2}u_x^2$ in future studies.

2.4 Frame Element Total Potential Energy

The following general assumptions will be considered in the analysis:

a) Elements are straight and prismatic between nodes in the undeformed state.

b) Stressing the elements does not appreciably change their cross-sectional area.

c) The external loads are applied at the nodes and are assumed to be conservative in that their directions remain unaltered as the structure deforms.

d) The final resulting stresses are within the elastic range and the material is linearly elastic, i.e.,

$$\sigma = E\varepsilon \qquad (2.5)$$

e) The elements are rigidly connected at the joints unless otherwise specified.

The strain energy density of a general prestrained frame element induced due to the application of external loads is defined as (Fig. 2).

$$dU = \int_0^{\varepsilon_p} \sigma \, d\varepsilon + \int_{\varepsilon_p}^{\varepsilon_p + \varepsilon_d} \sigma \, d\varepsilon \qquad (2.6)$$

Under the assumption of ideal linear elastic material behaviour (Eq. 2.5), and upon integrating Eq. 2.6, the

following relationship, results,

$$dU = \frac{E}{2}(\varepsilon_d + \varepsilon_p)^2 \qquad (2.7)$$

or

$$dU = \frac{E}{2}\varepsilon^2 \qquad (2.8)$$

where ε is the total strain in the element defined as

$$\varepsilon = \varepsilon_p + u_x - yv_{xx} + \frac{1}{2}(v_x^2 + u_x^2) \qquad (2.9)$$

Integrating Eq. 2.8 over the volume V results in the strain energy stored in the element:

$$U_s = \frac{E}{2} \int_V \varepsilon^2 \, dV \qquad (2.10)$$

Integrating Eq. 2.10 over the cross-section and by substituting Eq. 2.9 into Eq. 2.10 results in the nonlinear integral form of the prestrained frame element strain energy

$$U_s = \frac{EA}{2} \int_0^s \left\{ [\varepsilon_p + u_x + \frac{1}{2}(v_x^2 + u_x^2)]^2 + \frac{I}{A} v_{xx}^2 \right\} dx$$

$$(2.11)$$

In light of the interpretation of the development of the element strain energy discussed in Section 2.2, the work done by the element end forces is expressible as

$$W_s = P_q u_q + M_p \theta_p + M_q \theta_q \qquad (2.12)$$

under the assumption of small rotation with respect to the x axis, θ_p and θ_q may be replaced by v_{x_p} and v_{x_q}, respectively; therefore, Eq. 2.12 reads

$$W_s = P_q u_q + M_p v_{x_p} + M_q v_{x_q} \qquad (2.13)$$

The total potential energy of a structural element is simply the strain energy of the element minus the potential of the loads acting on the element:

$$\pi_p = U_s - \bar{W}_s \qquad (2.14)$$

Therefore, Eqns. 2.11 and 2.13 give the integral form of the frame element potential energy as expressed with respect to the moving x, y axes, which can be written as

$$\pi_p = \left[\left(\frac{EA}{2} \int_0^s \left\{ [\epsilon_p + u_x + \tfrac{1}{2}(v_x^2 + u_x^2)]^2 + \frac{I}{A} v_{xx}^2 \right\} dx \right) - \left\{ P_q u_q + M_p v_{x_p} + M_q v_{x_q} \right\} \right] \qquad (2.15)$$

The variational derivation of the governing differential equations as well as the boundary conditions are presented in Appendix A and the interpretation of the boundary conditions is discussed in a subsequent section.

2.5 Field Equations and Boundary Conditions

The following set of field equations and boundary conditions are obtained after performing the variational process on the total potential energy integral expression shown in Eq. 2.15.

Field Equations

$$\frac{d}{dx} \left\{ [\epsilon_p + u_x + \tfrac{1}{2}(v_x^2 + u_x^2)] + u_x[\epsilon_p + u_x + \tfrac{1}{2}(v_x^2 + u_x^2)] \right\} = 0$$

$$(2.16)$$

$$\frac{I}{A} v_{xxxx} - \frac{d}{dx}[\varepsilon_p + u_x + \frac{1}{2}(v_x^2 + u_x^2)]v_x = 0 \qquad (2.17)$$

Boundary Conditions Equations

$$\left\{ AE\left([\varepsilon_p + u_{x_q} + \frac{1}{2}(v_{x_q}^2 + u_{x_q}^2)] + u_{x_q}[\varepsilon_p + u_{x_q} + \frac{1}{2}(v_{x_q}^2 + u_{x_q}^2)] \right) \right.$$
$$\left. - P_q \right\} \delta u_q = 0 \qquad (2.18.a)$$

$$\left\{ -AE\left([\varepsilon_p + u_{x_p} + \frac{1}{2}(v_{x_p}^2 + u_{x_p}^2)] + u_{x_p}[\varepsilon_p + u_{x_p} + \frac{1}{2}(v_{x_p}^2 + u_{x_p}^2)] \right) \right.$$
$$\left. \right\} \delta u_p = 0 \qquad (2.18.b)$$

$$\left\{ -AE\left(\frac{I}{A} v_{xxx_q} - v_{x_q}[\varepsilon_p + u_{x_q} + \frac{1}{2}(v_{x_q}^2 + u_{x_q}^2)] \right) \right\} \delta v_q = 0 \qquad (2.18.c)$$

$$\left\{ AE\left(\frac{I}{A} v_{xxx_p} - v_{x_p}[\varepsilon_p + u_{x_p} + \frac{1}{2}(v_{x_p}^2 + u_{x_p}^2)] \right) \right\} \delta v_p \qquad (2.18.d)$$

$$\left\{ EIv_{xx_q} - M_q \right\} \delta v_{x_q} = 0 \qquad (2.18.e)$$

$$\left\{ EIv_{xx_p} + M_p \right\} \delta v_{x_p} = 0 \qquad (2.18.f)$$

Equations 2.16 through 2.18 were obtained with the nonlinear term $\frac{1}{2}u_x^2$ retained in the strain-deformation relationship (Eq. 2.9). A similar set of equations is obtained when the term $\frac{1}{2}u_x^2$ is omitted from the strain-deformation equation as follows:

Field Equations

$$\frac{d}{dx}(\varepsilon_p + u_x + \frac{1}{2}v_x^2) = 0 \qquad (2.19)$$

$$\frac{I}{A} v_{xxxx} - \frac{d}{dx}(\varepsilon_p + u_x + \frac{1}{2}v_x^2)v_x = 0 \qquad (2.20)$$

Boundary Conditions Equations

$$\left\{ AE(\varepsilon_p + u_{x_q} + \frac{1}{2}v_{x_q}^2) - P_q \right\} \delta u_q = 0 \qquad (2.21.a)$$

$$\left\{ -AE(\varepsilon_p + u_{x_p} + \frac{1}{2}v_{x_p}^2) \right\} \delta u_p = 0 \qquad (2.21.b)$$

$$\left\{ -AE[\frac{I}{A} v_{xxx_q} - v_{x_q}(\varepsilon_p + u_{x_q} + \frac{1}{2}v_{x_q}^2)] \right\} \delta v_q = 0 \qquad (2.21.c)$$

$$\left\{ AE[\frac{I}{A} v_{xxx_p} - v_{x_p}(\varepsilon_p + u_{x_p} + \frac{1}{2}v_{x_p}^2)] \right\} \delta v_p = 0 \qquad (2.21.d)$$

$$\left\{ EIv_{xx_q} - M_q \right\} \delta v_{x_q} = 0 \qquad (2.21.e)$$

$$-\left\{ EIv_{xx_p} + M_p \right\} \delta v_{x_p} = 0 \qquad (2.21.f)$$

Equation 2.16 describes the governing differential equation in the x direction which may be rewritten as

$$\frac{d}{dx} \left\{ (1 + u_x)[\varepsilon_p + u_x + \frac{1}{2}(v_x^2 + u_x^2)] \right\} = 0 \qquad (2.22)$$

In order to simplify the solution of the governing differential equations (Eqns. 2.16 and 2.17), the assumption that the direct axial strain u_x is negligible compared to unity is applied. Therefore, Eqn. 2.22 reduces to

$$\frac{d}{dx}[\varepsilon_p + u_x + \frac{1}{2}(v_x^2 + u_x^2)] = 0 \qquad (2.23)$$

which is the final form of the governing differential equation in the longitudinal x direction in case of retaining

the nonlinear term $\frac{1}{2}u_x^2$ in the strain-displacement relation-
ship. Equation 2.19 gives the governing differential
equation in the x direction when the term $\frac{1}{2}u_x^2$ is omitted;
the assumption that u_x is negligible compared to unity
needs not be applied in this case.

Equation 2.17 shows the governing differential
equation in the y direction when the term $\frac{1}{2}u_x^2$ is retained
in the strain-deformation relationship. Incorporating
Eqn. 2.23 into Eqn. 2.17, the final form of the governing
differential equation in the y direction is obtained as.

$$\frac{I}{A} v_{xxxx} - [\epsilon_p + u_x + \frac{1}{2}(v_x^2 + u_x^2)]v_{xx} = 0 \qquad (2.24)$$

In case of omitting the term $\frac{1}{2}u_x^2$, Eqn. 2.24 reads

$$\frac{I}{A} v_{xxxx} - (\epsilon_p + u_x + \frac{1}{2}v_x^2)v_{xx} = 0 \qquad (2.25)$$

From Figure 1, the following imposed boundary condi-
tions apply

$$u_p = 0 \qquad\qquad (2.26.a)$$

$$v_p = 0 \qquad\qquad (2.26.b)$$

$$v_q = 0 \qquad\qquad (2.26.c)$$

Therefore

$$\delta u_p = 0 \qquad\qquad (2.27.a)$$

$$\delta v_p = 0 \qquad\qquad (2.27.b)$$

$$\delta v_q = 0 \qquad\qquad (2.27.c)$$

On the other hand, u_q, v_{x_p} and v_{x_q} are not prescribed a priori and can take any arbitrary values; therefore, the following set of natural boundary conditions applies:

$$u_q = s - \ell \qquad (2.28.a)$$

$$v_{x_p} = \theta p \qquad (2.28.b)$$

$$v_{x_q} = \theta q \qquad (2.28.c)$$

u_q, v_{x_p} and v_{x_q} need not be zero which automatically implies that the expressions between the braces { } in Eqns. 2.18.a, 2.18.e, 2.18.f and also in Eqns. 2.21.a, 2.21.e, 2.21.f have to be equal to zero.

At this point, the writer would like to draw attention to the questionnable interpretation of the boundary condition (Eqn. 2.28.a) given by Bogner in Ref. 25. Bogner, who limited the formulations to the analysis of pin ended truss-type structures, classified the boundary condition given in Eq. 2.28.a as an imposed boundary condition. It is the writer's opinion that there is no justification to classify Eqn. 2.28.a as an imposed boundary condition, since it was always found that when the structure's total potential energy is minimum, the expression between the braces { } in Eqns. 2.18.a or 2.21.a is equal to zero in the limit when the direction of the tangent at q coincides with the direction of the chord defined by the x axis. Meanwhile, the variable s, defining the chord

length, which appears on the right-hand side of Eqn. 2.28.a
is a function of the unknown displacements at the end of
the element. Therefore, the value of s may not be prescribed
a priori and imposed on the element. As will be seen later
the misleading interpretation of that boundary condition
(Eqn. 2.28.a) affects the force-deformation relationship
in the axial direction.

2.6 Axial-Bending Coupling Constant (k^2)

Integrating Eqn. 2.23 with respect to x results in

$$\varepsilon_p + u_x + \frac{1}{2}(v_x^2 + u_x^2) = \text{constant} \qquad (2.29)$$

Multiplying both sides by $\frac{A}{I}$ results in the axial-bending
coupling constant, k^2, defined as

$$k^2 = \frac{A}{I}[\varepsilon_p + u_x + \frac{1}{2}(v_x^2 + u_x^2)] \qquad (2.30)$$

In case of omitting the nonlinear term $\frac{1}{2}u_x^2$ from the strain-
deformation relationship, the constant k^2 takes the form

$$k^2 = \frac{A}{I}(\varepsilon_p + u_x + \frac{1}{2}v_x^2) \qquad (2.31)$$

At this stage the formulations are split into three divisions
according to the value of the constant k^2 being negative,
zero or positive, respectively.

2.6.1 Compression-Bending Coupling ($k^2 < 0$)

In this case, the numerical value of k^2, as defined
in Eq. 2.30 or Eq. 2.31 is negative which implies compressive
strains along the deformed controidal axis of the element.
Substituting Eqn. 2.30 into Eqn. 2.24, the governing

differential equation in the transverse direction is

$$v_{xxxx} - k^2 v_{xx} = 0 \qquad (2.32)$$

Defining

$$k_1^2 = -k^2 \qquad (2.33)$$

Equation 2.32 reads

$$v_{xxxx} + k_1^2 v_{xx} = 0 \qquad (2.34)$$

The solution to Eqn. 2.34 takes the form

$$v(x) = A_1 \sin k_1 x + B_1 \cos k_1 x + C_1 x + D_1 \qquad (2.35)$$

The constants of integration A_1, B_1, C_1 and D_1 are determined from the following imposed and natural boundary conditions.

at x = 0

$$v = 0 \qquad (2.36.a)$$

$$v_x = \theta_p \qquad (2.36.b)$$

at x = s

$$v = 0 \qquad (2.36.c)$$

$$v_x = \theta_q \qquad (2.36.d)$$

The expressions for the four integration constants are listed below.

$$A_1 = \frac{\theta_p(1 - k_1 s \sin k_1 s - \cos k_1 s) + \theta_q(\cos k_1 s - 1)}{k_1(2 - 2\cos k_1 s - k_1 s \sin k_1 s)} \qquad (2.37.a)$$

$$B_1 = \frac{\theta_p(\sin k_1 s - k_1 s \cos k_1 s) + \theta_q(k_1 s - \sin k_1 s)}{k_1(2 - 2\cos k_1 s - k_1 s \sin k_1 s)} \qquad (2.37.b)$$

$$C_1 = \frac{\theta_p(1 - \cos k_1 s) + \theta_q(1 - \cos k_1 s)}{(2 - 2\cos k_1 s - k_1 s \sin k_1 s)} \qquad (2.37.c)$$

$$D_1 = \frac{\theta_p(k_1 s \cos k_1 s - \sin k_1 s) + \theta_q(\sin k_1 s - k_1 s)}{k_1(2 - 2\cos k_1 s - k_1 s \sin k_1 s)} \qquad (2.37.d)$$

A linear displacement function is assumed for the displacement in the axial direction as follows

$$u(x) = \frac{s-\ell}{s} x \qquad (2.38)$$

The constant k_1 is calculated from the following relationship

$$\frac{-I\, k_1^2}{A} = \begin{Bmatrix} u_q \\ \theta_p \\ \theta_q \end{Bmatrix}^T \begin{bmatrix} D_{11} & 0 & 0 \\ 0 & D_{22} & D_{23} \\ 0 & D_{32} & D_{33} \end{bmatrix} \begin{Bmatrix} u_q \\ \theta_p \\ \theta_q \end{Bmatrix} \qquad (2.39)$$

where

$$D_{11} = \frac{1}{u_q^2} \left\{ \frac{s-\ell}{s} + \varepsilon_p + \frac{1}{2}\left(\frac{s-\ell}{s}\right)^2 \right\} \qquad (2.40.a)$$

$$D_{22} = \left\{ (k_1 s)^3 + (k_1 s)^2 (-\sin k_1 s \cos k_1 s - 2\sin k_1 s) + \right.$$

$$(k_1 s)(-4\cos^2 k_1 s + 2\cos k_1 s + 2) +$$

$$\left. (2\sin k_1 s \cos k_1 s - 2\sin k_1 s) \right\} \Big/$$

$$\left\{ 4k_1 s(2 - 2\cos k_1 s - k_1 s \sin k_1 s)^2 \right\} \qquad (2.40.b)$$

$$D_{23} = \left\{ (k_1 s)^3 (-\cos k_1 s) + (k_1 s)^2 (3\sin k_1 s) + \right.$$

$$(k_1 s)(-6 + 6\cos k_1 s) + (2\sin k_1 s - 2\sin k_1 s \cos k_1 s) \right\} \Big/$$

$$\left\{ 4k_1 s(2 - 2\cos k_1 s - k_1 s \sin k_1 s)^2 \right\} \qquad (2.40.c)$$

also $D_{32} = D_{23}$

and $D_{33} = D_{22}$

due to the symmetry of the problem with respect to the end

rotations θ_p and θ_q.

In case of omitting the nonlinear term $\frac{1}{2}u_x^2$, the

term D_{11}, only, will be changed and reads

$$D_{11} = \frac{1}{u_q^2}\left\{ \frac{s-\ell}{s} + \varepsilon_p \right\} \tag{2.41}$$

When the term $\frac{1}{2}u_x^2$ is omitted, the constant k_1^2 may be found

by obtaining the exact displacement function in the axial

direction and satisfying the axial end conditions as follows:

Substituting Eq. 2.33 into Eq. 2.31 results in

$$k_1^2 = \frac{-A}{I} (\varepsilon_p + u_x + \frac{1}{2}v_x^2) \tag{2.42.a}$$

rearranging terms

$$u_x = \frac{-I}{A} k_1^2 - \varepsilon_p - \frac{1}{2}v_x^2 \tag{2.42.b}$$

integrating both sides with respect to x results in

$$u(x) = \frac{-I}{A} k_1^2 x - \varepsilon_p x - \int \frac{1}{2}v_x^2 dx + R$$

where R is the integration constant. The value of the inte-

gral $\int \frac{1}{2}v_x^2 dx$ is obtained from Eq 2.35. The two constants

k_1^2 and R are determined from the two boundary conditions

shown in Eqns. 2.26.a and 2.28.a. The resulting expression

for k_1^2 is identical to the expression shown in Eq. 2.39 with

D_{11} shown in Eq. 2.41 and $D_{22} = D_{33}$ and $D_{23} = D_{32}$ given in Eqns. 2.40.b and 2.40.c, respectively.

Notice that the parameter k_1 appears on both sides of Eq. 2.39 and it is virtually impossible to separate it on one side of the equation. Therefore, an iterative procedure is employed to find the value of the parameter k_1. The starting value for the iteration is based on assuming a cubed polynomial for the transverse displacement instead of the trigonometric displacement function (Eq. 2.35). More details about finding the compression-bending coupling parameter k_1 are given in Appendix B.

Substituting Eq. 2.30 (or Eq. 2.31 in case of omitting the term $\frac{1}{2}u_x^2$) into Eq. 2.11, the element strain energy can be rewritten as

$$U_s = \frac{EA}{2} \int_0^s (\frac{k_1^4 \, I^2}{A^2} + \frac{I}{A} v_{xx}^2) \, dx \qquad (2.43)$$

The expressions for $v(x)$ as well as k_1^2 have already been defined in Eqns. 2.35 and 2.39, respectively. Therefore, the element strain energy, as calculated with respect to the Eulerian coordinates x and y, is

$$U_s = \frac{1}{2} \begin{Bmatrix} u_q \\ \theta_p \\ \theta_q \end{Bmatrix}^T \begin{bmatrix} k_{11} & 0 & 0 \\ 0 & k_{22} & k_{23} \\ 0 & k_{32} & k_{33} \end{bmatrix} \begin{Bmatrix} u_q \\ \theta_p \\ \theta_q \end{Bmatrix} \qquad (2.44)$$

where

$$k_{11} = \frac{E \; s \; k_1^4 \; I^2}{A \; u_q^2} \tag{2.45.a}$$

$$k_{22} = EI \; k_1 \; \{(k_1s)^3 + (k_1s)^2(-2\sin k_1s + \sin k_1s \cos k_1s) + (k_1s)$$

$$(-2\cos k_1s + 2\cos^2 k_1s) + (-2\sin k_1s \cos k_1s + 2\sin k_1s)\}$$

$$\Big/ 2(2 - 2\cos k_1s - k_1s \sin k_1s)^2 \tag{2.45.b}$$

$$k_{23} = EI \; k_1 \; \{(k_1s)^3(-\cos k_1s) + (k_1s)^2(\sin k_1s) +$$

$$(k_1s)(2\cos k_1s - 2\cos^2 k_1s) + (-2\sin k_1s + 2\sin k_1s \cos k_1s)\}$$

$$\Big/ 2(2 - 2\cos k_1s - k_1s \sin k_1s)^2 \tag{2.45.c}$$

Again $k_{33} = k_{22}$

$\qquad k_{32} = k_{23}$

which shows the inherent symmetry of the problem with respect to the end rotations.

2.6.2 Case Of No Axial Force ($k^2=0$)

In this case the numerical evaluation of the constant k^2 yields a zero (or a negligible) quantity which implies zero (or very small) strains along the deformed central axis of the element, respectively.

The governing differential equation (Eq. 2.32) reduces to the form

$$v_{xxxx} = 0 \qquad (2.46)$$

The solution to Eq. 2.46 is

$$v(x) = A_2 x^3 + B_2 x^2 + C_2 x + D_2 \qquad (2.47)$$

The constants A_2, B_2, C_2 and D_2 can be determined from the same boundary conditions given in Eqns. 2.36.a through 2.36.d and the resulting constants are

$$A_2 = \frac{\theta_p + \theta_q}{s^2} \qquad (2.48.a)$$

$$B_2 = -\frac{2\theta_p + \theta_q}{s} \qquad (2.48.b)$$

$$C_2 = \theta_p \qquad (2.48.c)$$

$$D_2 = 0 \qquad (2.48.d)$$

The integral form of the strain energy (Eq. 2.43) reduces to

$$U_s = \frac{EA}{2} \int_0^s \frac{I}{A} v_{xx}^2 dx \qquad (2.49)$$

and the expression of the element strain energy is

$$U_s = \frac{1}{2} \begin{Bmatrix} u_q \\ \theta_p \\ \theta_q \end{Bmatrix}^T \begin{bmatrix} k_{11} & 0 & 0 \\ 0 & k_{22} & k_{23} \\ 0 & k_{32} & k_{33} \end{bmatrix} \begin{Bmatrix} u_q \\ \theta_p \\ \theta_q \end{Bmatrix} \qquad (2.50)$$

where

$$k_{11} = 0 \qquad (2.51.a)$$

$$k_{22} = \frac{4EI}{s} \qquad (2.51.b)$$

$$k_{23} = \frac{2EI}{s} \qquad (2.51.c)$$

Also

$$k_{33} = k_{22}$$

$$k_{32} = k_{23}$$

2.6.3 Bending-Tension Coupling ($k^2 > 0$)

In this case the numerical value of the constant k^2 is positive, meaning tensile strains exist along the deformed centroidal axis of the element.

The governing differential equation is shown in Eq. 2.32. The solution of this governing differential equation is

$$v(x) = A_3 \sinh kx + B_3 \cosh kx + C_3 x + D_3 \qquad (2.52)$$

The constants of integration are determined from the four boundary conditions shown in Eqns. 2.36.a through 2.36.d and are defined below

$$A_3 = \frac{\theta_p(\cosh ks - ks \sinh ks - 1) + \theta_q(1 - \cosh ks)}{k(2\cosh ks - 2 - ks \sinh ks)} \qquad (2.53.a)$$

$$B_3 = \frac{\theta_p(ks \cosh ks - \sinh ks) + \theta_q(\sinh ks - ks)}{k(2\cosh ks - 2 - ks \sinh ks)} \qquad (2.53.b)$$

$$C_3 = \frac{\theta_p(\cosh ks - 1) + \theta_q(\cosh ks - 1)}{(2\cosh ks - 2 - ks \sinh ks)} \qquad (2.53.c)$$

$$D_3 = \frac{\theta_p(\sinh ks - ks \cosh ks) + \theta_q(ks - \sinh ks)}{k(2\cosh ks - 2 - ks \sinh ks)} \qquad (2.53.d)$$

The constant k is evaluated using the same procedure previously employed in the case of compression-bending coupling and its numerical value is obtained from the following relationship,

$$\frac{I\,k^2}{A} = \begin{Bmatrix} u_q \\ \theta_p \\ \theta_q \end{Bmatrix}^T \begin{bmatrix} D_{11} & 0 & 0 \\ 0 & D_{22} & D_{23} \\ 0 & D_{32} & D_{33} \end{bmatrix} \begin{Bmatrix} u_q \\ \theta_p \\ \theta_q \end{Bmatrix} \qquad (2.54)$$

where

$$D_{11} = \frac{1}{u_q^2}\left\{\frac{s-\ell}{s} + \varepsilon_p + \frac{1}{2}\left(\frac{s-\ell}{s}\right)^2\right\} \qquad (2.55.a)$$

$$D_{22} = \left\{(ks)^3(-1) + (ks)^2(\sinh ks \cosh ks + 2 \sinh ks) + \right.$$
$$(ks)(-4\cosh^2 ks + 2\cosh ks + 2) +$$
$$\left.(2\sinh ks \cosh ks - 2 \sinh ks)\right\} \Big/$$
$$\left\{4ks(-2 + 2\cosh ks - ks \sinh ks)^2\right\} \qquad (2.55.b)$$

$$D_{23} = \left\{(ks)^3(\cosh ks) + (ks)^2(-3\sinh ks) + \right.$$
$$(ks)(-6 + 6\cosh ks) +$$
$$\left.(2\sinh ks - 2\sinh ks \cosh ks)\right\} \Big/$$
$$\left\{4ks(-2 + 2\cosh ks - ks \sinh ks)^2\right\} \qquad (2.55.c)$$

Also $D_{32} = D_{23}$

$\quad D_{33} = D_{22}$

In case of omitting the term $\frac{1}{2}u_x^2$ from the strain-deformation relationship, the expression of D_{11} reads

$$D_{11} = \frac{1}{u_q^2}\left\{\frac{s-\ell}{s} + \varepsilon_p\right\} \tag{2.56}$$

Notice that the parameter k has to be obtained via employing an iterative procedure, as was done in determining k_1, since it appears on both sides of Eq. 2.54. The starting value for the iteration as well as the iterative scheme employed are shown in Appendix B.

The strain energy in that case is

$$U_s = \frac{1}{2}\begin{Bmatrix} u_q \\ \theta_p \\ \theta_q \end{Bmatrix}^T \begin{bmatrix} k_{11} & 0 & 0 \\ 0 & k_{22} & k_{23} \\ 0 & k_{32} & k_{33} \end{bmatrix} \begin{Bmatrix} u_q \\ \theta_p \\ \theta_q \end{Bmatrix} \tag{2.57}$$

where

$$k_{11} = \frac{ES\ k^4\ I^2}{A\ u_q^2} \tag{2.58.a}$$

$$k_{22} = EIk\left\{(ks)^3 + (ks)^2(-2\sinh ks + \sinh ks \cosh ks) + \right.$$

$$(ks)(2\cosh ks - 2\cosh^2 ks) + (2\sinh ks \cosh ks - 2\sinh ks)\left.\right\}$$

$$\Big/ 2(-2 + 2\cosh ks - ks \sinh ks)^2 \tag{2.58.b}$$

$$k_{23} = EIk\left\{(ks)^3(-\cosh ks) + (ks)^2(\sinh ks) + \right.$$

$$(ks)(-2\cosh ks + 2\cosh^2 ks) +$$

$$\left.(2\sinh ks - 2\sinh ks \cosh ks)\right\}$$

$$\left/ 2(-2 + 2\cosh ks - ks \sinh ks)^2 \right. \qquad (2.58.c)$$

Also $k_{33} = k_{22}$

$$k_{32} = k_{23}$$

2.7 Analytic Gradient Components

The analytic gradient components of the element strain energy with respect to the element end global displacements $\bar{u}_p$, $\bar{v}_p$, $\bar{\lambda}_p$, $\bar{u}_q$, $\bar{v}_q$ and $\bar{\lambda}_q$, are required to formulate the gradient vector of the total potential energy function of the structure. This will be accomplished in three steps as follows.

2.7.1 Gradient Vector Defined in the Eulerian (x,y) Coordinates

The vector $\{G_e\}$ defines the analytic gradient components of the element strain energy with respect to the displacements u_q, θ_p and θ_q.

$$\{G_e\} = \begin{Bmatrix} \dfrac{\partial U_s}{\partial u_q} \\[2ex] \dfrac{\partial U_s}{\partial \theta_p} \\[2ex] \dfrac{\partial U_s}{\partial \theta_q} \end{Bmatrix} \qquad (2.59)$$

While the strain energy would ideally be expressed as a function of u_q, θ_p and θ_q only, the particular expressions of the strain energy derived herein, Eqns. 2.44 and 2.57, involve k_1 or k, respectively, as a fourth variable subject, however, to a constraint, Eqns. 2.39 and 2.54, respectively. However, the vector $\{G_e\}$ can be obtained as follows

a) <u>for $k^2 < 0$</u>

$$\{G_e\} = \begin{Bmatrix} \dfrac{\partial U_s}{\partial u_q} + \dfrac{\partial U_s}{\partial k_1}\dfrac{\partial k_1}{\partial u_q} \\[2ex] \dfrac{\partial U_s}{\partial \theta_p} + \dfrac{\partial U_s}{\partial k_1}\dfrac{\partial k_1}{\partial \theta_p} \\[2ex] \dfrac{\partial U_s}{\partial \theta_q} + \dfrac{\partial U_s}{\partial k_1}\dfrac{\partial k_1}{\partial \theta_q} \end{Bmatrix} \qquad (2.60)$$

where the partial derivatives on the right hand side are obtained from Eqns. 2.44 and 2.39.

b) <u>for $k^2 = 0$</u>

In this case, the vector $\{G_e\}$ is directly obtained as shown in Eq. 2.59 where the partial derivatives on the

right hand side in Eq. 2.59 are evaluated from the strain

energy expression, Eq. 2.50.

c) <u>for k²>0</u>

$$\{G_e\} = \begin{Bmatrix} \dfrac{\partial U_s}{\partial u_q} & + & \dfrac{\partial U_s}{\partial k}\dfrac{\partial k}{\partial u_q} \\[3mm] \dfrac{\partial U_s}{\partial \theta_p} & + & \dfrac{\partial U_s}{\partial k}\dfrac{\partial k}{\partial \theta_p} \\[3mm] \dfrac{\partial U_s}{\partial \theta_q} & + & \dfrac{\partial U_s}{\partial k}\dfrac{\partial k}{\partial \theta_q} \end{Bmatrix} \qquad (2.61)$$

The partial derivatives on the right hand side are

evaluated from Eqns. 2.54 and 2.57.

2.7.2 Gradient Vector Defined in the Local $\tilde{x},\tilde{y}$ Coordinates

The gradient vector $\{G_e\}$ of the element strain energy

with respect to the six displacement components $\tilde{u}_p,\, \tilde{v}_p,\, \tilde{\lambda}_p,$

$\tilde{u}_q,\, \tilde{v}_q$ and $\tilde{\lambda}_q$ is obtained by transforming the gradient

vector $\{G_e\}$ from the x,y Eulerian coordinates to the local

Lagrangian coordinates $\tilde{x},\tilde{y}$ using the following relationships,

Fig. 1.

$$u_q = s - \ell \qquad (2.62)$$

$$\theta_p = \tilde{\lambda}_p - \theta_r \qquad (2.63)$$

$$\theta_q = \tilde{\lambda}_q - \theta_r \qquad (2.64)$$

Notice that both of the chord length s and the rigid body

rotation θ_r are, in turn, nonlinear functions of the four

displacements $\tilde{u}_p$, $\tilde{v}_p$, $\tilde{u}_q$ and $\tilde{v}_q$ according to the following relationships,

$$s = \left\{ (\ell + \tilde{u}_q - \tilde{u}_p)^2 + (\tilde{v}_q - \tilde{v}_p)^2 \right\}^{\frac{1}{2}} \qquad (2.65)$$

$$\theta_r = \sin^{-1} \frac{\tilde{v}_q - \tilde{v}_p}{s} \qquad (2.66)$$

The gradient vector $\{\tilde{G}_e\}$ of the element strain energy can be obtained via the following multiplication operation

$$\left\{ \tilde{G}_e \right\}_{6 \times 1} = \left[\; \tilde{T} \; \right]_{6 \times 3} \left\{ G_e \right\}_{3 \times 1} \qquad (2.67)$$

where $\{G_e\}$ is defined in Eq. 2.59.

$$\left\{ \tilde{G}_e \right\}^T = \left(\frac{\partial U_s}{\partial \tilde{u}_p}, \; \frac{\partial U_s}{\partial \tilde{v}_p}, \; \frac{\partial U_s}{\partial \tilde{\lambda}_p}, \; \frac{\partial U_s}{\partial \tilde{u}_q}, \; \frac{\partial U_s}{\partial \tilde{v}_q}, \; \frac{\partial U_s}{\partial \tilde{\lambda}_q} \right)$$

The nonlinear transformation matrix $[T]$ is given as

$$
\begin{bmatrix} \tilde{T} \end{bmatrix}_{6\times3} = \begin{bmatrix}
\dfrac{\partial u_q}{\partial \tilde{u}_p} & \dfrac{\partial \theta_p}{\partial \tilde{u}_p} & \dfrac{\partial \theta_q}{\partial \tilde{u}_p} \\[2ex]
\dfrac{\partial u_q}{\partial \tilde{v}_p} & \dfrac{\partial \theta_p}{\partial \tilde{v}_p} & \dfrac{\partial \theta_q}{\partial \tilde{v}_p} \\[2ex]
\dfrac{\partial u_q}{\partial \tilde{\lambda}_p} & \dfrac{\partial \theta_p}{\partial \tilde{\lambda}_p} & \dfrac{\partial \theta_q}{\partial \tilde{\lambda}_p} \\[2ex]
\dfrac{\partial u_q}{\partial \tilde{u}_q} & \dfrac{\partial \theta_p}{\partial \tilde{u}_q} & \dfrac{\partial \theta_q}{\partial \tilde{u}_q} \\[2ex]
\dfrac{\partial u_q}{\partial \tilde{v}_q} & \dfrac{\partial \theta_p}{\partial \tilde{v}_q} & \dfrac{\partial \theta_q}{\partial \tilde{v}_q} \\[2ex]
\dfrac{\partial u_q}{\partial \tilde{\lambda}_q} & \dfrac{\partial \theta_p}{\partial \tilde{\lambda}_q} & \dfrac{\partial \theta_q}{\partial \tilde{\lambda}_q}
\end{bmatrix}
\qquad (2.68)
$$

The elements of the $[\tilde{T}]$ matrix are given, explicitly, in Appendix C.

2.7.3 Gradient Vector Defined in the Global $\bar{X}, \bar{Y}$ Coordinates

Finally, the $\{\tilde{G}_e\}$ vector, given in Eq. 2.67 is transformed from the local $\tilde{x}, \tilde{y}$ coordinates to the global $\bar{X}, \bar{Y}$ coordinates via the linear transformation matrix as shown in the following relationship.

$$
\left\{ \bar{G}_e \right\}_{6\times1} = \begin{bmatrix} \bar{T} \end{bmatrix}_{6\times6} \left\{ \tilde{G}_e \right\}_{6\times1}
\qquad (2.69)
$$

where $\{\tilde{G}_e\}$ is defined in Eq. 2.67,

$$\{\bar{G}_e\}^T = \left(\frac{\partial U_s}{\partial \bar{u}_p}, \; \frac{\partial U_s}{\partial \bar{v}_p}, \; \frac{\partial U_s}{\partial \bar{\lambda}p}, \; \frac{\partial U_s}{\partial \bar{u}_q}, \; \frac{\partial U_s}{\partial \bar{v}_q}, \; \frac{\partial U_s}{\partial \bar{\lambda}q} \right)$$

represents the analytic gradient components of the element strain energy with respect to the six global displacements $\bar{u}_p$, $\bar{v}_p$, $\bar{\lambda}_p$, $\bar{u}_q$, $\bar{v}_q$, and $\bar{\lambda}_q$. $[\bar{T}]$ is the linear transformation matrix. The elements of this matrix are the direction cosines of the undeformed frame member with respect to the global $\bar{X}, \bar{Y}$ axes. The $[\bar{T}]$ matrix is given in Appendix C.

2.8 Force-Deformation Relationships

The total potential energy of the frame element is basically expressible as

$$\pi_p = U_s - W_s$$

where U_s is the strain energy expression and is given in either of Eqns. 2.44, 2.50 or 2.57 depending on the value of the constant k^2 being negative, zero or positive, respectively. W_s is the work done by the developed end force defined with respect to the (x,y) Eulerian coordinates. W_s is explicitly given in Eq. 2.12.

Applying the principle of stationary potential energy to the discrete element, the following relationships result:

$$\frac{\partial \pi_p}{\partial u_q} = \frac{\partial U_s}{\partial u_q} - P_q = 0 \qquad (2.70.a)$$

$$\frac{\partial \pi_p}{\partial \theta_p} = \frac{\partial U_s}{\partial \theta_p} - M_p = 0 \qquad (2.70.b)$$

$$\frac{\partial \pi_p}{\partial \theta_q} = \frac{\partial U_s}{\partial \theta_q} - M_q = 0 \qquad (2.70.c)$$

which implies that

$$P_q = \frac{\partial U_s}{\partial u_q} \qquad (2.71.a)$$

$$M_p = \frac{\partial U_s}{\partial \theta_p} \qquad (2.71.b)$$

$$M_q = \frac{\partial U_s}{\partial \theta_q} \qquad (2.71.c)$$

Alternatively, the value of M_p and M_q can also be obtained via Eqns. 2.18.e, 2.18.f as

$$M_p = -EIv_{xx_p} \qquad (2.72.a)$$

$$M_q = EIv_{xx_q} \qquad (2.72.b)$$

which yield the same values obtained for the M_p and M_q expressions shown in Eqns. 2.71.b and 2.71.c. It should be noticed that the agreement between the value of the force components M_p, M_q as obtained using either of the expressions given in Eqns. 2.71.b and 2.72.a and Eqns. 2.71.c and 2.72.b, respectively, is expected since the procedure is basically the same. In Eqns. 2.72.a and 2.72.b, the variational principle was applied to the integral form of the element potential energy function.

Meanwhile, the expressions shown in Eqns. 2.71.b and 2.71.c were obtained by minimizing the element potential energy expression form (Eqns. 2.44, 2.50 or 2.57). Equation 2.71.a gives the axial force along the chord line defined by the x axis (Fig. 1). If the natural boundary conditions shown in Eq. 2.18.a (or Eq. 2.21.a) are employed to obtain the value of P_q, the resulting force represents the component of axial force as given by Eq. 2.71.a along the tangent at q. In the limit, when the number of elements comprising the frame member is increased, the value of P_q obtained from either Eq. 2.71.a or Eq. 2.18.a (or Eq. 2.21.a) will be the same. For small deflection problems, the difference between P_q as obtained from Eq. 2.71.a or Eq. 2.18.a (or Eq. 2.21.a) is negligible.

Bogner in Ref. 25 gives a force-deformation relationship which is questionnable as to whether static equilibrium in the deformed configuration in the cases of large deflection problems of trusses can be satisfied. The suggested formulations when applied to the truss element exactly satisfied equilibrium in the deformed configuration. In order for Bogner's formulations to satisfy the equilibrium in the deformed state, the axial force must be obtained by differentiating the strain energy expression given by Bogner with respect to the displacement u_q; the numerical value of the resulting expression gives the value of the axial force which satisfies the equilibrium in the deformed configuration.

Since the displacements u_p, v_p and v_q are imposed to be zero with respect to the Eulerian coordinates (Fig. 1), therefore the corresponding force components P_p, V_p and V_q are obtained from the static equilibrium of the discrete element as follows:

$$P_p = -P_q \qquad (2.73.a)$$

$$V_p = \frac{1}{s}(M_p + M_q) \qquad (2.73.b)$$

$$V_q = \frac{-1}{s}(M_p + M_q) \qquad (2.73.c)$$

CHAPTER III

METHOD OF ANALYSIS

3.1 General

This chapter describes the energy search method as applied in the present work. The introduction of the optimization techniques into the structural analysis problem through the principle of stationary potential energy is explained.

The energy search method retains the flexibility of discrete element idealizations while improving the prediction of the structural behaviour by avoiding some of the customary linearizing assumptions. The flexibility of the energy search method in accounting for elements going out of service under loading is illustrated. The relative ease of handling the situations where some of the displacements are prescribed is also shown.

The method of Fletcher-Reeves is explained as the algorithm used to minimize the total potential energy function. Detailed formulations of the method are given in Appendix D.

The concept of scaling the variables defining the space of search is explained in this chapter with the necessary formulations given in Appendix D.

3.2 Total Potential Energy of a Structural System

For a structural system of I elements, the strain energy is, simply, the scaler sum of the individual element

strain energies:

$$U = \sum_{i=1}^{I} U_s^{(i)} \qquad\qquad (3.1)$$

Where I is the total number of elements contributing to the total strain energy of the structure and $U_s^{(i)}$ is the strain energy of the i <u>th</u> frame element given in Eqns. 2.44, 2.50 or 2.57, depending on whether the element is in compression-bending coupling, only bending or tension-bending coupling, respectively.

If any element goes out of service during the search process, the contribution of that element into the structural strain energy is simply neglected. This situation is usually encountered when tension elements, which exhibit no stiffness in compression (e.g., cables) slacken under certain loading conditions. It should be mentioned that since the strain energy is a scalar quantity, it can be numerically evaluated with respect to any system of coordinates. For simplicity, the element strain energy, in the present study, is calculated with respect to the Eulerian moving coordinates (x,y) shown in Fig. 1.

The work term is, basically, the scalar sum of the external loads times the corresponding displacements which can be expressed as

$$W = \sum_{j=1}^{J} P_j D_j \qquad\qquad (3.2)$$

where J is the total number of independent non-zero displacements

which represents the structure's degrees of freedom. P_j and D_j are the j th load and the corresponding j th displacement, respectively. Notice that the work term is a linear function of the displacements while the strain energy is generally a nonlinear function of the displacements.

Expression 3.1 defining the total structure's strain energy when coupled with Eq. 3.2, which gives the work done by the external loads, describes the total potential energy of the structure which can be cast in the following form:

$$\Pi_p = \sum_{i=1}^{I} U_s^{(i)} - \sum_{j=1}^{J} P_j D_j \qquad (3.3)$$

Notice that Π_p is finally a direct function of the global displacements defined by the global displacements vector {D}. The J components of the independent degrees of freedom together with the potential energy function itself, Π_p, are considered coordinates in a J+1 dimensional space. The potential energy expression (Eq. 3.3) defines a hypersurface in this space.

3.3 Function Minimization

The principle of stationary potential energy (Ref. 23) states that,

> "Of all displacement states {D} which satisfy geometric admissibility, that which makes the potential Π_p stationary satisfies the equilibrium conditions and is the actual displacement state {D}*."

The above principle can be stated mathematically, as

IF

$$\frac{\partial \Pi_p(\{D\})}{\partial D_j}\Bigg|_{\{D\} = \{D\}^*} = 0 \; ; \quad j = 1, 2, \ldots, J \qquad (3.4)$$

Then

$$\Pi_p(\{D\}^*) \text{ is stationary at } \{D\}^*.$$

Furthermore, if

$$\Pi_p(\{D\}^*) < \Pi_p(\{D\}) \qquad (3.5)$$

for all $\{D\}$ in the vicinity of $\{D\}^*$, then the associated equilibrium position is stable. The principle of stationary potential energy is equivalent to the displacement method.

According to the principle of stationary potential energy, the structural analysis problem is viewed as a special case of the mathematical programming problem known as unconstrained minimization where the variables can take any arbitrary values to minimize the potential energy function Π_p. The structural analysis problem, as described from the mathematical programming standpoint is described as,

Given $\Pi_p(\{D\})$

Find $\{D\}$

such that $\Pi_p(\{D\})$ is minimum.

The necessary condition for the occurrence of a local minimum at $\{D\} = \{D\}^*$ is

$$\frac{\partial \Pi_p(\{D\}^*)}{\partial D_j^*} = 0; \qquad j = 1, 2, \ldots, J \qquad (3.6)$$

Since Π_p, when derived for geometrically nonlinear structures is a highly nonlinear function of the displacement {D}, therefore Eq. 3.6 is simply a set of J nonlinear equations representing the first derivative of the potential energy function with respect to each of the generalized coordinates {D}. The most obvious approach to finding the minimum of Π_p is to solve Eq. 3.6. Unfortunately, the task of solving a large set of nonlinear equations may be very difficult. The function Π_p may be so complex, such as the kind encountered in the present study, that it is virtually impossible to write it out in a closed form. The use of the mathematical programming techniques in minimizing the potential energy function allows powerful numerical methods of unconstrained minimization to be used.

3.4 Unconstrained Minimization Techniques

Several methods are included under the unconstrained minimization category. Some of these methods are known as non-gradient methods.(Ref. 28) where only the numerical value of the function is required during the search to detect the function minimum. Other methods are classified as gradient methods where both the function value as well as its first derivative with respect to each of the unknown variables are required numerically for the minimization process. Box in Ref. 29 presented a comparison between several gradient and non-gradient optimization methods. Box came to the conclusion that the method developed by

Fletcher and Powell (Ref. 30) is the most consistently
successful. In the same paper, Box recommended the method
of Fletcher and Reeves (Ref. 31) as the second choice.
It is worth mentioning that both of the two previously
mentioned methods possess quadratic convergence, i.e., the
property that they will converge to the minimum in a finite
number of steps if applied to a quadratic function (if
linearized formulations are used to obtain the potential
energy function, then the energy function is a quadratic
and the minimum will be found in a finite number of itera-
tions).

3.5 Fletcher-Reeves Method

This is a quadratically convergent method which is
guaranteed, apart from round-off errors to detect the
minimum of a quadratic function of J variables in at most
J steps. The algorithm is explained in Ref. 31 and was
successfully used in the analysis of nonlinear truss-type
structures (Ref. 26) and is recalled again in the present
analysis. Both the function value $\Pi_p(\{D\})$ as well as the
first derivative $\dfrac{\partial \Pi_p(\{D\})}{\partial D_j}$ must be numerically available.

The first step during the minimization is taken
from the starting point $\{D_o\}$ along the steepest descent
direction defined by $\dfrac{-\partial \Pi_p(\{D_o\})}{\partial D_{oj}}$. Further directions of
travel are taken along the conjugate directions which are
a system of linearly independent directions generated
according to certain relationships. The details of Fletcher

Reeves method are given in Appendix D. In this work, sub-
routine DFMCG from the IBM system/360 scientific subroutine
package was used to locate the minimum of the total
potential energy functional.

3.6 Gradient Vector of the Structure

A basic requirement for the method of Fletcher-
Reeves is the evaluation of the analytic graident of the
total potential energy of the structure defined as,

$$\frac{\partial \Pi_p(\{D\})}{\partial D_j}, \text{ where } j = 1, 2, \ldots, J$$

with respect to each of the J degrees of freedom. Since
the total potential energy of the structure is expressible
as

$$\Pi_p = \sum_{i=1}^{I} U_s^{(i)} - \sum_{j=1}^{J} P_j D_j \qquad (3.7)$$

where I is the number of elements and J is the number of
the non-zero degrees of freedom defining the space of
search, therefore the analytic gradient vector of the
total potential energy function is expressible as

$$\left\{ \frac{\partial \Pi_p(\{D\})}{\partial D_j} \right\}_{Jx1} = \sum_{i=1}^{I} \{\bar{G}_e^{(i)}\}_{6x1} - \{P\}_{Jx1} \qquad (3.8)$$

Notice that $\{\bar{G}_e^{(i)}\}$ is the element strain energy gradient
vector with respect to the six-end displacements defined
in the global coordinates. Evaluating $\{\bar{G}_e^{(i)}\}$ has been
explained in Chapter II. The vectorial summation

$\sum_{i=1}^{I} \{\bar{G}_e^{(i)}\}$ is accomplished via the variable correlation

scheme which is explained in Ref. 32.

The relative ease in handling the problems where some of the displacements are prescribed a priori is apparent when using a gradient function minimization technique. The procedure is to set the gradient component, that corresponds to the prescribed displacement, to zero in the global gradient vector defined in Eq. 3.8 to keep the value of the prescribed displacement unaltered during the search.

3.7 Scaling Transformation

The method of Fletcher-Reeves, which is used in the present work, although requiring modest storage is sometimes characterized with convergence difficulties. Fortunately, the incorporation of a scaling transformation technique proved to effectively improve the convergence of the nonlinear potential energy function of the structure.

The scaling transformation, as applied in this work, was first proposed by Fox and Stanton (Ref. 33) and was successfully used in the cases of linear and nonlinear analysis in references 33, 26, respectively.

The scaling transformation can be accomplished by a simple multiplication of the individual degrees of freedom by appropriate constants to rescale the coordinates defining the search space to reduce the eccentricity of the

objective function. The variance of the eigenvalues, and consequently, the diagonal elements, of the Hessian matrix of the objective function gives a good idea of the performance of the function when minimizing using a gradient method. The general conclusion is that the closer the conditioning number of the matrix of second partials to unity, the better are the convergence characteristics of the objective function.

The concept of scaling transformation as given in Ref. 33 is based on Gerschgorin's theorem which guarantees that every eigenvalue of the Hessian matrix lies in at least one of the disks centered at a_{ii} and of radii = $\sum_{i \neq j} |a_{ij}|$. Figure 3 gives a graphical description of the possible range of the eigenvalues for an unscaled and scaled matrix. In the unscaled case, the circles are not only large, but are centered at widely different points. The circles of the scaled matrix are all centered at the same point and their radii are tightly bounded above. This can be achieved by the scaling transformation described in the following.

Consider the linearized form of the potential energy function,

$$\mathbb{I}_p(\{D\}) = \frac{1}{2}\{D\}^T [K] \{D\} - \{D\}^T \{P\} \qquad (3.9)$$

where $\{D\}$ is the unscaled vector of independent degrees of freedom, $\{P\}$ is the work equivalent load vector and $[K]$ is the conventional unscaled linear stiffness matrix.

.now introduce the transformation defined by

$$\{z\} = [R]^{-1}\{D\} \qquad (3.10)$$

$$[\bar{K}] = [R]^T[K][R] \qquad (3.11)$$

$$\{\bar{P}\} = [R]^T\{P\} \qquad (3.12)$$

where $\qquad [R] = (r_{jj}) \qquad (3.13)$

and $\qquad r_{jj} = \dfrac{1}{(k_{jj})^{\frac{1}{2}}} \qquad (3.14)$

In this case, the matrix of second partials of the total potential energy is simply the master stiffness matrix of the linear structure.

The potential energy in the scaled coordinates is defined by

$$\Pi_p(\{Z\}) = \frac{1}{2}\{Z\}^T [\bar{K}] \{Z\} - \{Z^T\} \{\bar{P}\} \qquad (3.15)$$

Notice that the value of the potential energy is the same whether it is calculated with reference to the scaled or the unscaled coordinates. Inside the minimization subroutine, used in the present study, the value of the potential energy was calculated using the unscaled displacement vector, while the unknown displacements as well as the gradient components were always referred to the scaled coordinates.

In the nonlinear formulations, the elements of the matrix of second partials (stiffness matrix in linear formulations) are still functions of the displacements; however, previous experience (Refs. 22,26) revealed that linearizing the matrix of second partials is sufficient to significantly improve the convergence of the potential

energy function. Derivation of the scaling factors for the frame element is shown in Appendix D.

CHAPTER IV

NUMERICAL EVALUATION

General

This chapter is devoted to the numerical evaluation
of the developed formulations and method of analysis.
Different analysis examples are solved and compared with
other analytical solutions and experimental test results to
show the potential and capability of the developed method.

The examples were selected to cover the various
degrees of geometric nonlinearity as classified by Mallett
and Marcal in Ref. 9. The analysis of structures exhibiting
linear behaviour up to the point of instability represents
the basic class of geometric nonlinear behaviour. On the
other hand, the analysis of structures having snap-through
type buckling, where the structure jumps from a stable
position to another stable configuration traversing a region
of unstable equilibrium, represents the highest degree of
geometric nonlinearity.

Example 1

This example investigates the problem of stability of
frames in light of the present method and formulations. Two
portal frames, one hinged and another fixed, are employed
in the analysis. The dimensions as well as the material
properties are all given in Figs. 4-a and 4-b.

Two reference solutions are given, one by Timoshenko

and Gere (Ref. 34) who predicted the buckling load of the hinged frame and another by Connor, Logcher and Chan in Ref. 8 who analyzed the fixed portal frame up to the instability limit.

The example aims to check the capability of the developed method of analysis to predict the buckling load of frame structures. Meanwhile, it also shows the agreement between the solution obtained by the present method and the solution using previous methods of analysis. Moreover, the post-buckling behaviour is investigated in the cases where the structure possesses some post-buckling stiffness. In the following, the analysis of the hinged frame will be discussed, then the analysis of the fixed frame will be covered.

(a) The Hinged Frame

To obtain the buckling load using the present formulations, a lateral displacement of $\Delta = 0.1$ inches was prescribed at the top of the left column as shown in Fig. 5. The axial force was incremented in the presence of the prescribed displacement and the horizontal transverse force at the left corner was calculated at the end of the analysis. The vertical load was plotted versus the calculated horizontal force (Fig. 5) which is found to be decreasing as the axial load increases. The buckling load is defined as the axial load which produces a lateral displacement, equal to Δ in the presence of no lateral force. The value of the

buckling load obtained using the present method is shown in Fig. 5 and is equal to 1170 Kips. Instability, as it pertains to this frame, is described as the mutual degradation of the bending and membrane stiffnesses as a result of increasing the axial load up to the buckling load. At the critical point, defining the buckling load, even a zero lateral load, will theoretically produce a lateral displacement.

The stability analysis of pin-ended portal frames was investigated by Timoshenko and Gere in Ref. 34. The solution by Timoshenko and Gere is based on studying the equilibrium in the deformed configuration while neglecting axial deformations, and then satisfying the compatibility condition at the corner joint between the column and the horizontal beam. The value of the buckling load, as predicted by Timoshenko and Gere is equal to 1176 Kips which is in good agreement with the value obtained by using the present method. The small discrepancy is simply attributed to neglecting the axial deformations in the solution by Timoshenko and Gere.

(b) The Fixed Frame

The solution using the present method is based on applying a small perturbing horizontal force in the presence of the axial load. The axial load is increased gradually, and the corresponding horizontal displacement is calculated. The plot in Fig. 6 shows the load-deflection curve of the

fixed frame. It is clear that the frame exhibits consider-
able bending stiffness in the region A-B, after which the
structure loses its bending stiffness at a fast rate and
finally buckles. No solution was obtained at an axial load
of 4700 Kips which is considered as the buckling load for
the fixed frame. Increasing the axial load beyond the
buckling load shows some post-buckling stiffness represented
by part C-D in Fig. 6 which is characterized by a considerable
increase in the deflection for a small increase in the axial
load; notice the change in the horizontal scale in Fig. 6.

In Ref. 8, Connor, Logchar and Chan presented non-
linear formulations for the rigid joint space frame which
were applied to the stability analysis of the same fixed
portal frame. The nonlinear term $\frac{1}{2}(\frac{dv}{dx})^2$ was retained in
the strain-displacement relationship, but Lagrangian
(initial state) coordinates were used in the analysis. The
resulting nonlinear equations were solved by the method of
successive substitution which is characterized by first-
order convergence. The predicted behaviour according to
Connor, Logchar and Chan (Ref. 8) is shown in Fig. 6 by
the dotted curve and the buckling load was found to be
4800 Kips which is in good agreement with the value predicted
using the present method (4700 Kips). The small discrepancy
between the two solutions is simply attributed to the fact
that Connor, Logchar and Chan formulated the equilibrium
equations with respect to the undeformed local coordinates

and therefore the use of the formulations was restricted to the cases where the squares of the rotation angles are negligible compared to unity. Also the definition of the axial force as given by Connor, Logchar and Chan appears to be inconsistent.

The present method of analysis proved to be capable to handle the stability of frames. The post-buckling behaviour was also predicted whenever the structure possesses a considerable post-buckling stiffness. The comparison with previous analytical solutions showed good agreement.

Example 2

This example investigates the behaviour of a fixed-fixed beam under an increasing central vertical load and a uniform axial tensile prestrain. Figure 7 shows the beam dimensions and the necessary data for the analysis.

By means of this example, the solution obtained, using the formulations developed in the present study, is compared with the experimental test results. At the same time, this example shows the capability of the method of analysis in considering the cases where initial prestrains are induced in the structure. The effect of including and excluding the nonlinear term $\frac{1}{2}u_x^2$ is also studied in this example. Finally, the linear solution is also given to show the erroneous behaviour obtained by the linear formulations when compared with the behaviour obtained experimentally.

In the experimental analysis, the edges of the beam were welded to two very rigid steel blocks and then a uniform prestrain of approximately 80µε was applied. The ends were tightly bolted to the loading frame, then the external load was applied gradually in 20 lbs. increments up to a load of 100 lbs. It proved extremely important to guarantee the complete fixity of the beam ends in the horizontal direction since a very small slippage at the beam ends is enough to cancel the tension-bending coupling which is the main reason of the nonlinear behaviour in this particular example. The strain throughout the beam was monitored by means of four strain gauges at the two quarter points near the beam edges as shown in Fig. 7. The vertical deflection was measured by means of a dial gauge located at the beam centre. The beam was also unloaded gradually to make sure that the initial prestrain did not change while loading which implies that no slippage took place and also to assure that the beam is still in the elastic range. The dotted curve in Fig. 8 represents the dial gauge readings for the central deflection at the different loading levels. The maximum deflection, as measured under the load of 100 lbs. was found to be 0.66 inches.

The dash-dot line in Fig. 8 shows the behaviour predicted using the conventional linear analysis based on the undeformed geometry (i.e., there is no contribution from the axial force on the transverse deflection) and a

linear strain-displacement relationship which implies that the strain along the centroidal axis due to bending rota- tion is negligible. According to the conventional linear analysis, the vertical deflection under a load of 100 lbs. was found to be 2.88 inches.

The solid continuous line in Fig. 8 represents the analytical solution obtained by the formulations presented in Chapter 2 where only the nonlinear term $\frac{1}{2}v_x^2$ was retained in the basic strain-deformation relationship (Eq. 2.4). A vertical deflection of 0.54 inches was obtained corresponding to a vertical load of 100 lbs. The circled points on the same plot (Fig. 8) were obtained by adding the nonlinear term $\frac{1}{2}u_x^2$ to the strain-deformation relationship as shown in Eq. 2.4.

The comparison between the experimental results and the analytical solution, using the present method and formulations, shows good agreement as can be noticed from Fig. 8. The two curves, corresponding to the experimental and the present analyses, have almost the same trend, although the theoretical model always overestimates the rigidity which is attributed to the following two reasons:

1. Although care was taken to prevent the horizontal slippage by tightening the end block's nuts with the loading frame, there is a possibility of a very slight slippage of the end blocks due to the high tensile force developed at the beam ends.

2.   The inaccuracy in determining the real prestrain
     was evident due to the difficulty in estimating
     the original prestrain due to the effect of the
     weight of the beam.

Furthermore, the finite element method generally
leads to stiffer behaviour which can be remedied by using
more elements. Of special interest is the relative ease of
the present formulations in considering the effect of the
initial axial prestrains on the behaviour of the structure.
The initial prestrain is simply one of the element properties
in the input data to the computer program.

The comparison between the linear solution and the
experimental test results demonstrates clearly the error
that may be obtained from the linear analysis, even at very
low load values. Also, it is the writer's opinion that any
nonlinear analysis employing a third degree polynomial as
an approximation to the deflection curve (Refs. 21, 27), will
give an inaccurate estimate to the behaviour of that parti-
cular beam, especially at high vertical load values. This
claim is supported by Young's paper (Ref. 17) which showed
that the customary assumption of a cubed polynomial to the
true deflection curve is highly misleading in the cases of
large axial force. In this particular example, the value
of the axial force which corresponds to a vertical load of
100 lbs. was found to be equal to approximately 1600 lbs.
(tension); the non-dimensional factor ϕ, defined by Young

as $P\ell^2/EI$, is equal to 147.5 which is very large, and even transcends the range given in Young's paper, and results in significant error if the assumption of a cubed polynomial is used to describe the transverse displacement curve.

Finally, the introduction of the nonlinear term $\frac{1}{2}u_x^2$ into the strain-displacement relationship, even in this case of very large axial force, has a negligible effect on the behaviour of the beam; this is believed to be due to the use of the efficient Eulerian coordinates system in the present study. The same conclusion was obtained in the special case of pin ended (truss) elements by Jagannathan Epstein and Christiano in Ref. 20.

Example 3

The A frame shown in Fig. 9 was solved using the present formulations and method of analysis. The structural dimensions, as well as the section properties, and the material constants are shown in Fig. 9.

The basic purpose of this example is to demonstrate the capability of the present method and formulations to analyze structures exhibiting snap-through buckling which is accompanied by large rotations and deflections. According to the classification given by Mallet and Marcal in Ref. 9, this class of problems is considered the highest degree in the hierarchy of geometric nonlinearity. Meanwhile, the results obtained by using the present method of analysis is compared with the solution obtained by Mallett and Berke in

Ref. 24 who solved the same A frame. Finally the merit of retaining the nonlinear term $\frac{1}{2}u_x^2$ in the strain-displacement relationship is also investigated.

The continuous solid curve in Fig. 10 represents the solution obtained by prescribing the vertical load and calculating the corresponding vertical displacement using the proposed function minimization method. Part A-B shows the nonlinear behaviour of the structure in the pre-buckling zone. The deformations are still in the small deflection range, but the nonlinearity is basically attributed to the bending-compression coupling which is completely ignored in the linear analysis. The structure buckles at a vertical load of 3.8 Kips when the vertical deflection was 2.98 inches. A small increment of 0.1 Kip in the vertical load causes the vertical displacement under the load to jump a distance of 13.6 inches. This characterizes the snap-through of the frame apex to traverse the region of the unstable equilibrium to another stable equilibrium zone indicated by the curve C-E in Fig. 10. The structural deformed geometry before and after buckling is shown in Fig. 9 which indicates the dramatic change in the geometry as the frame snaps-through. It is interesting to realize that the snap-through was accompanied by a sudden change from the compression-bending coupling state to the tension-bending coupling state as the load is increased beyond point C (Fig. 10). The part of the curve in the unstable region (dash-dot curve) was obtained by

prescribing the displacement and calculating the load using the same function minimization technique.

Mallett and Berke in Ref. 24 solved the same frame. The agreement between the behaviour predicted using both Mallett and Berke solution and the present formulations is exact in the region A-B. Mallett and Berke overestimated the buckling load by about 0.4 Kips and the reason is believed to be due to the artificial stiffness included in their formulations because of employing assumed displacement modes.

In the post-buckling region, it is apparent that the solution by Mallett and Berke overestimates the structural rigidity and thus yields smaller displacements. The reason is again the artificial stiffness due to both the approximate displacement functions as well as the system of the Eulerian coordinates employed by Mallett and Berke. In the next example, the effectiveness of Mallett and Berke Eulerian coordinates will be discussed in more detail.

The difference between the results obtained using the present method and the method proposed by Mallett and Berke (Ref. 24) in the unstable region, is basically attributed to the difference in the force-deformation relationships employed in both formulations. Worthy of special mention, is that the force equilibrium was exactly satisfied at each loading level using the force-deformation relationship developed in the present study.

The effect of introducing the nonlinear term $\frac{1}{2}u_x^2$, besides the nonlinear term $\frac{1}{2}v_x^2$, into the strain-displacement relationship is investigated. The circled dots in Fig. 10 show the effect of retaining the nonlinear term $\frac{1}{2}u_x^2$ in the formulations. It is apparent that the effect is very small and can be ignored in this case of bending-compression coupling which agrees with the recommendation given in Ref. 20 concerning the truss element.

Example 4

The analysis of the diamond square frame shown in Fig. 11-a is considered. The geometry as well as the section properties are shown in the same figure.

Fig. 11-b shows the structure after deformations as the load is increased up to 60 lbs. The problem represents a very large deflection case where the ratio of the deflections to the original dimension, in the direction of the displacement, reaches a value of 0.45 at a load of 60 lbs.

The analysis of this example is presented to check the consistency of the formulations developed for the bending-tension coupling case, since the frame is subjected to this type of coupling under the specified tensile load (Fig. 11-b). Moreover, this example is employed to clearly demonstrate the difference between the formulations developed in the present analysis and the formulations developed in Ref. 21, and were used to analyze the same frame in Ref. 24

by Mallett and Berke.   The same frame was solved using an
exact analysis by Jenkins and Seitz in Ref. 35, therefore,
a comparison will be performed between the solution using
the present formulations and the solution by Jenkins and
Seitz.   The example also demonstrates the reliability of
the present method of analysis in handling problems of
large deformations and rotations (a rotation of about 30°
was reported at a load level of 60 lbs.).

The exact solution by Jenkins and Seitz (Ref. 35)
is given as the reference solution.   Jenkins and Seitz used
the exact moment rotation relationship to express the
moment equilibrium equations and the resulting complicated
integral was solved using elliptic integral forms after
satisfying the end conditions.   The solution by Jenkins
and Seitz, although lengthy and complicated, is restricted
to the analysis of the simple geometry of the diamond
frame considered herein with the simple loadings (axial
tension or compression).   Exact agreement was found between
Jenkins and Seitz' solution and the solution obtained by
the present analysis as shown in Fig. 12.

The same frame was analyzed by Mallett and Berke
in Ref. 24 who employed the energy search approach in the
analysis. It is clear from Fig. 12 that the solution by
Mallett and Berke deviates from the solution obtained using
the exact analysis (Ref. 35) and the deviation increases as
the load increases which is attributed to the following

reasons:

1. The basic modes used by Mallett and Berke (i.e., cubed polynomial) do not accurately reflect the coupling between the transverse and the axial stiffnesses.

2. The Eulerian axes proposed by Mallett in Ref. 24 are shown in Fig. 13-a; it is believed that the Eulerian coordinates employed by Mallett and Berke do not justify the use of the small rotation strain-displacement relationship (Eq. 2.4) unless a larger number of elements is employed to model the frame member.

The two foregoing handicaps in Mallett and Berke's solution were avoided in the present study by using the exact displacement functions to describe the transverse and axial deformations; this minimized the artificial stiffness which might be included if assumed displacement modes were used. Also, the Eulerian axes employed in the present work and shown in Fig. 13-b were specifically chosen in order to justify the use of the small rotation strain-displacement relationship Eq. 2.4. The same number of elements (8 elements) to model the square frame was used in both of the two solutions using the present formulations and the solution by Mallett and Berke (Ref. 24).

Example 5

The proposed formulations and method of analysis are

applied to predict the complete behaviour of shallow arches under increasing central vertical load. The circular aluminium arch shown in Fig. 14-a was solved using the present formulations and was also tested experimentally (Ref. 36) as well as analyzed using nonlinear finite elements formulations by Marcal (Ref. 37). The dimensions as well as the material properties are all shown in Fig. 14-a.

The present example aims to show the capability of the developed formulations and method of analysis to predict the buckling load of flexible shallow arches under increasing vertical load. The behaviour of the arch in the unstable region after buckling was also predicted using the present method of analysis. The formulations were also used to follow the behaviour of the arch in the post-buckling zone.

In order to solve the arch using the present formulations, the circular arch was modeled as eight straight frame elements as shown in Fig. 14-b. The solid continuous line in Fig. 16 represents the solution obtained by the present analysis. In the portion A-B of the curve, the load was gradually increased and the corresponding vertical displacement was calculated and plotted. As can be noticed from Fig. 16, the arch possesses considerable stiffness in that portion of the curve. Increasing the load beyond point B is characterized by a significant decrease in the arch stiffness which finally leads to buckling at a load of 33 lbs. Increasing the load beyond point B was also characterized

by convergence problems and the solutions were then obtained by prescribing the displacement of the arch apex and calculating the corresponding load. Experience indicated that any iterative solution will have convergence problems as the load is increased near the "Peak" carrying capacity. This conclusion was reported by Zienkiewicz in Ref. 38 and a convenient solution then is to proceed immediately prescribing displacements and computing the corresponding loads. The writer would like to emphasize the relative ease of the employed gradient function minimization technique in considering the situations where some of the displacements are prescribed a priori. Figs. 15-a, 15-b represent the arch before and after buckling, respectively.

The circular arch was tested experimentally by Gjelsvik and Bodner and the results are reported in Ref. 36. The details of the experimental set up as well as the technique employed to obtain the unstable region of the load-deflection curve are given in the same paper. According to the experimental analysis, buckling occurs at a vertical load of 31 lbs. The complete experimental load-deflection curve is represented by the dotted curve in Fig. 16.

The dash-dot curve in Fig. 16 represents the finite element solution by Marcal (Ref. 37). Marcal introduced an initial displacement matrix in addition to the initial

stress matrix. Marcal showed that the initial displacement matrix was found to be of the same order as the initial stress matrix, but appears not to have been previously recognized in finite element analysis. The initial displacement matrix, is, basically, obtained as a result of writing the nonlinear strain-displacement relationship in an incremental form.. In the finite element solution by Marcal, the arch was represented by sixteen straight beam-column elements and the buckling was predicted to take place at a vertical load of 27.2 lbs. which is in reasonable agreement with the value obtained experimentally. No behaviour was predicted in the post-buckling region since the procedure was a load-controlled type of analysis.

The present method of analysis and formulations proved to be capable to predict the behaviour of flexible arches under increasing vertical loads. The buckling load obtained by using the present analysis is in good agreement with the buckling load obtained experimentally. The small discrepancy between the present finite element solution and the experimental analysis is attributed to the fact that the theoretical model usually overestimates the real rigidity of the structure as a result of the approximations embodied in the formulations.

CHAPTER V

GUYED TOWERS

5.1 General

A guyed tower is a practical structure that may
exhibit geometrically nonlinear behaviour. Such towers
are frequently designed to heights of 1500 ft. to transmit
and/or receive high frequency signals for various electronic
communication systems. More recently, tall towers are
being designed and utilized for supporting collectors in
solar energy applications and have been proposed for off-
shore oil operations. The nonlinear behaviour of a guyed
tower may significantly complicate the analysis of this
structural system; it is this nonlinear aspect which
generates the interest in the problem.

The mathematical model for a guyed tower is essen-
tially a flexible beam-column with elastic supports.
Guyed towers exhibit most, if not all, of the geometrically
nonlinear aspects. The amplification of deflections and
bending stresses due to the beam-column action is evident.
At the same time, the tower may undergo large deflections
under severe wind conditions, which may necessitate study-
ing the equilibrium in the deformed configuration. The
tower is usually prestressed in the unloaded state due to
pretensioning the guys. Finally the change in the struc-
tural configuration due to the slackening of some guys on
the leeward side, may have to be taken into consideration.

Several studies have been published towards an adequate analysis of guyed towers. The following discussion gives a brief outline of the state-of-the-art of guyed tower analysis and design. In Ref. 39, Rowe investigated the amplification of stresses and displacements in guyed towers when changes in the geometry are included in the analysis. Analytical charts were included in the same reference which show immediately when refined methods of analysis are necessary in the design and what modifications should be made so that the ordinary methods of structural analysis give adequate results.

Dean in Ref. 40 gave the necessary formulations to consider the sag of the hanging cable which takes the form of the catenary under its own weight.

A stability analysis of guyed towers was presented in Ref. 41 by Hull who tried to find the mast critical moment of inertia that corresponds to specified wind forces. An interpretation to the influence of the mast moment of inertia and the stiffness of the supporting guys on the tower stability was given in the same paper. Hull suggested that increasing the stiffness of the guys is the most efficient means of increasing the buckling capacity of the tower up to the limit when the tower starts to buckle into a number of sine waves with nodes at the supporting points. At that stage, increasing the guys stiffness will be ineffective and the only way to increase

the buckling capacity is to increase the moment of inertia
of the mast itself.

Goldberg and Meyers in Ref. 42 presented a method
of analysis for guyed towers where the nonlinear behaviour
was considered and the effect of the wind on the cable
stiffness was also investigated. The technique employed
was based on transforming the nonlinear algebraic equili-
brium equations into a corresponding set of ordinary
differential equations which were then integrated numerically.
Reference 43 covered the complete analysis and construction
aspects of the cylindrical television mast which has been
built for the Independent Television Authority at Winter
Hill, Emley Moor and Belmont in Great Britain. Unfortunately,
the structure collapsed a few years later and was replaced
by a high concrete television tower of 1084 ft. whose
description is given in Ref. 44. The failure of the
previously mentioned cylindrical mast was discussed by
Williamson (Ref. 45) in a stability study of guyed towers
under ice loads.

Miklofsky and Abegg (Ref. 46) presented a simplified
systematic procedure for the design of guyed towers using
interaction diagrams which provide the designer with a
graphical visualization of the design range without resort-
ing to a trial and error procedure.

In a good attempt to analyze guyed towers; Odly in
Ref. 47 presented a method of solution in which some

secondary effects such as the effect of ice loads and insulators located on the guys, shear deformations, initial imperfections in tower shaft, etc., were included. Odly started the solution by assuming a set of displacements at each joint to calculate the spring constants of the guys which were then used to obtain the tower deflections. The procedure was repeated until all assumed and computed values of deflections were in satisfactory agreement.

In a study of shear effects in the design of guyed towers (Ref. 48) Williamson and Margolin stressed the fact that in the cases where the secondary moments and deflections, due to the beam-column action, significantly affect the final moments and deflections, the shear deformations should be considered to achieve a safe design. The writers also presented a means for modifying the conventional moment distribution factors when the axial thrust and web flexibility are considered. Finally a formula was given to find the thickness of the fictious solid web which has the same shear rigidity as a flexible trussed web.

Livesley in Ref. 49 attributed the nonlinearity in guyed towers to both the stiffening of the guy cables with increasing tension and to the destabilizing effects of the axial thrust on the mast itself. In the same paper, a procedure was described for calculating the guy tension in the cases where specified deflections are not to be exceeded under a number of different loading conditions.

Goldberg and Gaunt in Ref. 50 presented a method for determining the response of guyed towers to increasing lateral wind loads until the conditions of instability are reached. The criterion for buckling was the occurrence of relatively large increase in deformations for small increase in the applied loads. A valuable study was also given to illustrate the influence of certain system parameters on the critical load of the tower.

Williamson in Ref. 45 examined the icing effects on special types of tall guyed communication tower called "top-loaded" towers where the upper most level of guys consists of an array of conducting cables which serve as a radiating element for an antenna system. The result of the study is expressed as a critical ice thickness which corresponds to the occurrence of the instability conditions in the tower.

More recently, Romstad and Chiesa in Ref. 51 proposed an equivalent one dimensional beam element to replace the actual truss tower element which dramatically reduced the number of the degrees of freedom included in the analysis.

5.2 Numerical Example

The nonlinear analysis of a planar three level guyed tower is presented to demonstrate the response of the tower under increasing wind loads (Fig. 17). The tower is modeled using three beam-column elements, pinned at the base and supported at the three levels by elastic guys. As far as

the tower shaft is concerned, the different geometric non-linear aspects are considered. The tower shaft is assumed to have infinite shear rigidity to justify neglecting the shear strains. The guys are considered straight elastic string elements (i.e. having no compressive stiffness). The effect of the large nodal displacement is considered by employing Eulerian moving coordinates to formulate the guy equilibrium equations. The formulations given by Bogner in Ref. 25 were used for the string element with the modifications suggested in Chapter II concerning the force-deformation relationship.

The dimensions and material properties of the tower shaft are given in Table 1 for each of the three spans. The structural properties of the guys, as well as the initial pretension in each guy, are given in Table 2. The shaft is initially subjected to compressive prestrains due to pretensioning the guys. The prestrain in each span of the tower is given in Table 1. The complete structure under the working load is shown in Fig. 17 where the vertical loads represent the weight of the tower shaft as well as any equipment that may be mounted on the tower. The horizontal loads represent the working wind loads acting on the structure. The vertical loads were kept constant throughout the analysis since they represent the dead load. The horizontal loads were gradually increased to simulate the effect of increasing wind velocity. A load parameter

γ is used as a multiplier to relate the current wind intensity to the working wind intensity. The three curves in Fig. 18 represent the load-deflection curves for the three guyed levels. The vertical axis in Fig. 18 represents the values of the load parameter γ while the horizontal axis gives the values of the deflection at the direction of the wind. The tower has a considerable stiffness until γ reaches the value of approximately 8 after which the structure loses its stiffness at a fast rate which is characterized by large increments in deflections for relatively small increments in loads. No solution was obtained at γ equals 10 and the instability limit is estimated to lie between γ equals 9.75 and 10.

The load-deflection curves were also plotted in the range from γ equals 0 to 1 which represents the working conditions. Figure 19 shows the load-deflection curves in this range. The sudden change in the direction of the load-deflection curve of level 1 is attributed to the slackening of the leeward guys at the first and second levels which takes place at γ equals approximately 0.37. The load-deflection curves of the second and the third levels abruptly change their directions at γ equals approximately 0.37 due to the slackening of the leeward guys at the first and the second levels and again change their directions at γ equals approximately 0.51 due to the slackening of the leeward guys at the third level.

In the working range, the nonlinearity is attributed

to the change in the structural configuration due to the fact that the cables lose their pretension and no longer effectively contribute to the stiffness of the structure. At higher load levels the nonlinearity is attributed to the beam-column action as well as the large deformations which necessitate studying the equilibrium in the deformed position.

More research is needed to cover the remaining nonlinear aspects in guyed towers, especially the nonlinear behaviour of the supporting cables. Generally, the cables are not straight in the undeformed state; they usually take the shape of a catenary. Also, the effect of blowing wind on the stiffness of the cables has been shown to be significant (Ref. 50) and should be considered.

CHAPTER VI

SUMMARY AND CONCLUSIONS

6.1 General

In this chapter, the conclusions, as well as an
overall evaluation of the proposed formulations and method
of analysis are given. The difficulties encountered during
the research are mentioned in order that they may be
avoided or remedied in future investigations. Finally,
the projection of the present study is given so that the
concepts developed may be extended to other more general
structures.

6.2 Summary

It has been shown that a geometric nonlinear analysis
of some structures, especially when the value of the axial
force is large, is essential since the linear solution for
these structures may give misleading results. In this
research, the exact displacement functions have been used
in order to describe the transverse displacements. Moving
Eulerian coordinates were used and proved to be a very
effective and powerful means to consider the problem of
large deflections in structures. As a by-product, the
Eulerian coordinates used in the present study were shown
to allow retaining only the nonlinear second order bending
strain term $(\frac{1}{2}v_x^2)$ without the need of including the second
order axial strain term $(\frac{1}{2}u_x^2)$ in the strain-displacement

relationship. Initial prestressing effects were considered
by directly incorporating the prestrain into the strain-
displacement equation. The various types of geometric
nonlinearity, as well as instability analyses, were
investigated including finite deflections, bifurication
and snap-through buckling and the method was found to be
valuable in following the behaviour of certain structures
in the post-buckling zone.

Generally, the finite element formulations developed
and the function minimization technique employed proved to
be a powerful flexible means for the geometric nonlinear
analysis of structures. The method is a direct procedure
in that there is no need to increment the applied loads;
meanwhile, the general static equilibrium of the structure
at any stage and under any combination of loading was
exactly satisfied. When plotting the load-deflection curve
for some structures, it was found more convenient to use
the displacement vector of the last step as the starting
displacement vector in the coming step. This does not
imply that the procedure is incremental; it is simply an
efficient means to reduce computer time, especially for
highly geometric nonlinear problems.

One of the main difficulties encountered in the
present study involved finding the value of the parameters
k^2 and k_1^2 given in Eqns. 2.39 and 2.54, respectively.
Since these cannot be obtained in a closed form, iterative

schemes have to be employed. Two different iterative procedures were used to find the value of k^2 and k_1^2 according to the ratio I/A. It is also suggested that more research is needed to study the nature of the k^2 and k_1^2 functions.

As previously mentioned, whenever the minimum of the function is detected, the formulations guarantee the exact satisfaction of the equilibrium in the deformed configuration, but in a few cases the equilibrium was not exactly satisfied due to problems concerning the convergence of the potential energy function. Some of the convergence problems were due to the failure in detecting the value of the parameters k^2 and k_1^2 while other convergence problems are believed to be due to the procedure employed in Fletcher-Reeves algorithm. Employing the powerful Fletcher-Powell minimization method may compensate for the convergence problems encountered.

6.3 Projection

The natural extension for the present work is to include the necessary formulations to consider the analysis of space structures. Moreover, material nonlinearity, as it pertains to skeletal structures, could be investigated; it is strongly believed that the concept of the plastic hinge, as a change in the structural configuration, could be best handled using the energy search method. In the present formulations, the loads were assumed applied at the

nodes, therefore the procedure should be extended to con-
sider the effect of distributed loads between the nodes.
Also, eccentric prestressing would be worth investigating
since most of the prestressed concrete frame structures
are subjected to this kind of prestressing. Elements
possessing initial curvature (e.g., curved beams, cables
under their own weight, etc.) could be reconsidered in
light of the moving coordinates concept developed in this
research. Finally, the geometric nonlinearity due to
dynamic effects using function minimization is an important
subject for extensive studies.

6.4 <u>Conclusions</u>

The following conclusions are derived from the
present study:

1. The method and formulations presented ensure
   that equilibrium is exactly satisfied with
   respect to the deformed geometry.

2. The moving Eulerian coordinates used in the
   study is a powerful means to consider the
   effects of large deformations in structures.

3. The Eulerian coordinates used justifies neglect-
   ing the second order axial strain term ($\frac{1}{2}u_x^2$) in
   the strain-displacement equation.

4. The method proposed is valid for the analysis
   of plane frames exhibiting large displacements
   and can be used to predict buckling loads as
   well as post-buckling behaviour (including
   snap-through buckling).

5. When the axial force is relatively large, the
   exact hyperbolic ($k^2 > 0$) and trigonometric ($k^2 < 0$)
   transverse displacement functions used herein
   give accurate results.

6. The energy search method used in the study proved to be an efficient powerful, yet flexible, solution procedure for the geometrical nonlinear analysis of structures.

$\overline{X}, u$

ELEMENT A.D.
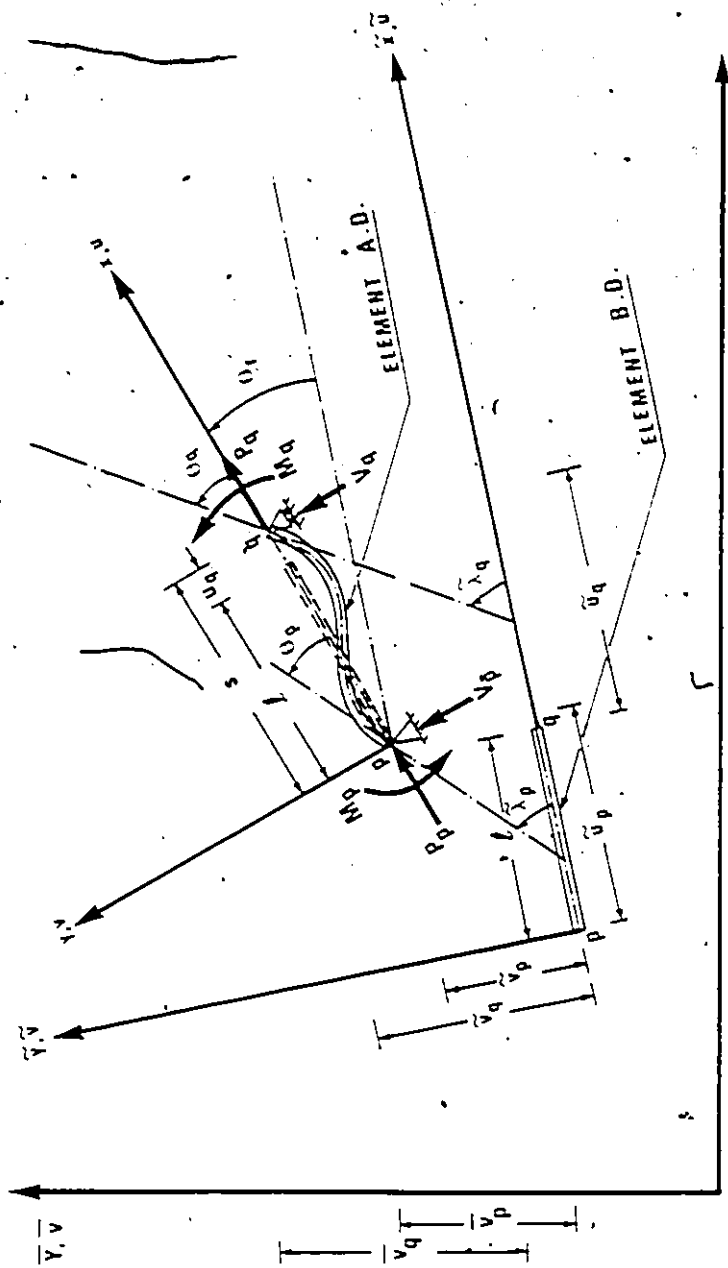
ELEMENT B.D.

A.D.=After Deformation
B.D.=Before Deformation

$\overline{Y}, v$

Fig. 1

Frame Discrete Element
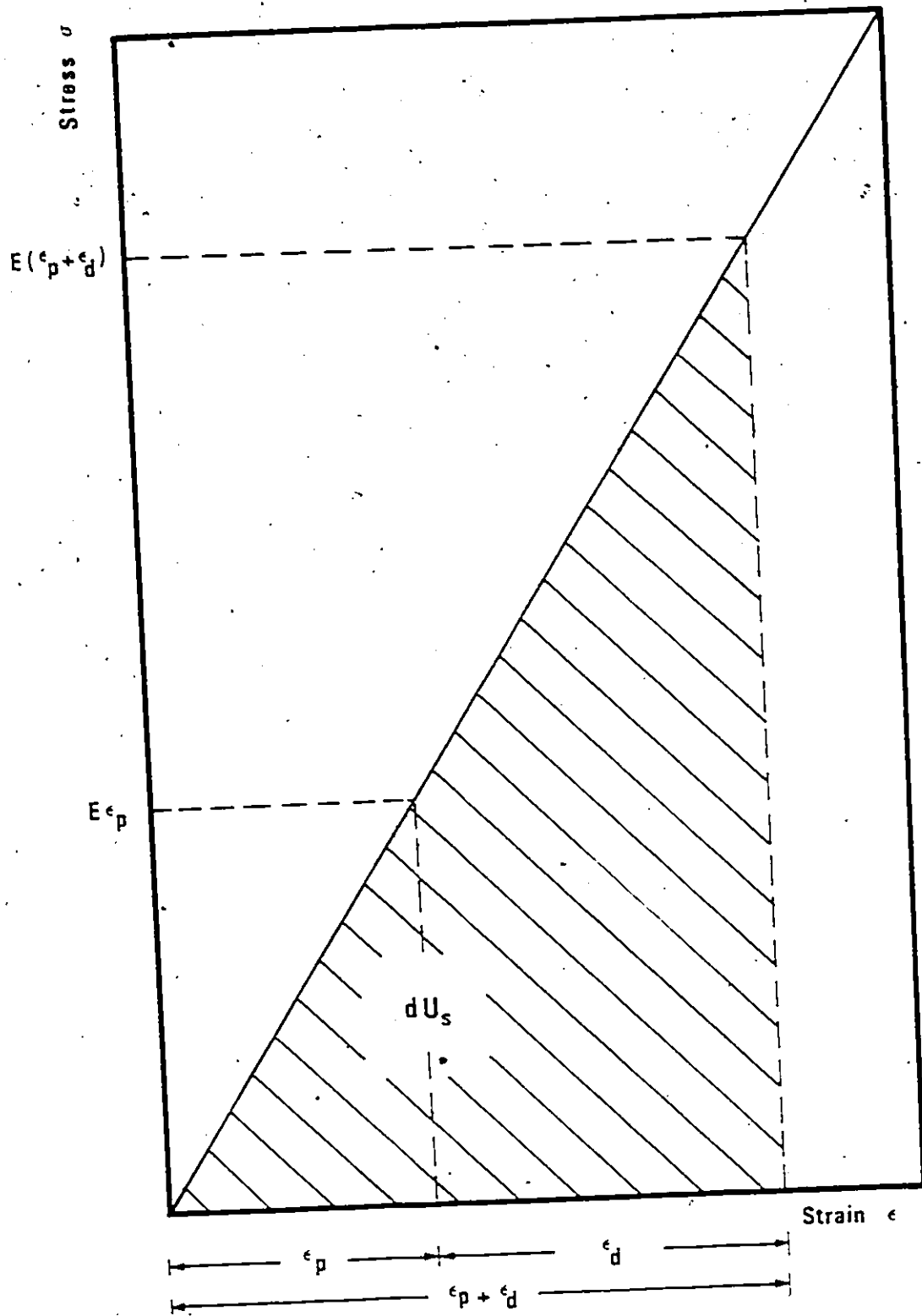
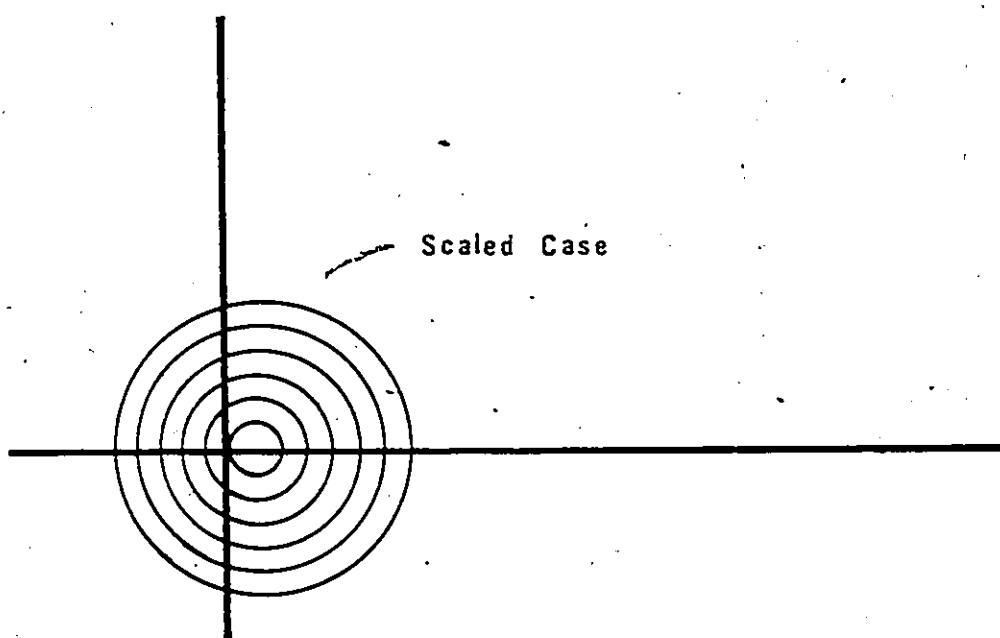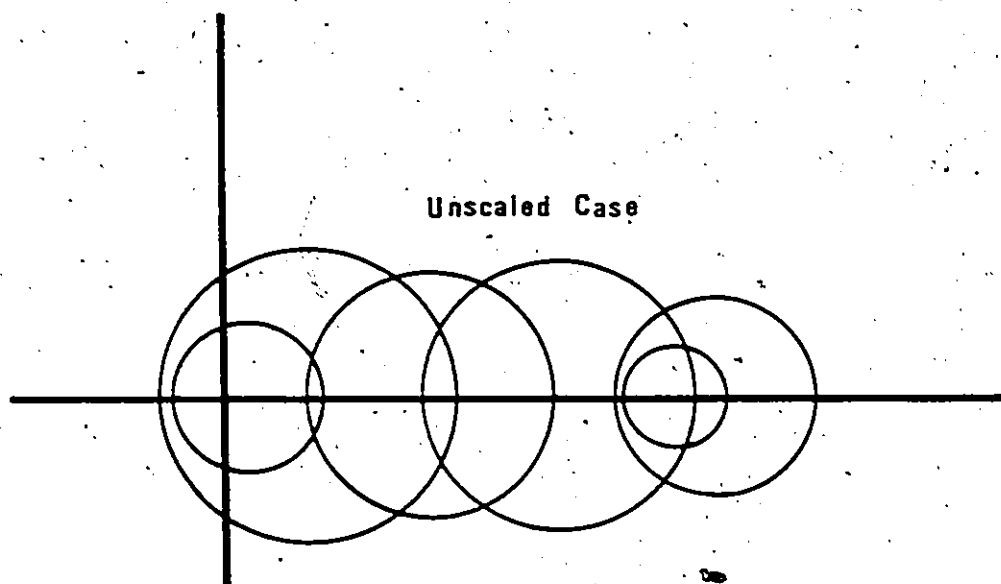Fig. 2   Strain Energy Desity in a Prestrained Frame Element

Unscaled Case

Scaled Case

Fig. 3

Gerschgorin Circles
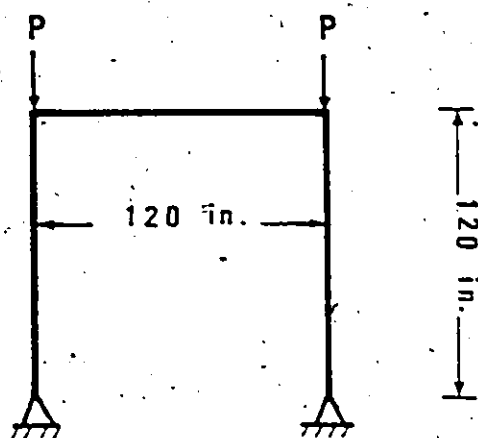
Fig. 4-a
Hinged Portal Frame

For All Members

$A = 11.77$ in.
$I = 310.1$ in.⁴

$I = 310.1$ i n^4.
$E = 3 \times 10^4$ ksi.
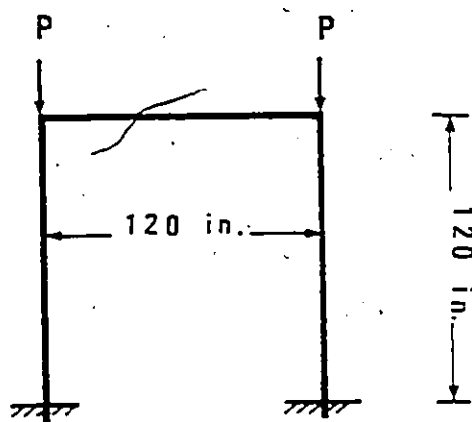
Fig. 4-b
Fixed Portal Frame

$(\; 1 \; \text{in.} = 25.4 \; \text{mm.} \; ; \; 1 \; \text{ksi.} = 6.9 \; \text{MN} / \text{m}^2 \;)$
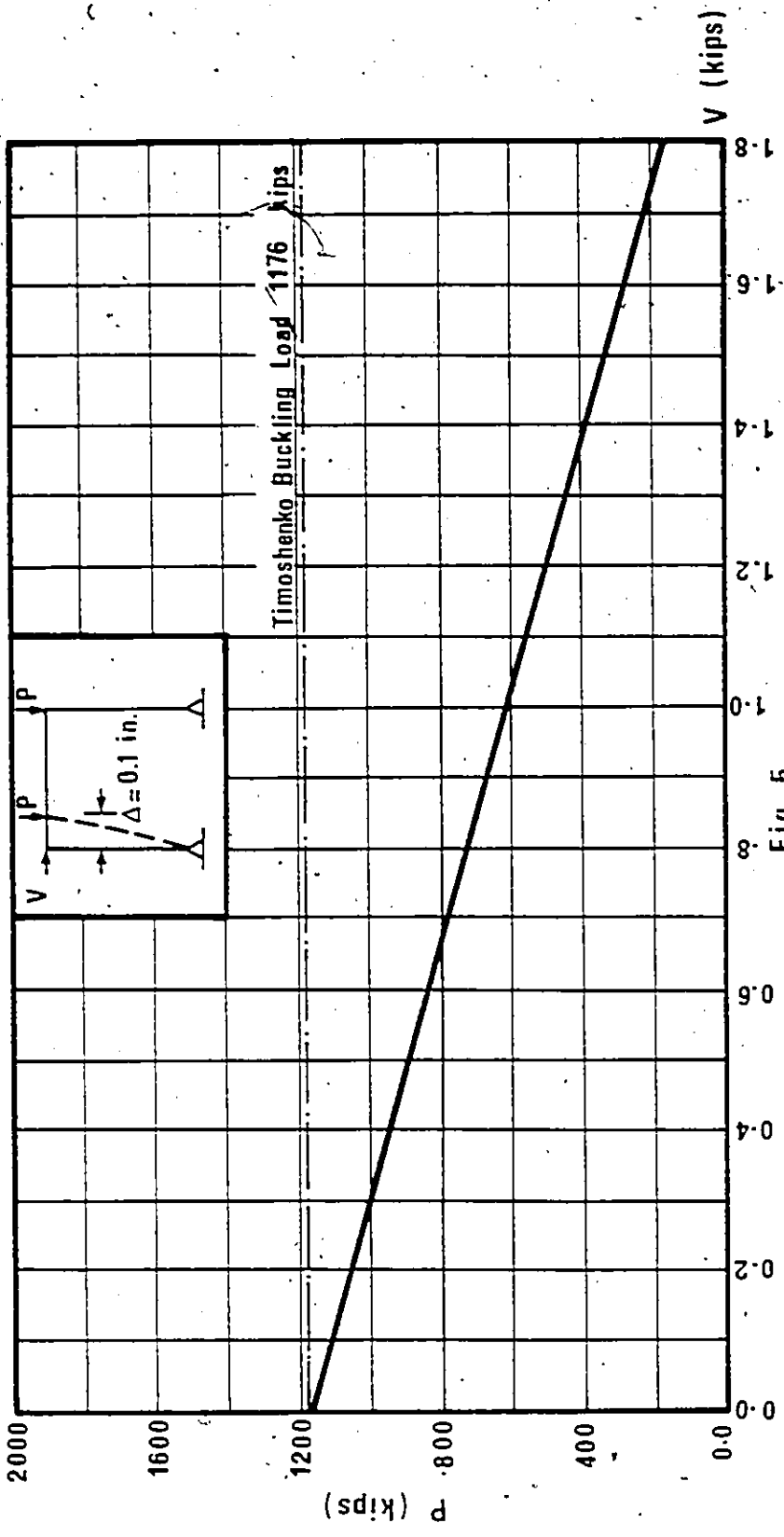
Fig.5 Buckling Load for the Hinged Frame

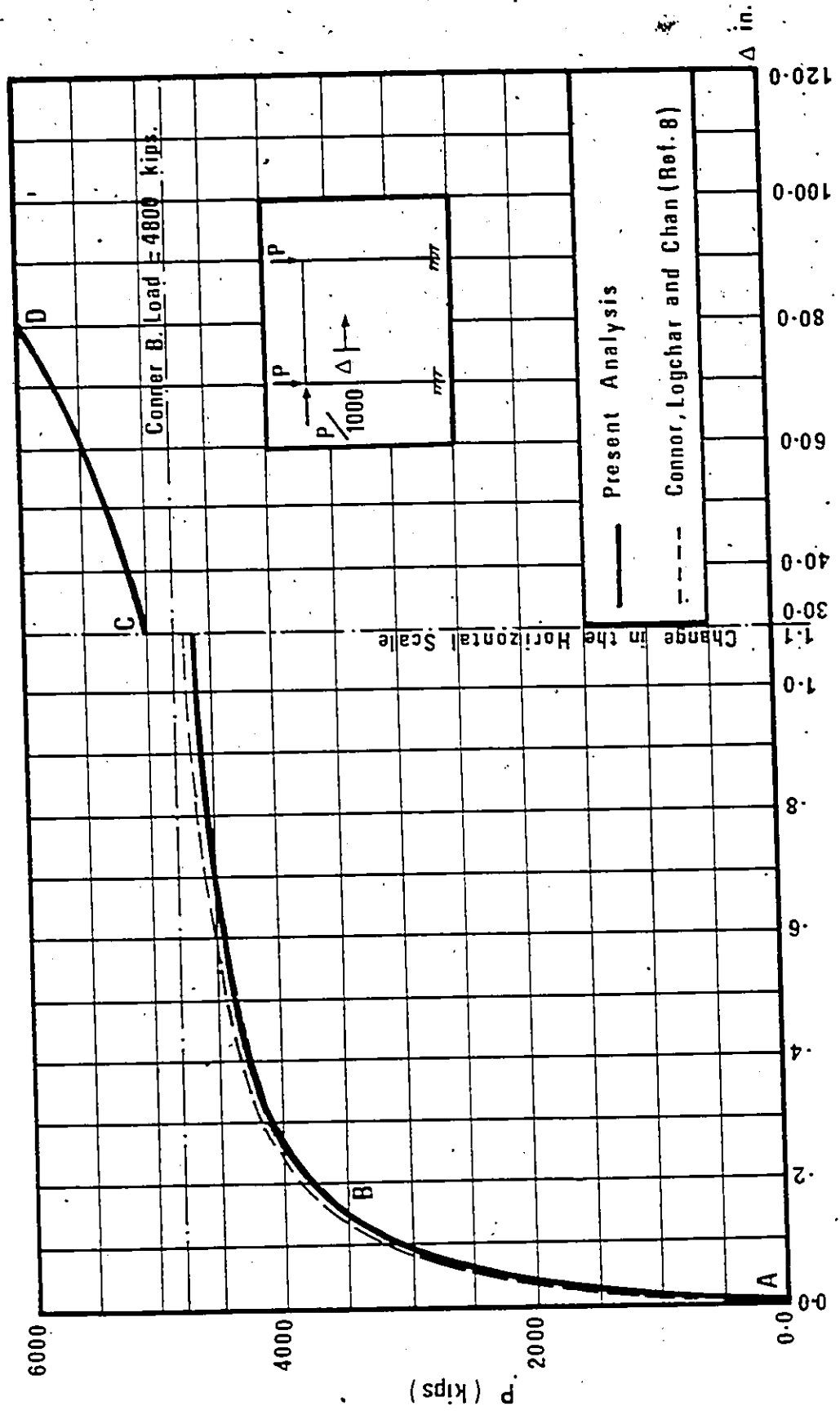(1 in. = 25.4 mm. ; 1 kip = 4.45 MN.)

94

Fig.6

Load - Deflection Curve for the Fixed Frame

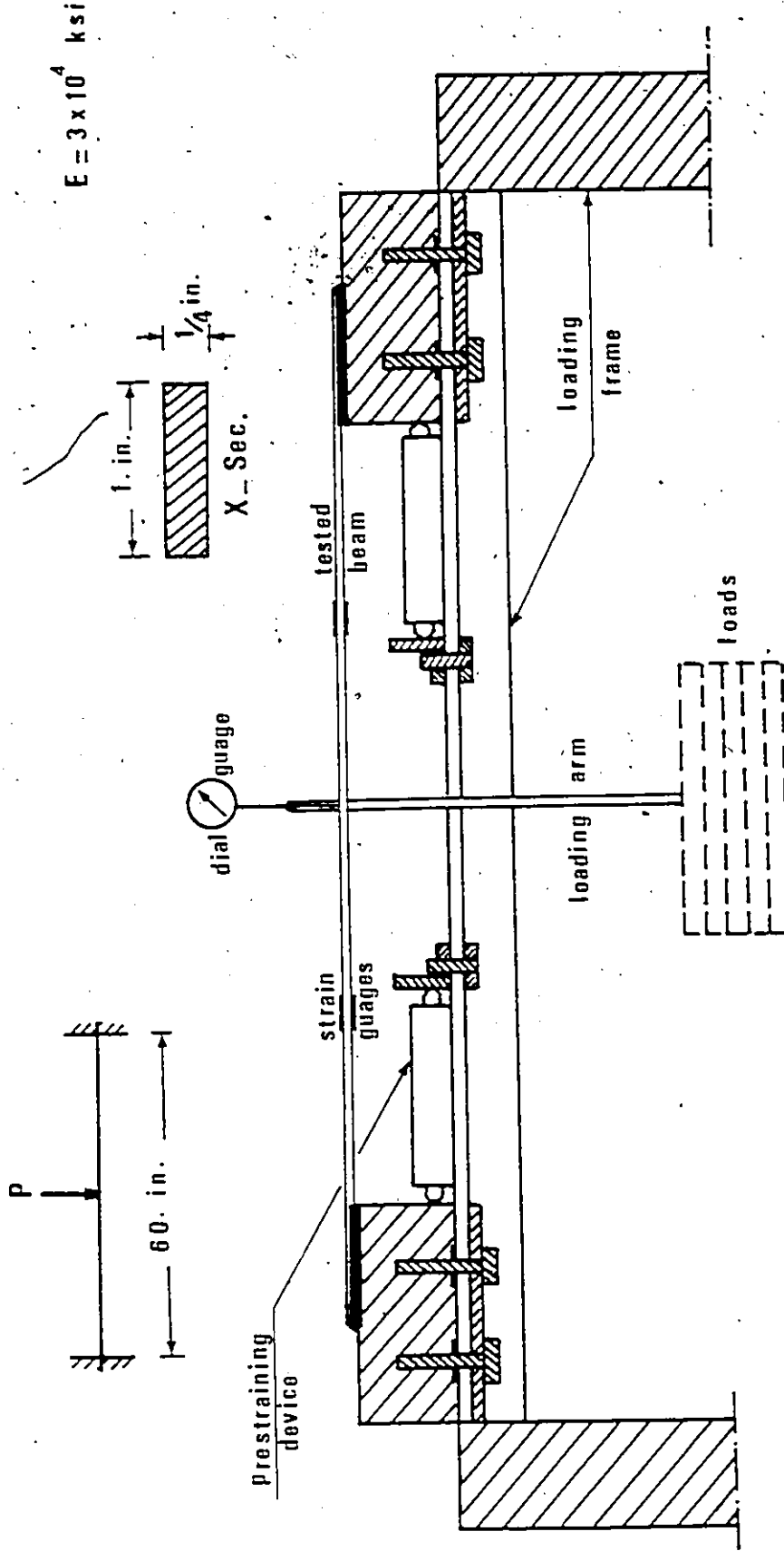(1 in. = 25.4 mm. ; 1 kip = 4.45 MN.)

Fig. 7

Schematic Drawing of the Experimental Set up

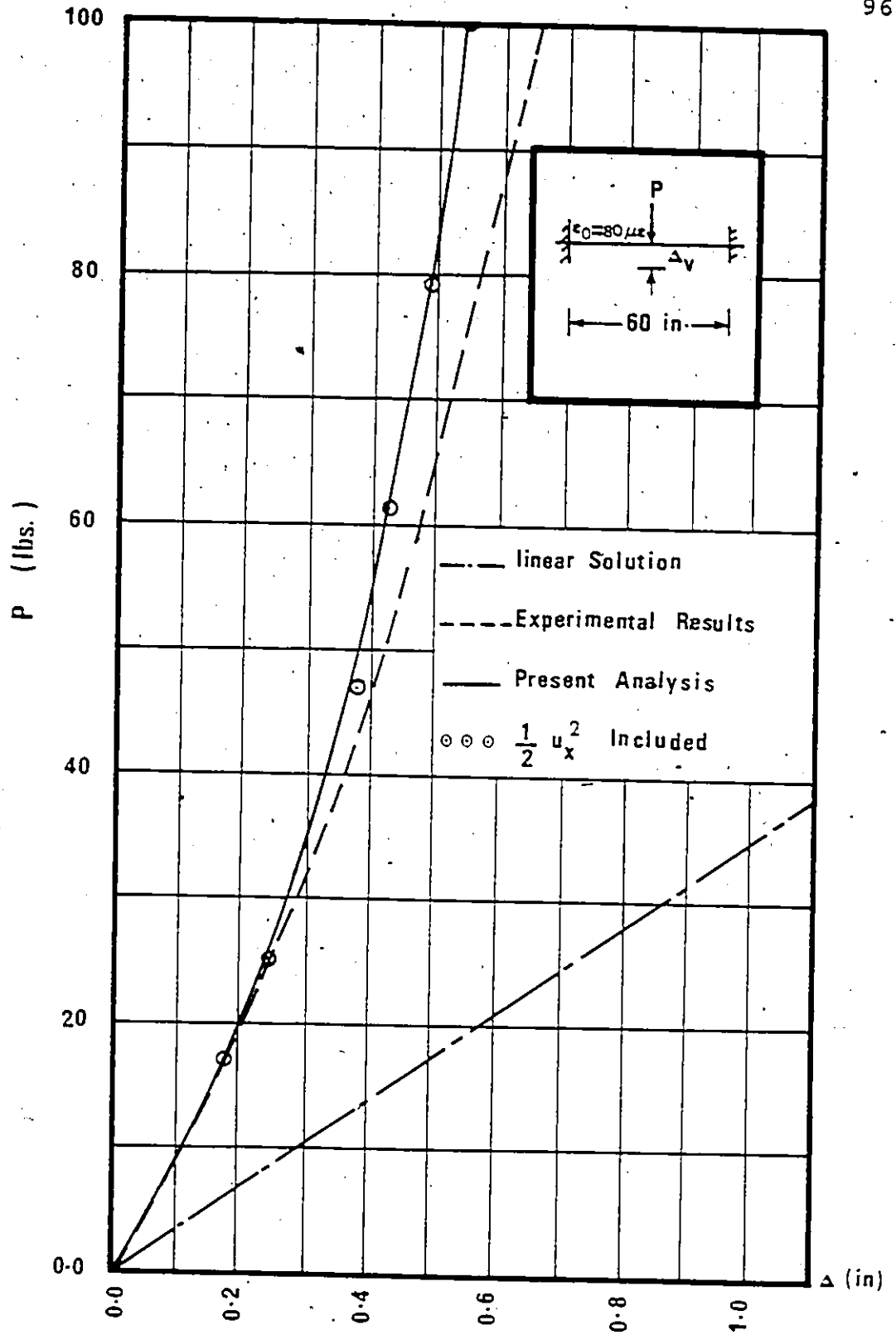(1 in. = 25.4 mm. ; 1 ksi = 6.9 MN/m^2)

Fig. 8   Load_Deflection Curve of the Fixed_Fixed Beam

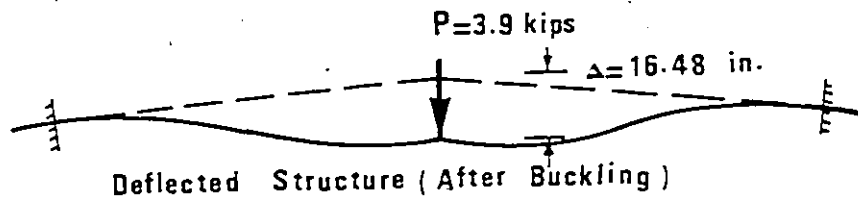(1 in. = 25.4 mm.   ,   1 lb. = 4·45 N)
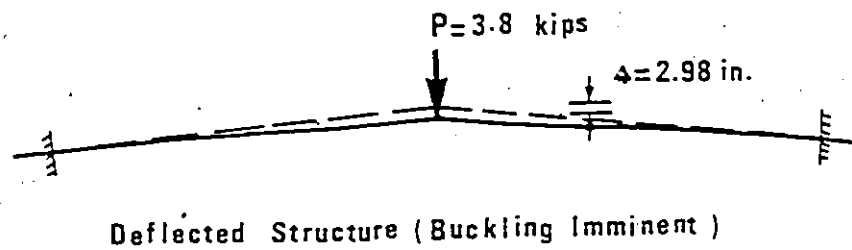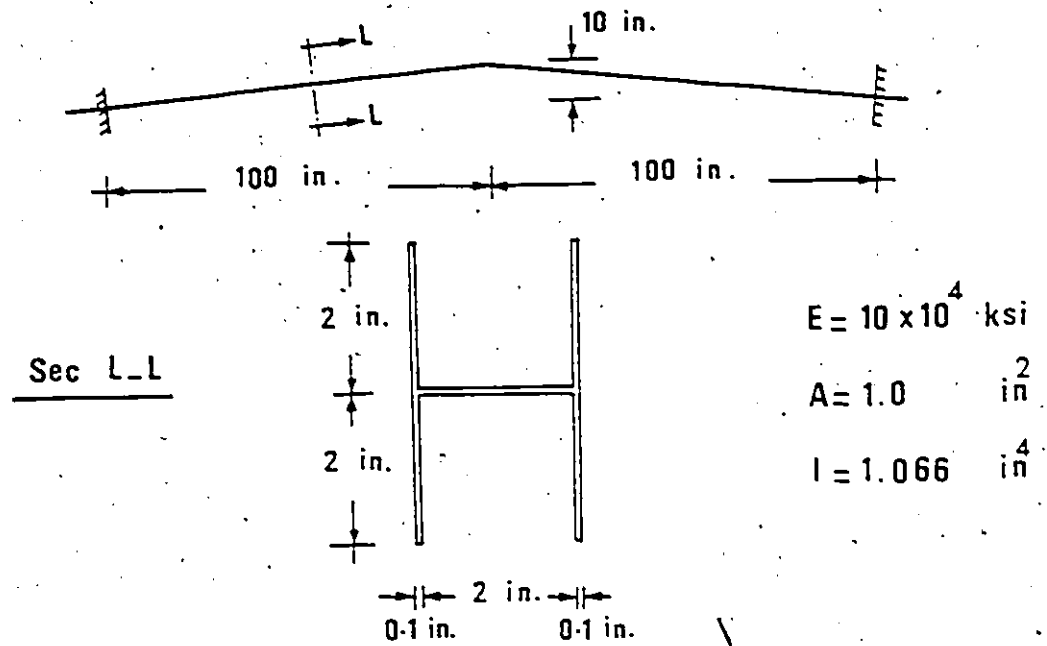
Fig.9.   A   Frame and Deflected Geometries

(1 in.= 25.4mm. , 1 kip.= 4.45 MN. .   1   ksi = 6.9 MN/m^2)
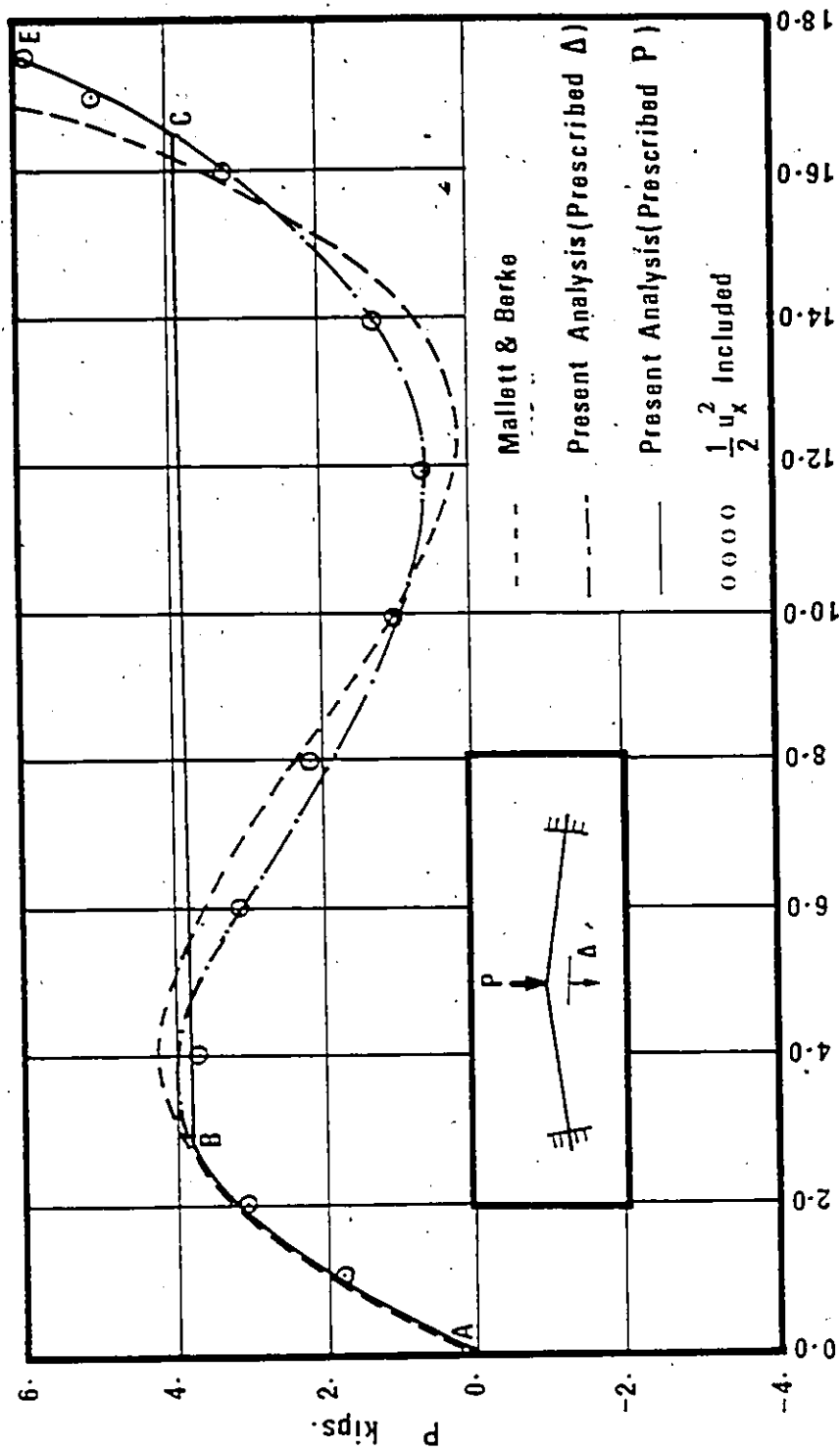
Fig. 10 Load–Deflection Curve of A Frame

(1 in. = 25.4 mm. ,   1 kip = 4.45 MN.)

E=10,000 ksi

Sec·m_m

1 in.

0·0625 in.
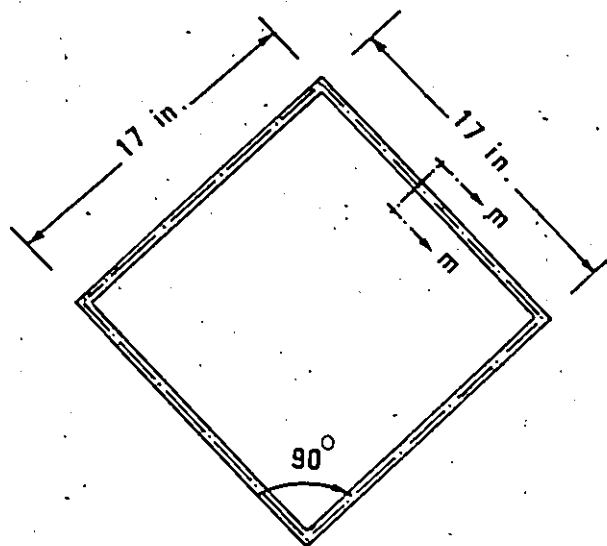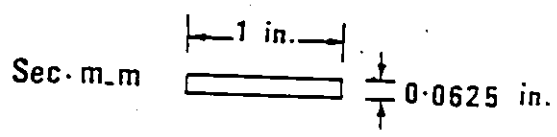
Fig.11_a Diamond Frame Before Deformation

Horiz.Scale= Vert. Scale

P=60 lbs·

P=60 lbs.
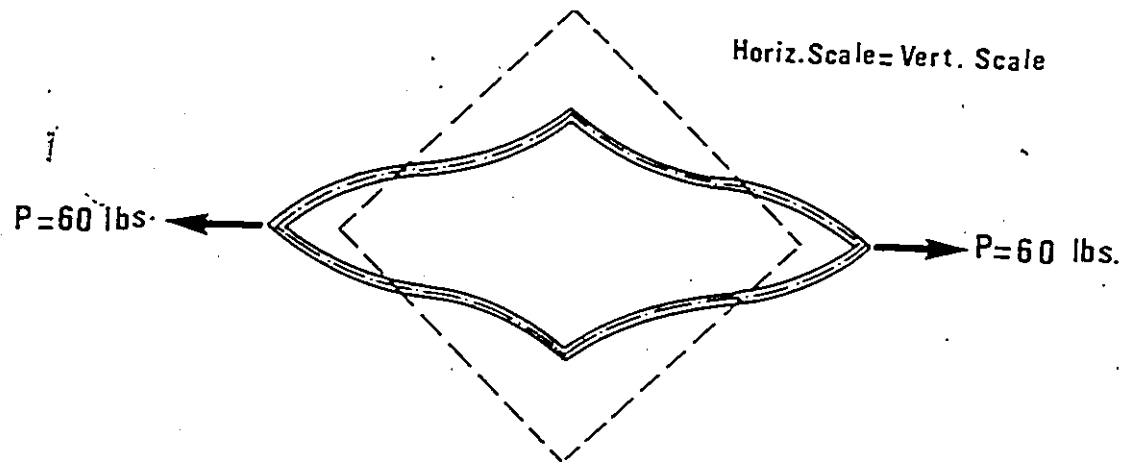
Fig.11_b   Diamond Frame After Deformation

(1 in. =25.4 mm. ,1 lb=4.45 N , 1 ksi ≈ 6.9 MN/m²)
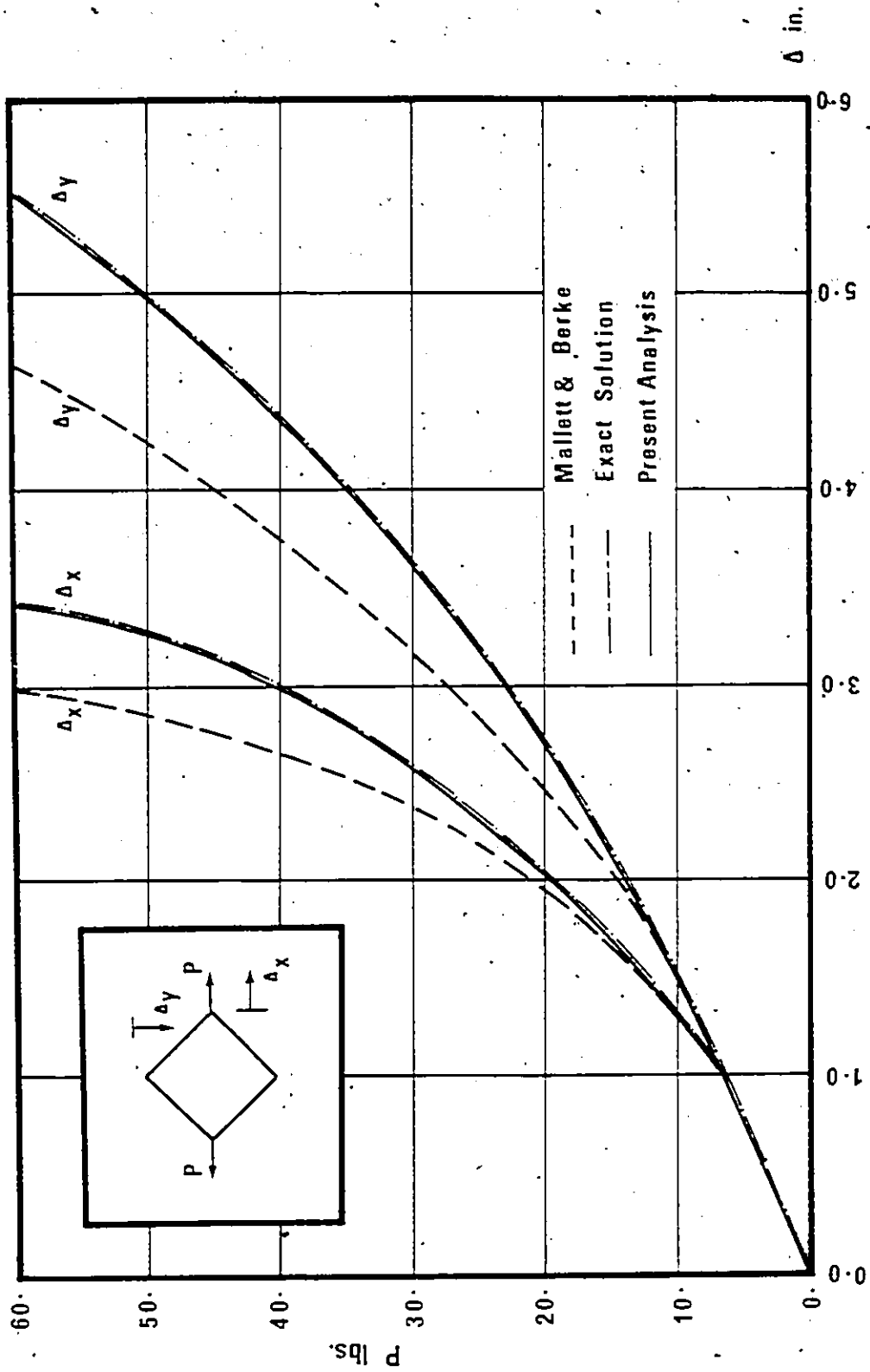
Fig.12 Load_Deflection Curves for Diamond Frame

(1 in. = 25.4 mm., 1 lb. = 4.45 N)

Sec. L_L

0.1875 in.

1 in.

rise = 1.09 in.

34 in.

Rad. = 133.11 in.

$(E = 10 \times 10^3 \text{ ksi})$

Fig. 14-a   Circular Arch

0.49 in.
0.817 in.
1.022 in.
1.09 in.

4.236 in. — 4.247 in. — 4.257 in. — 4.26 in. — 4.26 in. — 4.257 in. — 4.247 in. — 4.236 in.
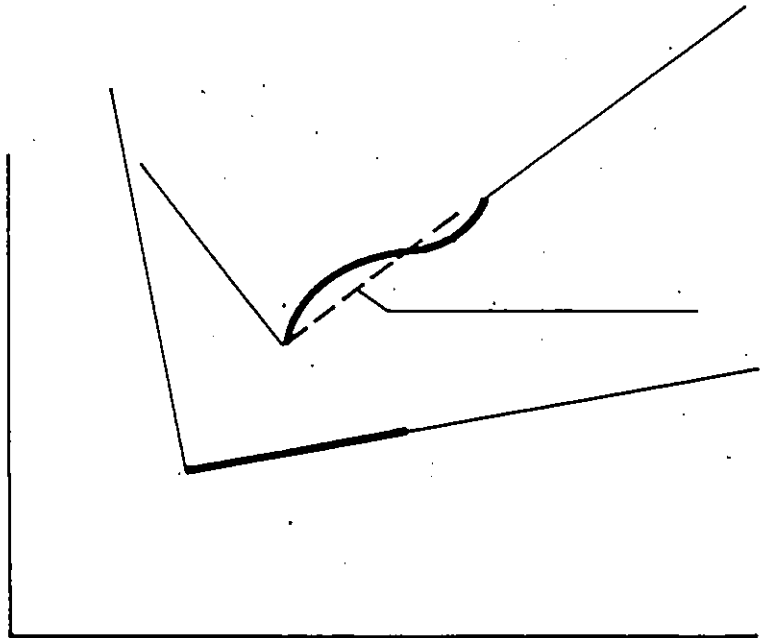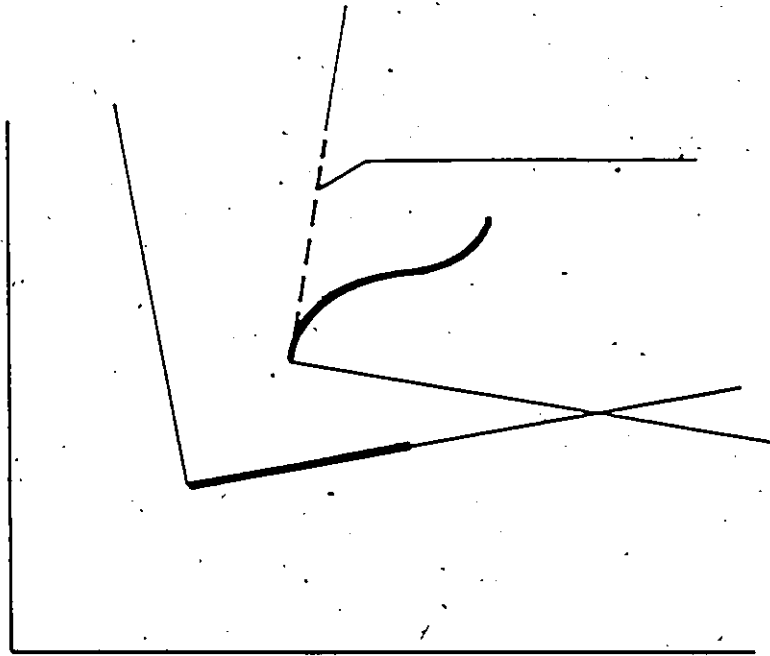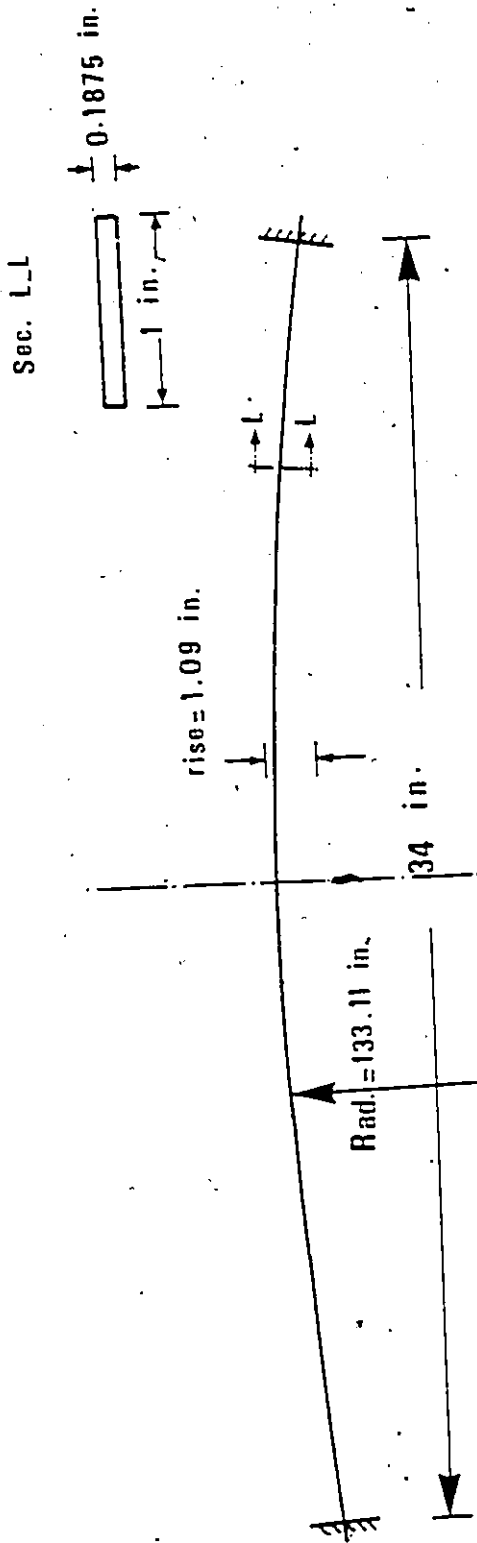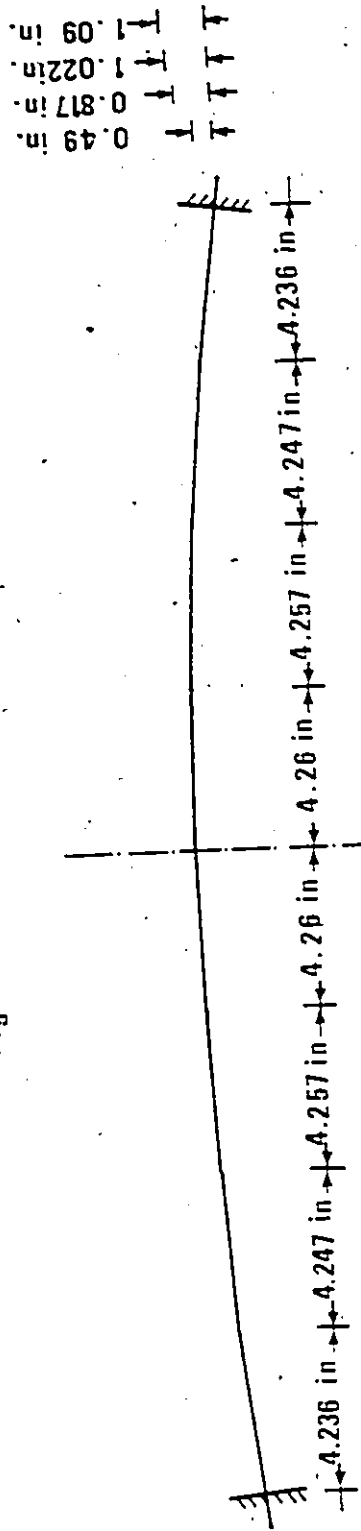
Fig. 14-b   Idealized Arch

(1 in. = 25.4 mm., 1 ksi = 6.9 MN/m^2)
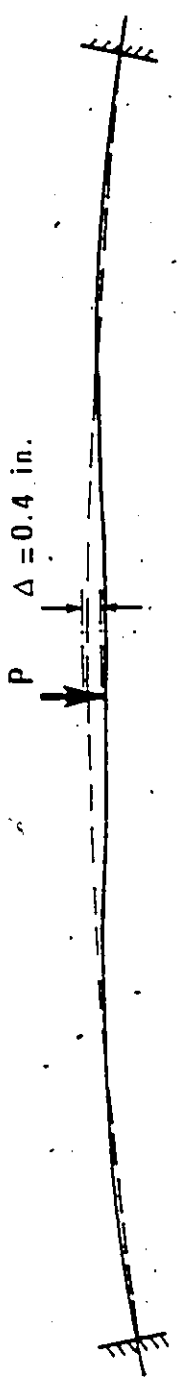
Fig. 15_a The Arch (Buckling Imminent)

P $\Delta = 0.4$ in.

$\Delta = 1.7$ in. P
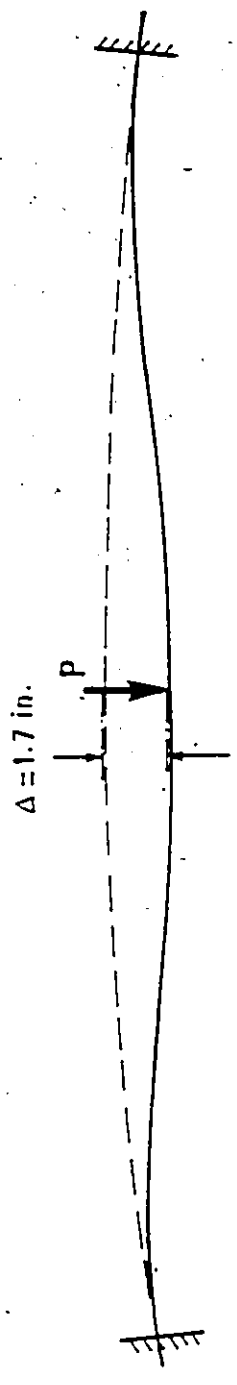
Fig. 15_b The Arch After Buckling

(1 in. = 25.4 mm.)
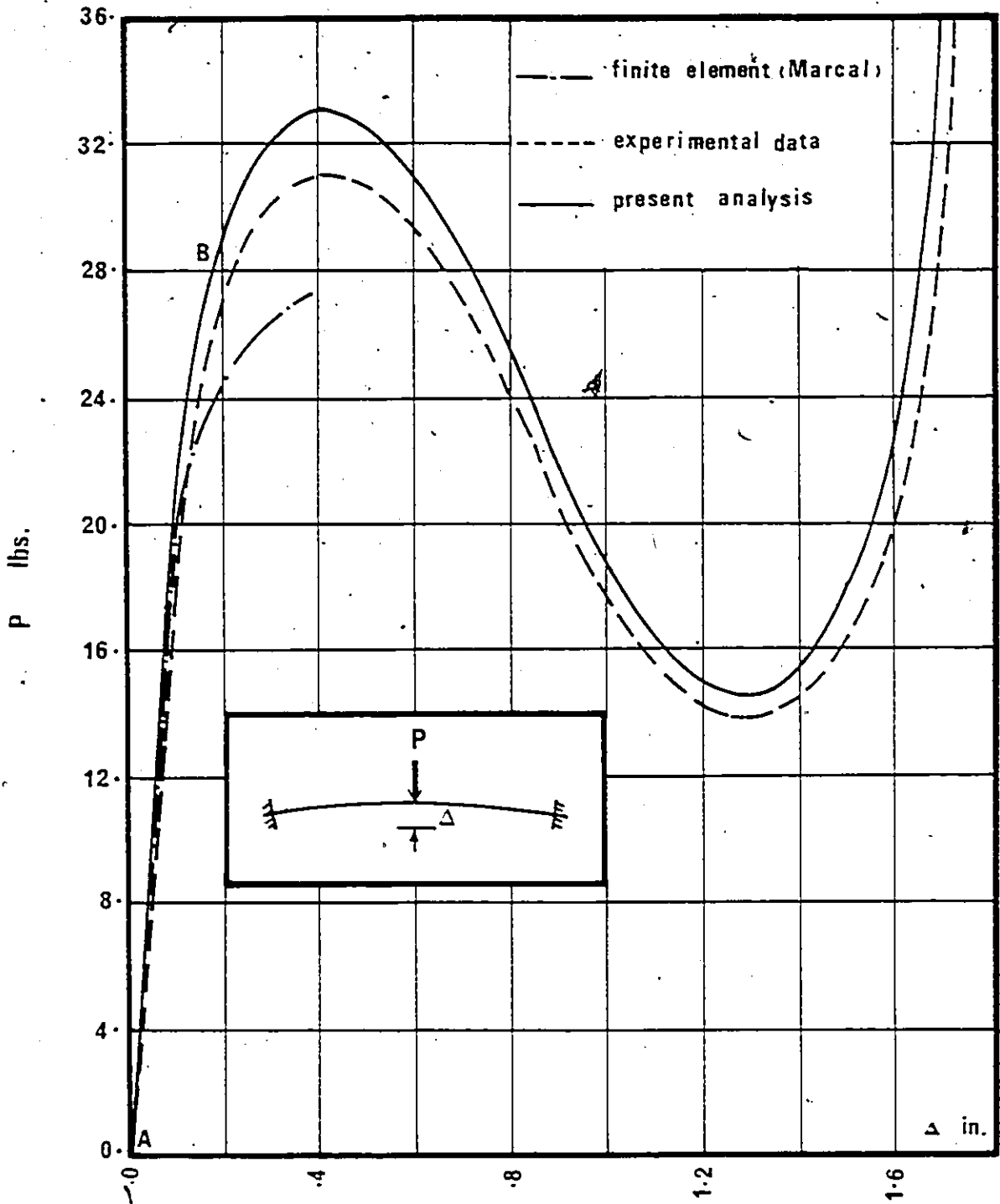
Fig.16   Load_Deflection Curve of the Shallow Arch

(1 in. = 25.4   mm , 1 · lb. = 4.45   N)
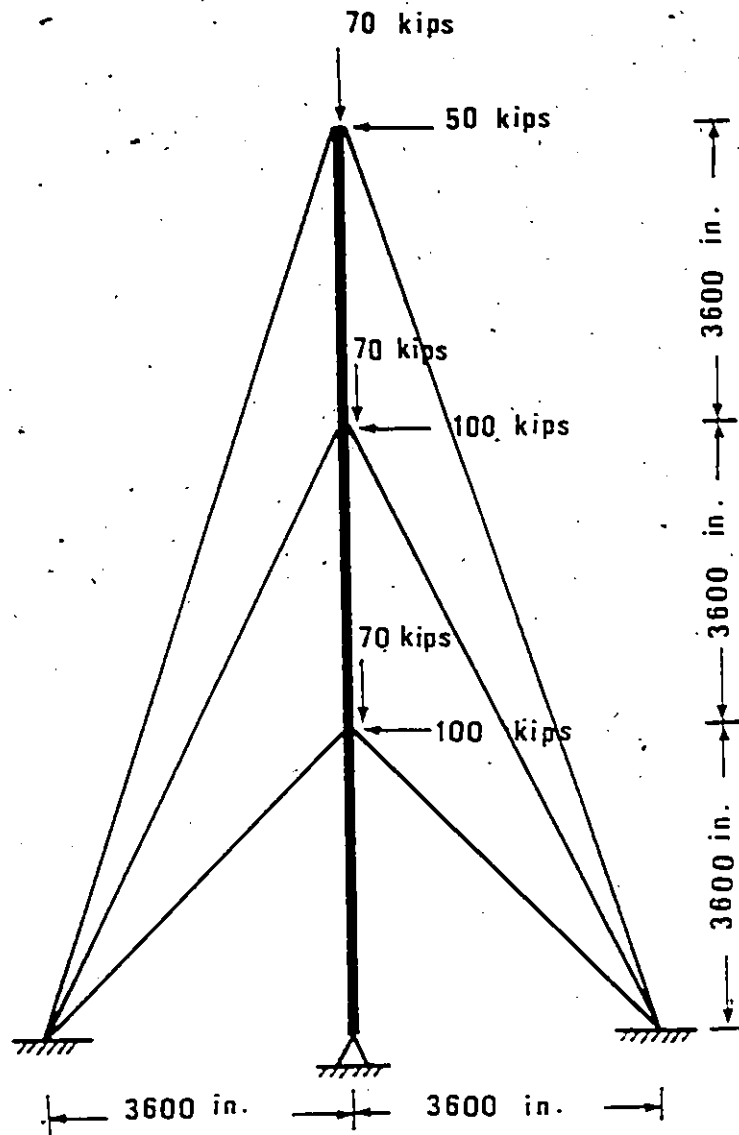
Fig. 17

Guyed Tower under Working Loads ($\gamma = 1.0$)

(1 in. = 25.4 mm. , 1 kip = 4.45 MN)
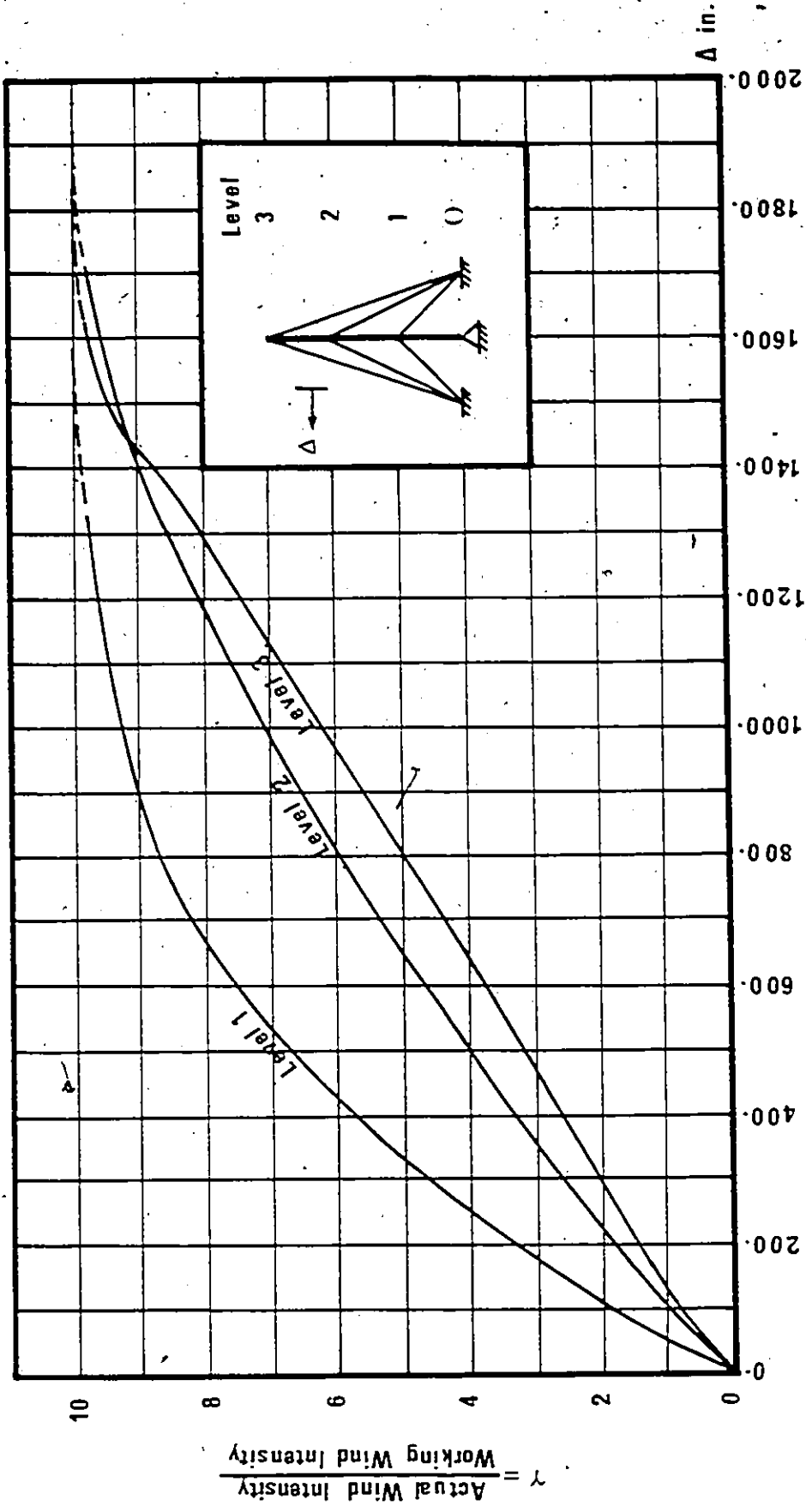
Fig. 18

Load_Deflection Curve for the Guyed Tower

(1 in. = 25.4 mm.)
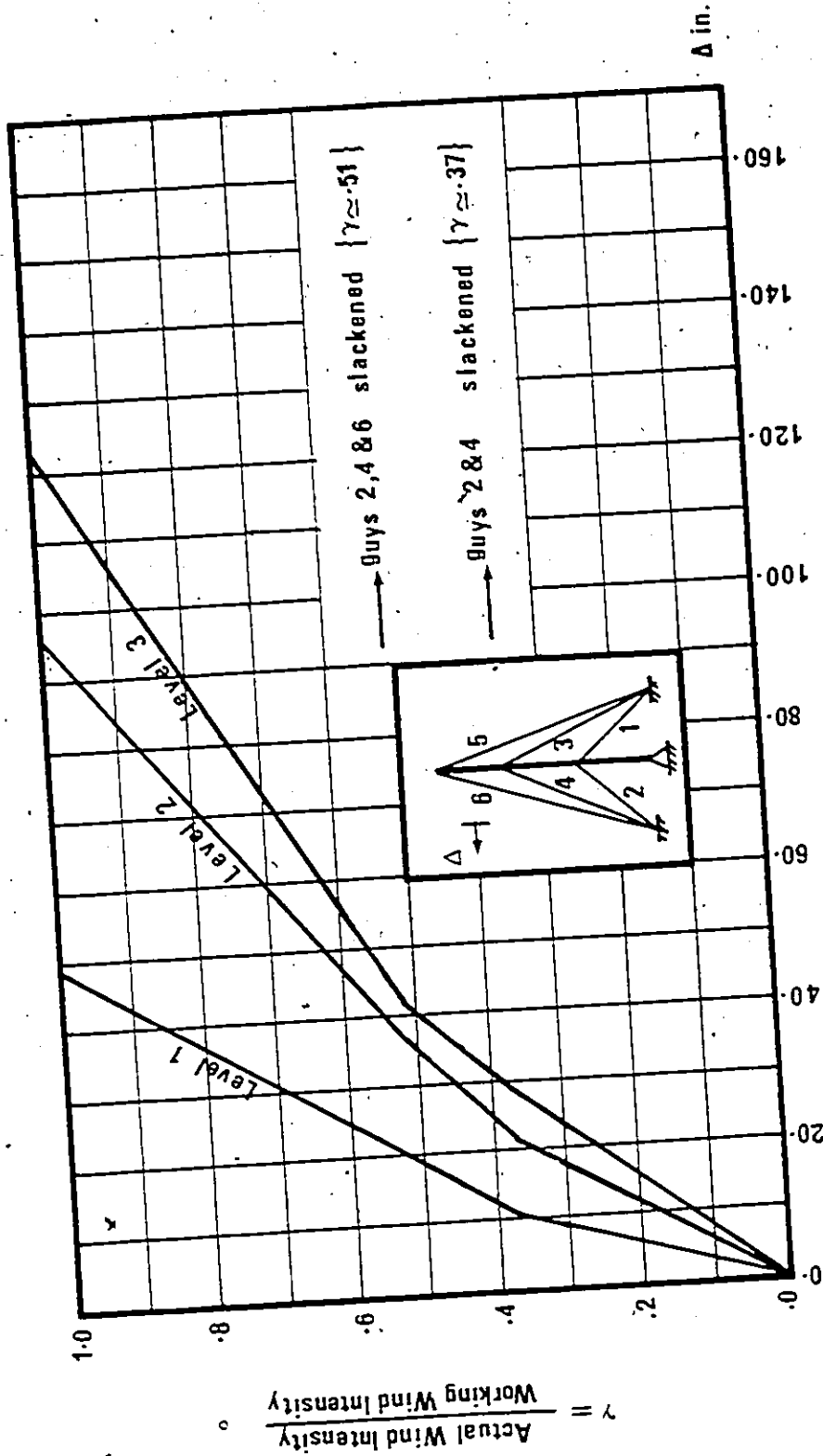
Fig. 19

Load – Deflection Curve for the Guyed Tower within the Working Range

(1 in.= 2 5.4 mm.)

Table (1)   Mast Properties (E = 30,000 ksi)

Span No.	Area (in^2)	Moment of Inertia (in^4)	Initial Prestrain in/in
1	60	300000	-1.16 $(10)^{-4}$
2	60	300000	-0.924 $(10)^{-4}$
3	60	300000	-0.527 $(10)^{-4}$

Table (2)   Guys Properties (E = 20,000 ksi)

Level No.	Area (in^2)	Initial Prestrain in/in
1	1.0	+ 0.15 $(10)^{-2}$
2	1.5	+ 0.13 $(10)^{-2}$
3	2.0	+ 0.125 $(10)^{-2}$

(1 in = 25.4 mm, 1 ksi = 6.9 MN/m^2)

REFERENCES

1. Saafan, S.A. and Brotton, D.M., "Elastic Finite
        Deflection Analysis of Rigid Frameworks by
        Digital Computers", International Symposium
        For the Use of Electronic Computers in Civil
        Engineering, October 1962, Lisbon, Portugal.

2. Saafan, S.A., "Nonlinear Behaviour of Structural Plane
        Frames", Journal of the Structural Division,
        ASCE, ST4, August 1963, pp. 557-579.

3. Poskitt, T.J., "Numerical Solution of Nonlinear
        Structures", Journal of the Structural Division,
        ASCE, ST4, August 1967, pp. 69-94.

4. Tezcan, S.S. and Krishna, P., "Numerical Solution of
        Nonlinear Structures", Discussion, Journal of
        the Structural Division, ASCE, ST6, June 1968,
        pp. 1613-1627.

5. Oran, C., "Tangent Stiffness in Plane Frames", Journal
        of the Structural Division, ASCE, ST6, June 1973,
        pp. 973-985.

6. Lee, S.L., Manuel, F.S. and Rossow, E.C., "Large
        Deflections and Stability of Elastic Frames",
        Journal of the Engineering Mechanics Division,
        ASCE, EM2, April 1968, pp. 521-545.

7. Przemieniecki, J.S., "Theory of Matrix Structural
        Analysis", McGraw-Hill Book Company, 1968,
        Chapter 15, pp. 384-391.

8. Connor, J.J., Logcher, R.D. and Chan, S.C., "Nonlinear
        Analysis of Elastic Framed Structures", Journal
        of the Structural Division, ASCE, ST6, June 1968,
        pp. 1525-1547.

9. Mallett, R.H. and Marcal, P.V., "Finite Element
        Analysis of Nonlinear Structures", Journal of the
        Structural Division, ASCE, ST9, September 1968,
        pp. 2081-2104.

10. Baron, F. and Venkatesan, M.S., "Nonlinear Formulations
        of Beam-Column Effects", Journal of the Structural
        Division, ASCE, ST4, April 1971, pp. 1305-1340.

11. Haisler, W.E., Stricklin, J.A. and Stebbins, F.J.,
    "Development and Evaluation of Solution Procedures
    for Geometrically Nonlinear Structural Analysis",
    AIAA Journal, Vol. 10, No. 3, March 1972, pp.
    264-272.

12. Turner, M.J., Dill, E.H., Martin, H.C. and Melosh, R.J.,
    "Large Deflections of Structures Subjected to
    Heating and External Loads", Journal of the Aero-
    space Science, Vol. 27, No. 2, Feb. 1960, pp. 97-
    106.

13. Stricklin, J.A., Haisler, W.E. and Riesemann, W.A.,
    "Self-Correcting Initial Value Formulations in
    Nonlinear Structural Mechanics", AIAA, Vol. 9,
    No. 10, October 1971, pp. 2066-2067.

14. Martin, H.C. and Carey, G.F., "Introduction to Finite
    Element Abalysis - Theory and Applications",
    McGraw-Hill Book Company, 1973, Chapter 6, pp.
    151-183.

15. Oran, C., "Tangent Stiffness in Space Frames", Journal
    of the Structural Division, ASCE, ST6, June 1973,
    pp. 987-1001.

16. Yang, T.Y., "Matrix Displacement Solution to Elastica
    Problems of Beams and Frames", International
    Journal of Solids Structures, Vol. 9, 1973,
    pp. 829-842.

17. Young, D., "Stiffness Matrix for a Beam with an Axial
    Force", AIAA, Vol. 11, No. 2, February 1973,
    pp. 246-247.

18. Martin, H.C., "On the Derivation of Stiffness Matrices
    For the Analysis of Large Deflection and Stability
    Problems", Matrix Methods in Structural Mechanics,
    Proceedings of the Conference held at Wright-
    Patterson Air Force Base, Ohio 26-28, October
    1965, pp. 697-715.

19. Bouchet, A.V. and Biswas, M., "Nonlinear Analysis of
    Towers and Stocks", Journal of the Structural
    Division, ASCE, ST8, August 1977, pp. 1631-1641.

20. Jagannathan, D.S., Epstein, H.I. and Christiano, P.,
    "Fictitious Strains due to Rigid Body Rotation",
    Technical Notes, Journal of the Structural Division,
    ST11, ASCE, November 1975, pp. 2472-2476.

21. Bogner, F.K., Mallett, R.H., Minich, M.D. and Schmit, L.A., "Development and Evaluation of Energy Search Methods of Nonlinear Structural Analysis", AFFDL-TR-65-113, Air Force Flight Dynamics Laboratory, Wright-Patterson Air Force Base, Ohio, 1965.

22. "Development in Discrete Element Finite Deflection Structural Analysis by Function Minimization", AFFDL-TR-68-126, Air Force Flight Dynamics Laboratory, Wright-Patterson Air Force Base, Ohio, September 1968.

23. Mallett, R.H., "A Mathematical Programming Approach to Nonlinear Structural Analysis", The Air Force Flight Dynamics Laboratory, Research Contract AF 33(615)-1022, Report No. EDC 2-65-10, November 1965.

24. Mallett, R.H. and Berke, L., "Automated Methods For The Finite Displacement Analysis of Three-Dimensional Truss and Frame Assemblies", AFFDL-TR-66-102, Air Force Flight Dynamics Laboratory, Wright-Patterson Air Force Base, Ohio, 1966.

25. Bogner, F.K., "Analysis of Tension Structures", AFFDL-TR-68-150, Air Force Flight Dynamics Laboratory, Wright-Patterson Air Force Base, Ohio, 1968.

26. El-Hakim, N.M., "Nonlinear Energy Search Analysis of Truss-Type Structural Systems", M.A.Sc. thesis, The Faculty of Graduate Studies, University of Windsor, 1975.

27. Holzer, S.M. and Somers, A.E., "Nonlinear/Solution Process: Energy Approach", Journal of the Engineering Mechanics Division, ASCE, EM4, August 1977, pp. 629-647.

28. Zangwill, W.I., "Minimizing a Function Without Calculating Derivatives", Computer Journal, Vol. 10, 1967, pp. 293-296.

29. Box, M.J., "A Comparison of Several Current Optimization Methods, and the Use of Transformations in Constrained Problems", Computer Journal, Vol. 9, 1966, pp. 67-77.

30. Fletcher, R. and Powell, M.J.D., "A Rapidly Convergent Descent Method for Minimization", Computer Journal, Vol. 6, 1963, pp. 163-168.

31. Fletcher, R. and Reeves, C.M., "Function Minimization By Conjugate Gradient", Computer Journal, Vol. 7, 1964, pp. 149-154.

32. Monforton, G.R., "Advanced Analysis of Structures", Course notes given at the University of Windsor, Civil Engineering Department, January 1976.

33. Fox, R.L. and Stanton, E.L., "Development in Structural Analysis by Direct Energy Minimization", AIAA Journal, Vol. 6, No. 6, June 1968, pp. 1036-1042.

34. Timoshenko, S.P. and Gere, J.M., "Theory of Elastic Stability", Second Edition, McGraw-Hill Book Company, 1961, Chapter 2, p. 66.

35. Jenkins, J.A. and Seitz, T.B., "Analysis of Large Deflections in Structures", Air Force Institute of Technology, Wright Patterson AFB, Ohio. School of Engineering, Rept. No. GAM Mech., 65 B-8, 151 p. June 1965.

36. Gjelsvik, A. and Bonder, S.R., "The Energy Criterion and Snap Buckling of Arches", Journal of Applied Mechanics Division, ASCE, EM5, October 1962, pp. 87-134.

37. Marcal, P.V., "Effects of Initial Displacement on Problems of Large Deflection and Stability", Tech. Report ARPA E54, Brown University, November 1967.

38. Zienkiewicz, "The Finite Element Method in Engineering Science", McGraw Hill Book Company, 1972, Chapter 19, pp. 413-434.

39. Rowe, R.S., "Amplification of Stress and Displacement in Guyed Towers", Journal of the Structural Division, ASCE, ST6, October 1958, pp. 1821-1 - 1821-20.

40. Dean, D.L., "Static and Dynamic Analysis of Guy Cables", Journal of the Structural Division, ASCE, ST1, January 1961, pp. 1-21.

41. Hull, F.H., "Stability Analysis of Multi-Level Guyed Towers", Journal of the Structural Division, ASCE, ST2, April 1962, pp. 61-80.

42. Goldberg, J.E. and Meyers, V.J., "A Study of Guyed Towers", Journal of the Structural Division, ST4, ASCE, August 1965, pp. 57-76.

43. Mears, T.F. and Charman, W.R., "The Design and Construction of Cylindrical Television Masts In Great Britain", The Structural Engineer, Vol. 44, No. 1, January 1966, pp. 5-15.

44. Bartak, A.J.J. and Shears, M., "The New Tower For The Independent Television Authority at Emley Moor, Yorkshire", The Structural Engineer, Vol. 50, No. 2, February 1972, pp. 67-80.

45. Williamson, R.A., "Stability Study of Guyed Towers Under Ice Loads", Journal of the Structural Division, ASCE, ST12, December 1973, pp. 2391-2408.

46. Miklofsky, H.A. and Abegg, M.G., "Design of Guyed Towers by Interaction Diagrams", Journal of the Structural Division, ASCE, ST1, February 1966, pp. 245-266.

47. Odley, E.G., "Analysis of High Guyed Towers", Journal of the Structural Division, ASCE, ST1, February 1966, pp. 169-197.

48. Williamson, R.A. and Margolin, M.N., "Shear Effects in Design of Guyed Towers", Journal of the Structural Division, ASCE, ST5, October 1966, pp. 213-235.

49. Livesley, R.K., "Automatic Design of Guyed Masts Subject to Deflection Constraints", International Journal for Numerical Methods in Engineering, Vol. 2, 1970, pp. 33-43.

50. Goldberg, J.E. and Gaunt, J.T., "Stability of Guyed Towers", Journal of the Structural Division, ASCE, ST4, April 1973, pp. 741-756.

51. Romstad, K.M. and Chiesa, M., "Approximate Analysis of Tall Guyed Towers", ASCE Fall Convention and Exhibit, San Francisco, Ca., October 17-21, 1977.

52. Schmit, L.A., Goble, G.G., Fox, R.L., Lasdon, L. and Moses, F., "Structural Synthesis", Summer Course Notes, Vol. 2, 1965, by Case Institute of Technology, Cleveland, Ohio.

APPENDIX A

VARIATIONAL ANALYSIS

It was shown in Chapter II that the frame element potential energy is expressible as (Eq. 2.15):

$$\pi_p = \left[\frac{EA}{2} \int_0^s \left\{ \left[\varepsilon_p + u_x + \frac{1}{2}(v_x^2 + u_x^2) \right]^2 + \frac{I}{A} v_{xx}^2 \right\} dx \right.$$

$$\left. - P_q u_q - M_p v_{x_p} - M_q v_{x_q} \right] \tag{A.1}$$

It is assumed that the element is in equilibrium under the forces P_q, M_p and M_q acting at the ends p and q. Applying arbitrary small virtual displacements δu, δv and δv_x to the element, from the principle of virtual work, the incremental work done by the external forces is equal to the increment in strain energy.

Since

$$\pi_p = U_s - W_s \tag{A.2}$$

Therefore

$$\delta\pi_p = \delta U_s - \delta W_x \tag{A.3}$$

The principle of virtual work implies that

$$\delta U_s = \delta W_s \tag{A.4}$$

or

$$\delta\pi_p = 0 \tag{A.5}$$

i.e., the variation of the element total potential energy with respect to the three virtual displacements (δu, δv, δv_x) is zero, which can be expressed as

$$\frac{\partial \pi_p}{\partial u} \delta u + \frac{\partial \pi_p}{\partial v} \delta v + \frac{\partial \pi_p}{\partial v_x} \delta v_x = 0 \qquad (A.6)$$

When the operator $(\frac{\partial}{\partial u} \delta u + \frac{\partial}{\partial v} \delta v + \frac{\partial}{\partial v_x} \delta v_x)$ operates on the element potential energy functional given in Eq. A.1, the following variation form results:

$\delta \pi_p =$

$$- AE \int_0^s \frac{d}{dx} \left\{ [\epsilon_p + u_x + \frac{1}{2}(v_x^2 + u_x^2)] + u_x[\epsilon_p + u_x + \frac{1}{2}(v_x^2 + u_x^2)] \right\} \delta u \, dx \qquad (A)$$

$$+ AE \int_0^s \frac{d}{dx} \left\{ v_{xxx} - v_x[\epsilon_p + u_x + \frac{1}{2}(v_x^2 + u_x^2)] \right\} \delta v \, dx \qquad (B)$$

$$+ \left(AE \, [\epsilon_p + u_{x_q} + \frac{1}{2}(v_{x_q}^2 + u_{x_q}^2)] + u_{x_q}[\epsilon_p + u_{x_q} + \frac{1}{2}(v_{x_q}^2 + u_{x_q}^2)] \right) - P_q \right) \delta u_q \qquad (C)$$

$$- \left\{ AE \, [\epsilon_p + u_{x_p} + \frac{1}{2}(v_{x_p}^2 + u_{x_p}^2)] + u_{x_p}[\epsilon_p + u_{x_p} + \frac{1}{2}(v_{x_p}^2 + u_{x_p}^2)] \right\} \delta u_p \qquad (D)$$

$$- \left\{ AE \, \frac{I}{A} v_{xxx_q} + v_{x_q}[\epsilon_p + u_{x_q} + \frac{1}{2}(v_{x_q}^2 + u_{x_q}^2)] \right\} \delta v_q \qquad (E)$$

$$+ AE \left\{ \frac{I}{A} v_{xxx_p} + v_{x_p}[\epsilon_p + u_{x_p} + \frac{1}{2}(v_{x_p}^2 + u_{x_p}^2)] \right\} \delta v_p \qquad (F)$$

$$+ \left\{ EI v_{xx_q} - M_q \right\} \delta v_{x_q} \qquad (G)$$

$$- \left\{ EI v_{xx_p} + M_p \right\} \delta v_{x_p} . \qquad = 0 \qquad (H)$$

Since δu, δv and δv_x are arbitrary non-zero virtual displacements, therefore, each of the expressions (A) through (H) should individually equal zero. Expressions A and B are valid for any point along the element, therefore they represent

the field equations given by Eqns. 2.16 and 2.17.
Expressions (C) through (H) describe the end conditions
which are shown in Eqns. 2.18.a through 2.18.f. The
interpretation of the boundary conditions is thoroughly
discussed in Chapter II.

APPENDIX B

EVALUATION OF COUPLING PARAMETERS (k_1 AND k)

As indicated in Chapter II, the value of the parameters k_1 and k must be obtained by using iteration since it is virtually impossible to obtain their values in a closed form. The parameter k is defined according to the following differential equation (i.e., Eq. 2.30).

$$k^2 = \frac{A}{I} \left[\varepsilon_p + u_x + \frac{1}{2}(v_x^2 + u_x^2) \right] \qquad (B.1)$$

In order to get a starting value for k to start the iteration, first and third degree polynomials are assumed for the axial and the transverse displacements, respectively. The two integration constants for the axial direction's first degree polynomial are determined from the two boundary conditions shown in Eqns. 2.26.a and 2.28.a. The resulting displacement function is in the form

$$u(x) = \frac{s - \ell}{s} x \qquad (B.2)$$

The four integration constants for the transverse direction's third degree polynomial are determined from the four boundary conditions shown in Eqns. 2.26.b, 2.26.c, 2.28.b and 2.28.c. The resulting displacement takes the form

$$v(x) = \frac{\theta_p + \theta_q}{s^2} x^3 + \frac{-2\theta_p - \theta_q}{s} x^2 + \theta_p x \qquad (B.3)$$

Back substituting into Eq. B.1, the following relationship is obtained which defines the approximate value of the

parameter k

$$\frac{Ik^2}{A} = \begin{Bmatrix} u_q \\ \vartheta_p \\ \vartheta_q \end{Bmatrix}^T \begin{bmatrix} D_{11} & 0 & 0 \\ 0 & D_{22} & D_{23} \\ 0 & D_{32} & D_{33} \end{bmatrix} \begin{Bmatrix} u_q \\ \vartheta_p \\ \vartheta_q \end{Bmatrix} \qquad (B.4)$$

where

$$D_{11} = \frac{1}{u_q^2} \left[\frac{s-\ell}{s} + \varepsilon_p + \frac{1}{2}\left(\frac{s-\ell}{s}\right)^2 \right] \qquad (B.5.a)$$

$$D_{22} = \frac{1}{15} \qquad (B.5.b)$$

$$D_{23} = \frac{-1}{60} \qquad (B.5.c)$$

Also

$$D_{33} = D_{22}$$

$$D_{32} = D_{23}$$

In case of omitting the nonlinear term $\frac{1}{2}u_x^2$ from the basic strain-displacement relationship (Eq. 2.4) the term D_{11} reads

$$D_{11} = \frac{1}{u_q^2} \left(\frac{s-\ell}{s} + \varepsilon_p \right) \qquad (B.6)$$

In case of compression-bending coupling the starting value of k_1 is taken as

$$k_1 = \sqrt{|k^2|} \qquad (B.7)$$

while for tension-bending coupling the starting value of
k is taken as

$$k = \sqrt{k^2} \qquad\qquad (B.8)$$

where k^2 has already been defined in Eq. B.4.

Two iterative procedures are employed according to
the value of the ratio I/A. For I/A less than or equal to
10, an incremental iterative procedure is used, while for
I/A greater than 10, a successive substitution scheme is
employed. In the incremental procedure, a step size equal
to k/10 (where k is given by Eq. B.4) is taken and the
generated value of k_1 (or k) is obtained according to the
expressions given in Eq. 2.39 (or Eq. 2.54). The iteration
stops if the difference between the absolute value of k_1^2
(or k^2) in two consecutive cycles is less than $(10)^{-6}$.
In the successive substitution procedure, the starting
value of k, given by Eq. B.4, is used to obtain a better
value for k_1 (or k) through Eq. 2.39 (or Eq. 2.54). The
generated value of k_1 (or k) is then used to get an improved
value for k_1 (or k). The procedure is repeated until the
absolute value of the difference between any two consecutive
values of k_1 (or k) is less than k/100000 (where k is given
by Eq. B.4).

APPENDIX C

NON-LINEAR AND LINEAR TRANSFORMATION

C.1 Non-Linear Transformation

To transform the gradient components of the element strain energy from the Eulerian (x,y) coordinates to the lagrangian local $(\tilde{x},\tilde{y})$ coordinates, Fig. 1, a non-linear transformation matrix $[\tilde{T}]_{6\times3}$ is employed. The elements of the $[\tilde{T}]$ matrix are shown below.

$$
\left[\tilde{T}\right]_{6\times3} =
\begin{bmatrix}
\dfrac{\partial u_q}{\partial \tilde{u}_p} & \dfrac{\partial \theta_p}{\partial \tilde{u}_p} & \dfrac{\partial \theta_q}{\partial \tilde{u}_p} \\[2em]
\dfrac{\partial u_q}{\partial \tilde{v}_p} & \dfrac{\partial \theta_p}{\partial \tilde{v}_p} & \dfrac{\partial \theta_q}{\partial \tilde{v}_p} \\[2em]
\dfrac{\partial u_q}{\partial \tilde{\lambda}_p} & \dfrac{\partial \theta_p}{\partial \tilde{\lambda}_p} & \dfrac{\partial \theta_q}{\partial \tilde{\lambda}_p} \\[2em]
\dfrac{\partial u_q}{\partial \tilde{u}_q} & \dfrac{\partial \theta_p}{\partial \tilde{u}_q} & \dfrac{\partial \theta_q}{\partial \tilde{u}_q} \\[2em]
\dfrac{\partial u_q}{\partial \tilde{v}_q} & \dfrac{\partial \theta_p}{\partial \tilde{v}_q} & \dfrac{\partial \theta_q}{\partial \tilde{v}_q} \\[2em]
\dfrac{\partial u_q}{\partial \tilde{\lambda}_q} & \dfrac{\partial \theta_p}{\partial \tilde{\lambda}_q} & \dfrac{\partial \theta_q}{\partial \tilde{\lambda}_q}
\end{bmatrix}
\tag{C.1}
$$

$$6 \times 3$$

120

The following relationships are used to determine the elements of the $[\widetilde{T}]$ matrix.

$$u_q = s - \ell \qquad\qquad (C.2)$$

$$\theta_p = \widetilde{\lambda}_p - \theta_r \qquad\qquad (C.3)$$

$$\theta_q = \widetilde{\lambda}_q - \theta_r \qquad\qquad (C.4)$$

$$s = \left\{ (\ell + \tilde{u}_q - \tilde{u}_p)^2 + (\tilde{v}_q - \tilde{v}_p)^2 \right\}^{\frac{1}{2}} \qquad (C.5)$$

$$\theta_r = \sin^{-1} \frac{\tilde{v}_q - \tilde{v}_p}{s} \qquad\qquad (C.6)$$

Fig. (1) illustrates the above geometrical relationships.

The elements of the $[\widetilde{T}]$ matrix are listed below:

$$\tilde{t}(1,1) = -\frac{1}{s} (\ell + \tilde{u}_q - \tilde{u}_p)$$

$$\tilde{t}(2,1) = -\frac{1}{\ell} (\tilde{v}_q - \tilde{v}_p)$$

$$\tilde{t}(3,1) = 0$$

$$\tilde{t}(4,1) = -\tilde{t}(1,1)$$

$$\tilde{t}(5,1) = -\tilde{t}(2,1)$$

$$\tilde{t}(6,1) = 0$$

$$\tilde{t}(1,2) = \frac{(-1)(\tilde{v}_q - \tilde{v}_p)(\ell + \tilde{u}_q - \tilde{u}_p)}{s^2 \sqrt{s^2 - (\tilde{v}_q - \tilde{v}_p)^2}}$$

$$\tilde{t}(2,2) = \frac{\sqrt{s^2 - (\tilde{v}_q - \tilde{v}_p)^2}}{s^2}$$

$$\tilde{t}(3,2) = 1$$

$$\tilde{t}(4,2) = -\tilde{t}(1,2)$$

$$\tilde{t}(5,2) = -\tilde{t}(2,2)$$

$$\tilde{t}(6,2) = 0$$

$$\tilde{t}(1,3) = \tilde{t}(1,2)$$

$$\tilde{t}(2,3) = \tilde{t}(2,2)$$

$$\tilde{t}(3,3) = 0$$

$$\tilde{t}(4,3) = -\tilde{t}(1,3)$$

$$\tilde{t}(5,3) = -\tilde{t}(2,3)$$

$$\tilde{t}(6,3) = 1$$

C.2 Linear Transformation

To transform the gradient components from the local $\tilde{x}, \tilde{y}$ coordinates to the global $\bar{X}, \bar{Y}$ reference axes, Fig. 1, the following linear transformation matrix is employed.

$$[\bar{T}]_{6\times6} = \begin{bmatrix} \ell_1 & m_1 & 0 & 0 & 0 & 0 \\ \ell_2 & m_2 & 0 & 0 & 0 & 0 \\ 0 & 0 & 1 & 0 & 0 & 0 \\ 0 & 0 & 0 & \ell_1 & m_1 & 0 \\ 0 & 0 & 0 & \ell_2 & m_2 & 0 \\ 0 & 0 & 0 & 0 & 0 & 1 \end{bmatrix} \qquad (C.7)$$

where ℓ_1, m_1 are the direction cosines of $\tilde{x}$ axis with respect to the global $\bar{X}, \bar{Y}$ axes, respectively. Similarily, ℓ_2, m_2 are the direction cosines of $\tilde{y}$ axis with respect to the global $\bar{X}, \bar{Y}$ axes, respectively.

APPENDIX D

FLETCHER-REEVES METHOD AND SCALING

TRANSFORMATION FORMULATIONS

D.1 Fletcher-Reeves Method

The method of Fletcher-Reeves employs conjugate directions as the directions of travel to detect the minimum of the function. The formulations are thoroughly explained in Ref. 31 and a good discussion is also presented in Ref. 52. The conjugate directions are generated according to the following relationship:

$$\vec{s}_{j+1} = -\vec{\nabla \Pi_p}_{j+1} + \beta_j \, \vec{s}_j \tag{D.1}$$

where

$\vec{s}_j$ is the conjugate direction defined in the j <u>th</u> step.

$\vec{s}_{j+1}$ is the generated conjugate direction in the j+1 <u>th</u> step.

$\vec{\nabla \Pi_p}_{j+1}$ is the vector defining the partial derivatives of the total potential energy of the structure in the j+1 <u>th</u> step with respect to each of the J generalized coordinates, which can be expressed mathematically as,

$$\overrightarrow{\nabla \Pi_p} = \begin{Bmatrix} \dfrac{\partial \Pi_p}{\partial D_1} \\[1em] \dfrac{\partial \Pi_p}{\partial D_2} \\ \vdots \\ \dfrac{\partial \Pi_p}{\partial D_{J-1}} \\[1em] \dfrac{\partial \Pi_p}{\partial D_J} \end{Bmatrix}_{J \times 1} \qquad (D.2)$$

$$\beta_j = \frac{(\overrightarrow{\nabla \Pi}_{p_{j+1}})^2}{(\overrightarrow{\nabla \Pi}_{p_j})^2} \qquad (D.3)$$

The starting vector $\{D_o\}$ is usually taken as the $\{0\}$ vector, but generally the starting point which leads as quickly as possible to the bottom of the minimization valley is the best choice. Finding $\{D_{j+1}\}$ along $\overrightarrow{s_j}$ when starting from $\{D_j\}$ is, essentially, a linear minimization of the potential energy function along the $\overrightarrow{s_j}$ direction. The overall efficiency of the minimization technique depends, mainly, on the linear minimization routine. The linear minimization can be cast in the following equations:

a) given

$$g(\alpha_j) = \Pi_p \overrightarrow{(D_j} + \alpha_j \overrightarrow{s_j}) \qquad (D.4)$$

b) required

$$\alpha_j^*, \text{such that}$$

$$\acute{g}(\overset{*}{\alpha}_j) = 0 \qquad\qquad (D.5)$$

Notice that $\acute{g}(\alpha_j) = \vec{s}_j^T \vec{\nabla \Pi}_p (\vec{D_j} + \alpha_j \vec{s_j})$ \qquad (D.6)

Determining $\overset{*}{\alpha}_j$ is accomplished in three stages. The first obtains a step size for use by the second stage and the second stage establishes bounds on $\overset{*}{\alpha}_j$; the third stage interpolates its value. Discussion of the three stages follows.

Stage 1

It is assumed that the value of the minimum of the quadratic function is known a priori as an estimate (Est.) and that it lies on the line $\vec{D_j} + \alpha_j \vec{s_j}$. Therefore, it follows that the value of $\overset{*}{\alpha}$ which detects the minimum is obtainable exactly as k_o where

$$k_o = 2(\text{Est} - \Pi_p\{D_j\})/\vec{s}_j^T \vec{\nabla \Pi}_{p_j} \qquad (D.7)$$

Equation D.7 is obtainable by studying the geometrical properties of a parabola. In fact, the minimum of Π_p will generally not lie on the line $(\vec{D_j} + \alpha_j \vec{s_j})$, so Eq. D.7 will be in error. One way to overcome this is to limit the value $\overset{*}{\alpha}$ to be less than or equal to one.

$$\overset{*}{\alpha} = \begin{cases} k_o & \text{if} \quad 0 < k_o < (\vec{s}_j^T \vec{s}_j)^{-\frac{1}{2}} & (D.8) \\ \\ (\vec{s}_j^T \vec{s}_j)^{-\frac{1}{2}} & \text{otherwise} & (D.9) \end{cases}$$

For linear analysis where the strain energy function is a quadratic function of the displacements {D}, the value of $\overset{*}{\alpha}_i$ could be obtained in a closed form (Eq. D.7). The iterative solution is only needed in non-quadratic functions.

Stage 2

Evaluate g, $\bar{g}(\alpha_j)$ at the points 0, h, 2h, 4h,...,a,b where b is the first value of the α_j at which $\bar{g}$ is non-negative or g has not decreased which implies that

$$a < \overset{*}{\alpha}_j < b \qquad \text{(D.10)}$$

Stage 3

A third degree polynomial is then fitted between a and b. The four integration constants of the polynomial are determined from the boundary conditions g_a, $\bar{g}_a$, g_b and $\bar{g}_b$. The α_e which corresponds to the minimum of the third degree polynomial is determined according to the following relationships.

$$\alpha_e = b - \left(\frac{\bar{g}(b) + w - z}{\bar{g}(b) - \bar{g}(a) + 2w} \right) (b - a) \qquad \text{(D.11)}$$

$$z = \frac{3\{g(a) - g(b)\}}{b - a} + \bar{g}(a) + \bar{g}(b) \qquad \text{(D.12)}$$

$$w = \{z^2 - \bar{g}(a)\, \bar{g}(b)\}^{\frac{1}{2}} \qquad \text{(D.13)}$$

If neither g(a) nor g(b) is less than $g(\alpha_e)$, then α_e is accepted as the estimate of the minimum along $\overrightarrow{s}_j$;

otherwise, according to $\overline{g}(\alpha_e')$ is positive or negative, the interpolation is repeated over the sub-interval $[a, \alpha_e]$ or $[\alpha_e, b]$, respectively.

Early experience in the optimization of some special functions proved that the procedure should revert periodically to the steepest descent direction defined as $(-\overrightarrow{\nabla \Pi_p})$ in place of the customary $\overrightarrow{s_j}$. Such restarts are not more frequent than every $(J+1)$ iterations. Although this method is supposed to minimize a quadratic of J variables in J iterations, it is found that an additional iteration is beneficial in compensating for the accumulation of rounding-off errors in the first J iterations.

The iteration stops if

$$\overrightarrow{\nabla \Pi_p} = 0 \qquad \qquad (D.14)$$

This condition is unlikely to be realized in practice because of the round-off errors; therefore, the iteration is continued for one more cycle of $(J+1)$ iterations starting from the steepest descent and the last value of $\{D\}$ until either of the two following criteria is satisfied.

a) $\quad \Pi_p(\{D\}^*) - \Pi_p(\{D\}) < \varepsilon_2 \qquad \qquad (D.15)$

b) $\quad \{D\}^* - \{D\} < \varepsilon_3 \qquad \qquad (D.16)$

Some general remarks about the application of the Fletcher-Reeves method, which are obtained from the employed IBM library subroutine, are reported herein,

1. The function should be decreasing along the conjugate direction, if for any reason the function increases by stepping along the conjugate direction, the linear search routine will be skipped and the step will be taken along the steepest descent.

2. The exit criterion for accepting $\{D\}^*$ as the minimum is

$$\sum_{j=1}^{J}\left\{\overrightarrow{\nabla \pi}_{p_j}{}^2\{D\}\right\} < Eps \qquad (D.17)$$

where Eps is a predetermined value by the user. A value of $(10)^{-6}$ was specified in the present analysis.

D.2 Scaling Transformation Formulations

In Chapter III, the diagonal matrix [R] was defined as.

$$r_{jj} = \frac{1}{(k_{jj})^{\frac{1}{2}}} \qquad j = 1,2,\ldots,J \qquad (D.18)$$

The matrix $[k_{jj}]$ is the matrix of second partials of the potential energy function. In the case of linear analysis, the matrix of second partials is the stiffness matrix of the structure. In case of nonlinear analysis, linearizing the matrix of second partials proved to be efficient in order to improve the convergence of the potential energy function. The following linearizations were introduced to

obtain the elements of the diagonal matrix $[\bar{K}]$.

1) A third degree polynomial for the transverse displacement was assumed.

2) The bowing effects in calculating the coupling coefficients k^2 were neglected.

3) The deformed length s was replaced by undeformed length ℓ.

Therefore, the elements of the diagonal matrix $[\bar{K}]$ for the frame element are

$$k_{11} = k_{44} = \frac{EA}{2}\left\{\left(\frac{1}{\ell} - \frac{(\bar{X}_q - \bar{X}_p)^2}{\ell^3}\right)(\varepsilon_p^2 + 2\varepsilon_p) + \frac{2(\bar{X}_q - \bar{X}_p)^2}{\ell^3}\right\} + \frac{12EI\ell_2^2}{\ell^3}$$

$$(D.19)$$

$$k_{22} = k_{55} = \frac{EA}{2}\left\{\left(\frac{1}{\ell} - \frac{(\bar{Y}_q - \bar{Y}_p)^2}{\ell^3}\right)(\varepsilon_p^2 + 2\varepsilon_p) + \frac{2(\bar{Y}_q - \bar{Y}_p)^2}{\ell^3}\right\} + \frac{12EIm_2^2}{\ell^3}$$

$$(D.20)$$

$$k_{33} = k_{66} = \frac{4EI}{\ell} \qquad\qquad (D.21)$$

VITA AUCTORIS

Hany Ahmed Mohamed El-Ghazaly

1950   Born on August 1st in Cairo, Egypt.

1968   Completed the secondary stage education
and joined the Faculty of Engineering,
Cairo University.

1973   Graduated with a B.Sc. (Distinction
with honors) in Civil Engineering,
Cairo University.

1973   Appointed as a teaching assistant in
the Civil Engineering Department,
Cairo University.

1975   In September 1975, enrolled in a
programme leading to the degree of
Master of Applied Science in Civil
Engineering at the University of
Windsor.